THE ROLES OF SMALL AND LONG NON-CODING RNAS IN REGULATING GENE EXPRESSION

APPROVED BY SUPERVISORY COMMITTEE

Yi Liu, Ph.D.

Steven McKnight, Ph.D.

Qinghua Liu, Ph.D.

Nicholas K. Conrad, Ph.D.

DEDICATION

To my parents-Wenyou Xue and Ai’e Xu and my wife-Lin Yu.

THE ROLES OF SMALL AND LONG NON-CODING RNAS IN REGULATING GENE EXPRESSION

by

ZHIHONG XUE

DISSERTATION

Presented to the Faculty of the Graduate School of Biomedical Sciences

The University of Texas Southwestern Medical Center at Dallas

In Partial Fulfillment of the Requirements

For the Degree of

DOCTOR OF PHILOSOPHY

The University of Texas Southwestern Medical Center at Dallas

Dallas, Texas

May, 2014

ACKNOWLEDGEMENT

I first want to thank my mentor, Dr. Yi Liu, for his guidance and support throughout the years. I thank Yi for giving me the opportunity to work with and learn from him. Yi tried his best to train me in every aspect during my pursuit for the Ph.D., including critical thinking, \hypothesis making, designing experiments, troubleshooting, and scientific presentation. The training in his lab and his scientific guidance have been critical to my success.

I am grateful to members of the Liu lab, both past and present. I would like to thank Dr. Liande Li and Dr. Heng-Chi Lee who taught me the basic techniques for RNA studies. I also want to thank Dr. Michael Chae, Dr. Joonseok Cha, Dr. Yunkun Dang, Dr. Qiuying Yang and Mian Zhou for the helpful discussion on my project. In addition, I want to thank Qiaohong Ye and Haiyan Yuan for the technical support.

My work was greatly benefited from the collaborations with several other labs. I am thankful to Dr. Ying Liu, Dr. Xuecheng Ye, and Dr. Chunyang Liang from Dr. Qinghua Liu's lab for helping me to set up the *in vitro* small RNA assays. I want to thank Dr. Yi Yang and Dr. Jun Liao from Dr. Youxing Jiang's lab for the technical support in protein purification. I appreciate the help from Dr. Jichen Yang from Dr. Guanghua Xiao's lab for the mathematic simulation of circadian clock in *Neurospora*. I also want to thank Dr. Oded Yarden for providing the *al-2*-containing plasmid, and Dr. J. Scott Butler for the yeast RRP46-TAP strain.

I greatly appreciate my dissertation committee members: Dr. Steven McKnight, Dr. Qinghua Liu and Dr. Nicholas K. Conrad for their continuous support. Their critical insights and invaluable advice have played an important role during my studies.

Finally, I would like to thank my parents Wenyou Xue and Ai'e Xu, and my wife Lin Yu for their patience, encouragement, support and understanding throughout the years.

THE ROLES OF SMALL AND LONG NON-CODING RNAS IN REGULATING GENE EXPRESSION

Publication No. _____

ZHIHONG XUE, Ph.D.

The University of Texas Southwestern Medical Center at Dallas, 2014

Mentor: YI LIU, Ph.D.

Recent studies have revealed that a large proportion of a eukaryotic genome is transcribed into non-coding RNAs (ncRNAs). Based on size, these RNAs can be classified as small non-coding RNAs (sRNAs) and large non-coding RNAs (lncRNAs). The ncRNA regulatory networks control various levels of gene expression and play significant roles in diverse biological processes.

Argonaute proteins, the core proteins in RNAi pathways, are required for the biogenesis of some sRNAs, including the PIWI-interacting RNAs and some microRNAs. How Argonautes mediate maturation of sRNAs independent of their slicer activity was not clear.

The maturation of the *Neurospora* miRNA-like sRNA, milR-1, requires the Argonaute protein QDE-2, Dicer, and exonuclease QIP. Here, I reconstituted this Argonaute-dependent sRNA biogenesis pathway *in vitro*, and demonstrated that QDE-2 mediates milR-1 maturation by recruiting exosome and QIP, and by determining the size of milR-1. QIP first separates the QDE-2-bound duplex milR-1 precursor and then mediates 3' to 5' trimming and maturation of milR-1 precursor together with exosome using a hand-over mechanism. Our results establish a biochemical mechanism of an Argonaute-dependent sRNA biogenesis pathway and critical roles of exosome in sRNA processing.

Natural antisense RNAs, which are mostly lncRNAs, are widely found in eukaryotic organisms and have been implicated in diverse physiological processes. The physiological importance of antisense RNAs and how they regulate sense RNAs are not clear. *frequency* (*frq*) encodes a core component of the *Neurospora* circadian oscillator. Here, I demonstrated that the simultaneous transcription of *qrf*, the long non-coding *frq* antisense RNA, represses *frq* transcription by inducing RNA polymerase II collision-triggered premature transcription termination and chromatin modifications. The expression of *frq* also inhibits the expression of *qrf* and surprisingly, drives the antiphasic rhythm of the *qrf* transcripts in the dark. The mutual inhibition of *frq* and *qrf* transcription forms a double negative feedback loop that is required for robust and sustained circadian rhythmicity. Our results establish antisense transcription as an essential feature in a eukaryotic circadian system and demonstrate the importance and mechanism of antisense RNA action. Together, the studies described in this dissertation shed light on the mechanisms of gene expression regulated by sRNAs and lncRNAs.

TABLE OF CONTENTS

PRIOR PUBLICATIONS

Xue, Z., Ye, Q., Anson, S.R., Yang, J., Xiao, G., Kowbel, D., Glass, N.L., Crosthwaite, S.K., Liu, Y. Transcriptional interference by sense and antisense of *frequency* forms a double negative feedback loop that is required for circadian gene expression. (under review)

Yang, Q., Li, L., **Xue, Z.**, Ye, Q., Zhang, L., Li, S., and Liu, Y. (2013). Transcription of the major *Neurospora crassa* microRNA-like small RNAs relies on RNA polymerase III. PLoS Genet 9, e1003227.

Zhang, Z., Chang, S.S., Zhang, Z., **Xue, Z.**, Zhang, H., Li, S., and Liu, Y. (2013). Homologous recombination as a mechanism to recognize repetitive DNA sequences in an RNAi pathway. Genes Dev 27, 145-150.

Dang, Y., Li, L., Guo, W., **Xue, Z.**, and Liu, Y. (2013). Convergent transcription induces dynamic DNA methylation at disiRNA loci. PLoS Genet 9, e1003761.

Xue, Z., Yuan, H., Guo, J., and Liu, Y. (2012). Reconstitution of an Argonaute-dependent small RNA biogenesis pathway reveals a handover mechanism involving the RNA exosome and the exonuclease QIP. Mol Cell 46, 299-310.

Dang, Y., Yang, Q., **Xue, Z.**, and Liu, Y. (2011). RNA Interference in Fungi: Pathways, Functions, and Applications. Eukaryotic Cell 10, 1148-1155.

Lee, H.-C., Li, L., Gu, W., **Xue, Z.**, Crosthwaite, S.K., Pertsemlidis, A., Lewis, Z.A., Freitag, M., Selker, E.U., Mello, C.C., Liu, Y. (2010). Diverse Pathways Generate MicroRNA-like RNAs and Dicer-Independent Small Interfering RNAs in Fungi. Molecular Cell.

LIST OF FIGURES

LIST OF ABBREVIATIONS

ncRNAs	non-coding RNAs
mRNAs	messenger RNAs
rRNAs	ribosomal RNAs
snRNAs	small nuclear RNAs
snoRNAs	small nucleolar RNAs
lncRNAs	long non-coding RNAs
miRNAs	microRNAs
siRNAs	small interfering RNAs
piRNAs	Piwi-interacting RNAs
Ago	Argonaute
dsRNA	double-stranded RNA
ssRNA	single-stranded RNA
RdRPs	RNA-dependent RNA Polymerases
milRNA	miRNA-like small RNAs
RISC	RNA-induced silencing complex
Pol II	RNA polymerase II
DMT	DNA methyltransferase
HMT	Histone methyltransferase
H3K9	Histone 3 Lysine 9
H3K36	Histone 3 Lysine 36
TI	Transcription Interference

aRNAs	aberrant RNAs
MSUD	Meiotic Silence of Unpaired DNA
qiRNAs	QDE-2-interacting small RNAs
disiRNAs	Dicer-independent small interfering RNAs
QA	quinic acid
QDE	quelling deficient
QIP	QDE-2 interacting protein
per	*period*
frq	*frequency*
WC	White Collar
LRE	Light Response Element
CT	circadian time
CTD	carboxy terminal domain
ChIP	Chromatin immunoprecipitation

CHAPTER ONE

INTRODUCTION

Our previous undertsanding of gene regulation has been centered on the central dogma in molecular biology: DNA→ mRNA→ Protein. RNAs were normally considered as the messengers that transfer genetic information from DNA to protein. However, studies of the last decade uncovered that the large proportion of a eukaryotic genome is transcribed and many of the transcripts do not encode for proteins (Rinn and Chang, 2012), thus the name non-coding RNAs (ncRNAs). Recent studies have demonstrated that ncRNAs is a critical part of gene regulatory networks that can control gene expression, including chromatin architecture/epigenetic memory, genomic integrity, transcription, RNA splicing/ 5'-capping/3'-polyadenylation/editing/ turnover, and translation (Costa, 2008; Mattick and Makunin, 2006; Ponting et al., 2009; Rinn and Chang, 2012; Sharma and Misteli, 2013; Wang and Chang, 2011; Zaratiegui et al., 2007). In contrast to diversity of ncRNAs species, only limited number of ncRNAs currently have experimentally-derived functions and mechanisms.

1.1 ncRNAs

Since the concept of messenger RNAs (mRNAs) was first established by F. Jacob & J. Monod in 1961 (Jacob and Monod, 1961), numerous RNAs of all shapes and sizes have been discovered (Rinn and Chang, 2012). In 1965, an alanine tRNA, the first non-coding RNA,

was characterized in baker's yeast (Holley et al., 1965). Studies of the past several decades demonstrated the presence of large numbers of ncRNAs (Rinn and Chang, 2012). The ncRNAs can be classified into housekeeping ncRNAs and regulatory ncRNAs. Housekeeping ncRNAs include ribosomal RNAs (rRNAs), tRNAs, small nuclear RNAs (snRNAs), and small nucleolar RNAs (snoRNAs), which are highly conserved, and usually constitutively expressed in eukaryotes (Ponting et al., 2009). Based on size, regulatory ncRNAs are arbitrarily divided into small regulatory RNAs (sRNAs) and large non-coding RNAs (lncRNAs) (Ponting et al., 2009). Since the discovery of the first sRNA in 1993, a large number of sRNAs have been identified in different organisms, including micoRNA (miRNAs), small interfering RNAs (siRNAs) and Piwi-interacting RNAs (piRNAs). The common features of sRNAs are their short length (~20-30 nucleotides), and their association with members of the Argonaute (Ago) family of proteins. These sRNAs guide the Ago proteins to their regulatory targets. The sRNAs differ in their origin, maturation process and mode of action (Czech and Hannon, 2011; Ghildiyal and Zamore, 2009). The lncRNAs are operationally defined as RNAs larger than 200pb that do not appear to have coding potential. In 1980s~1990s, genetic studies identified a few lncRNAs that regulate genomic imprinting and X chromosome inactivation (XIST, H19, AIR) (Ponting et al., 2009; Rinn and Chang, 2012). In the past decade, the advance in high-throughput RNA sequencing uncovered numerous lncRNAs that have been implicated in regulating the complexity of the organism, including development, differentiation, and metabolism. The lncRNAs are poorly conserved and they regulate gene expression by diverse mechanisms. (Wang and Chang, 2011). In my

dissertation studies, I will focus on the biogenesis pathways of sRNAs and the function and mode of action of lncRNAs.

1.2 Biogenesis of ncRNAs

1.2.1 Mechanisms of sRNAs biogenesis

Since the discovery of the first miRNA in *C. elegans*, various types of sRNAs with sizes ranging from 20-30 nt have been identified, which are generally categorized into three main classes: siRNAs, miRNAs and piRNAs (Ghildiyal and Zamore, 2009). As shown in Figure 1-1, both siRNAs and miRNAs are derived from double-stranded RNAs (dsRNAs) precursors that are recognized and processed by RNase III domain-containing ribonuclease Dicer to produce short duplexes (21~25 nt). The main differences between siRNAs and miRNAs are in two key aspects. First, siRNAs are produced from exogenous and endogenous dsRNAs (e.g., viral RNA) or endogenous transcripts from repetitive sequences (e.g., transposable elements). In many organisms, the RNA-dependent RNA polymerases (RdRPs) are required to generate dsRNAs from single-stranded RNAs (ssRNAs) or to amplify sRNA to make secondary siRNAs. On the other hand, miRNAs are derived from miRNA-encoding genes that produce ssRNA precursor transcripts which form hairpin-like structures. Second, siRNAs normally fully match their mRNA targets whereas miRNAs can target mRNAs with incomplete complementary sequences (Carthew and Sontheimer, 2009; Dang et al., 2011; Ghildiyal and Zamore, 2009; Liu and Paroo, 2010).

piRNAs acquired the name due to their association with Piwi clade of Argonaute family proteins, which have been identified in both vertebrates and invertebrates. piRNAs are

processed from single-stranded precursor transcripts that are mostly derived from repetitive elements, transposons, and large piRNA clusters in animal germ cells. piRNAs are distinct from siRNAs and miRNAs in size (26~31 nt), and lack of sequence conservation. Although the biogenesis mechanism of primary piRNAs is still not clear, a "ping-pong" mechanism has been identified to mediate the amplification of piRNAs from primary piRNAs (Czech and Hannon, 2011; Dang et al., 2011; Ghildiyal and Zamore, 2009; Liu and Paroo, 2010; Siomi and Siomi, 2009) (Figure 1-1).

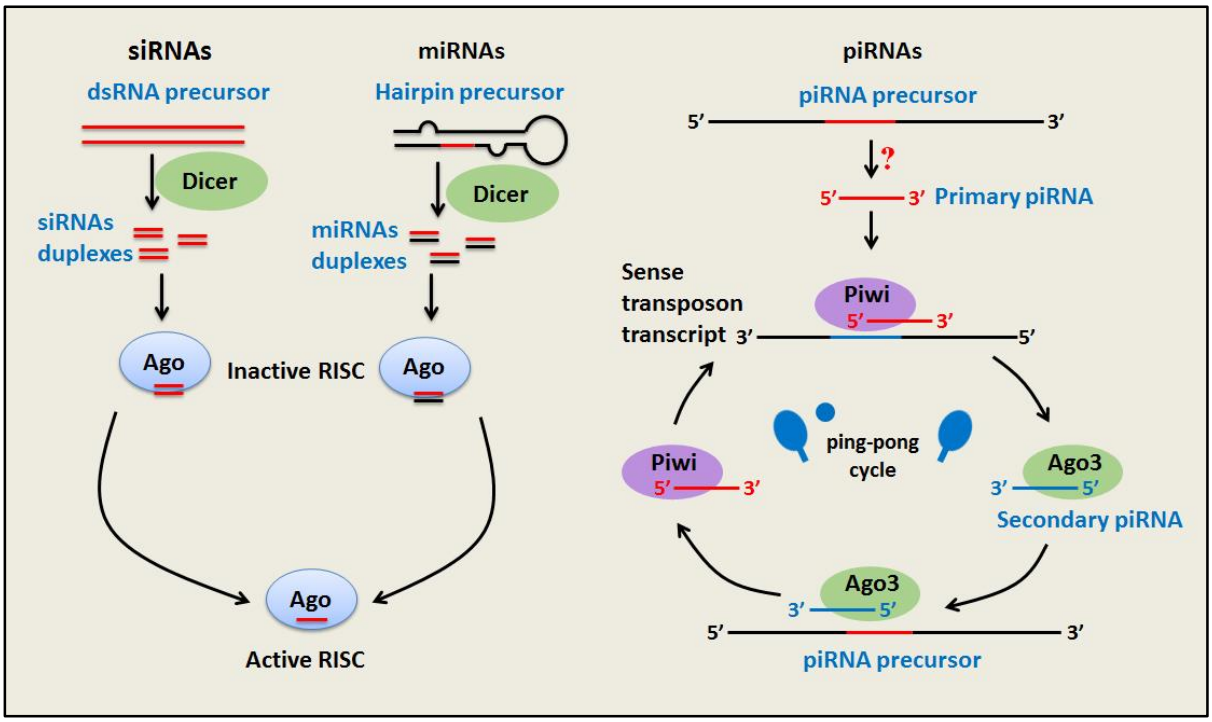

Figure 1-1 The mechanism of sRNAs biogenesis.
The schematic diagrams show the biogenesis mechanisms of siRNAs, miRNAs, and piRNAs. The siRNAs and miRNAs duplexes are generated by Dicer from dsRNAs and hairpin-liked single-stranded precursors, respectively. Afterwards, one strand of Ago-associated siRNAs or miRNAs duplex is removed to generate the active RNA-induced silencing complex (RISC). The primary piRNAs are produced from single-stranded precursors through unknown mechanisms. The piRNAs are further amplified through Piwi- and Ago3-dependent ping-pong cycle. (Adapted from Thomson and Lin, 2009)

1.2.2 Mechanisms of lncRNAs biogenesis

The majority of lncRNAs are transcribed by RNA polymerase II (Pol II), which are demonstrated by Pol II occupancy and histone modifications associated with Pol II transcription elongation (Wang and Chang, 2011). Based on their origins, lncRNAs can be classified into several categories: (1) sense RNAs or (2) antisense RNAs, where lncRNA transcripts overlap with another transcript on the same, or opposite strand, respectively; (3) bidirectional RNAs, where the expression of a lncRNAs and a neighboring transcript with opposite direction are initiated in close genomic proximity; (4) intronic, when a lncRNAs is derived from an intron of another transcript; (5) intergenic, where a lncRNA is located within the genomic interval between two genes (Ponting et al., 2009). It has suggested that ~5% - 30% of transcriptional units in diverse eukaryotes harbor *cis*-natural antisense transcripts (*cis*-NATs); the proportion is dependent on the depth of transcriptome-sequencing methods (Lapidot and Pilpel, 2006).

1.3 Biological functions of ncRNAs

1.3.1 Biological functions of sRNAs

The roles of sRNA was first suggested in homology-dependent gene silencing mechanisms in plants and fungi, which can be triggered by transgenes and recombinant viruses (Romano and Macino, 1992; Zaratiegui et al., 2007). It is now known that sRNA-mediated gene regulation plays important roles in chromatin structure, chromosome segregation, transcription, RNA processing, RNA stability, and translation in diverse biological processes. The general effects of sRNAs on gene expression are inhibitory, and

therefore were termed as gene silencing mechanism. The common theme of gene silencing is that sRNAs serve as the specific guides that direct bound effector proteins to target nuleic acid molecules via base-pairing interactions. The core component of the effector machinery is a member of the Argonaute protein family (Carthew and Sontheimer, 2009; Ghildiyal and Zamore, 2009; Siomi and Siomi, 2009).

In general, siRNA guides RISC to recognize its perfectly complementary mRNA, resulting in Ago-catalyzed mRNA cleavage at a single site within the duplex. Afterwards, RISC is regenerated through releasing the cleaved mRNA target that are further degraded by cellular exonucleases (Figure 1-2). In some cases, siRNAs are also capable of recognizing targets without perfect base-pairing, where they can silence targets by miRNA-like mechanisms involving in translational repression and exonucleolytic degradation. In addition, siRNAs can mediate heterochromatin formation by cooperating with nascent transcripts and RNA polymerases (RNA Pol II in fission yeast or RNA Pol IV/V in plants). In plants, target engagement results in the recruitment or activation of a DNA methyltransferase (DMT) that methylates the DNA, inducing heterochromatin formation. In fission yeast and probably in animals, the pathway requires a histone methyltransferase (HMT) which methylates lysine 9 of histone H3 (H3K9), leading to heterochromatin formation (Figure 1-2) (Carthew and Sontheimer, 2009; Ghildiyal and Zamore, 2009; Liu and Paroo, 2010; Moazed, 2009; Siomi and Siomi, 2009).

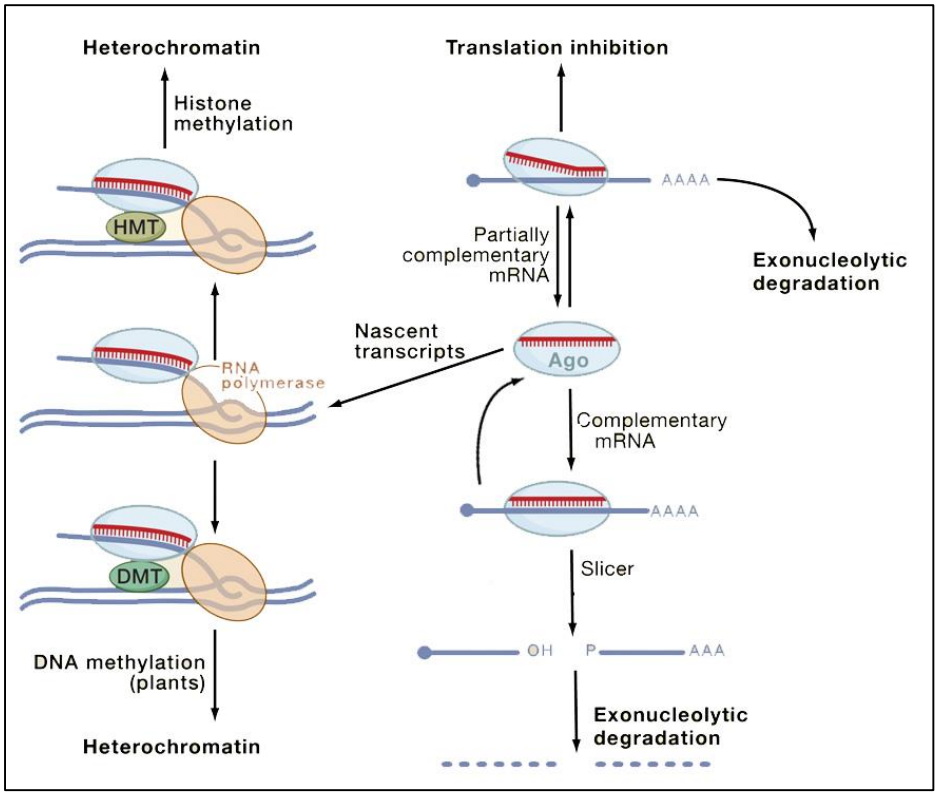

Figure 1-2 Mechanisms of siRNA silencing.
A schematic showing the known mechanisms of siRNAs-mediated silencing. (Adapted from Carthew and Sontheimer, 2009)

miRNAs regulate diverse biological processes, ranging from housekeeping functions to responses to environmental stress (Ghildiyal and Zamore, 2009). Almost all known miRNA-binding sites in animal mRNAs are located in the 3'UTR and normally present in multiple copies. Most of animal miRNAs bind with their targets with mismatches and bulges, although a key feature of recognition requires perfect base-pairing of miRNA nucleotides 2-8, representing the seed region. In contrast, most plant miRNAs are near-perfectly complementary to the coding sequence of their mRNA targets. The perfect miRNA-mRNA complementarity allows Ago-catalyzed cleavage of the mRNA strand, while mismatches

around the complementarity center exclude cleavage and promote translational repression (Bartel, 2004; Carthew and Sontheimer, 2009; Ghildiyal and Zamore, 2009; Liu and Paroo, 2010; Voinnet, 2009). The miRNAs-mediated translational repressions have been subject to ongoing debate. Various models of how miRNAs repress translation have been proposed. Normally, mRNAs recruit translation initiation factors and ribosomal subunits to form circularized structures that allow efficient translation (Figure 1-3 top). As shown in Figure 1-3, miRNAs can repress the translation initiation at the cap recognition stage or the ribosome large subunit 60S recruitment stage. Alternatively, miRNAs can lead to deadenylation of the mRNA and inhibit circularization of the mRNA. In addition, miRNAs can induce ribosomes to drop off prematurely at the post-initiation stage. Finally, miRNAs can promote mRNAs degradation via deadenylaiton and decapping (Carthew and Sontheimer, 2009; Fabian et al., 2010; Gu and Kay, 2010; Huntzinger and Izaurralde, 2011).

Like siRNAs and miRNAs, piRNAs guide PIWI proteins to mediate gene silencing, specifically the silencing of transposons. Similarly, PIWI proteins cleave the transposon RNA complementary with piRNAs, resulting in silencing. Mutations of PIWI proteins are correlated with increased expression of transposons. Transposons have a high potential to lead to deletion mutations on their host and PIWI proteins have been found to be essential for spermatogenesis in mice and germ-cell, stem-cell development in invertebrates. In addition, piRNAs have been shown to affect the methylation of transposons. However, how they act is not well understood (Fabian et al., 2010; Klattenhoff and Theurkauf, 2008; Meister, 2013; Thomson and Lin, 2009).

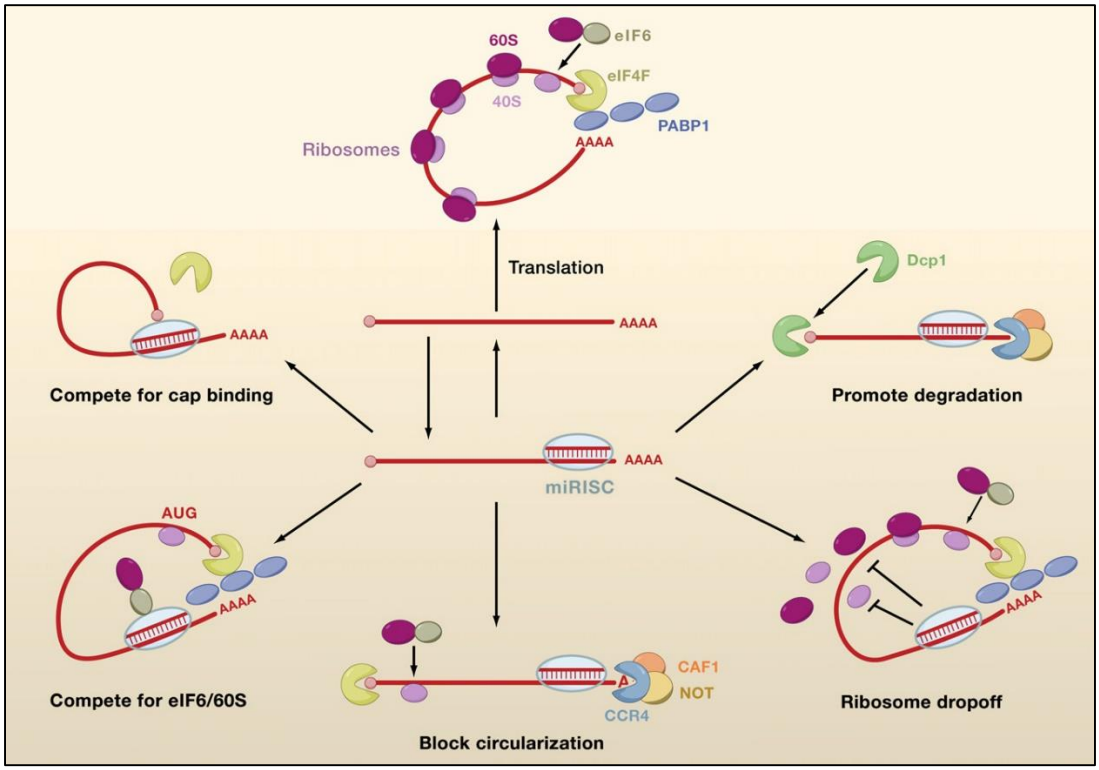

Figure 1-3 Possible mechanisms of miRNAs-mediated translational repression.
A schematic showing the published molecular models of miRNAs-mediated translational repression. eIF4F/ eIF6, initiation factors; Dcp1, mRNA-decapping enzyme 1A; PABP1, polyadenylate-binding protein 1; CAF1-CCR4-NOT, deadenylase complex. (Adapted from Carthew and Sontheimer, 2009)

1.3.2 Biological functions of lncRNAs

Various lncRNAs have been shown to modulate gene expression with diverse mechanisms. First, the transcription of lncRNAs can regulate the neighboring gene expression through transcription interference (TI) (Batista and Chang, 2013). TI was specifically defined as the suppressive influence of one transcriptional process, directly and *in cis* on a second transcriptional process (Mazo et al., 2007; Shearwin et al., 2005). As shown in Figure 1-4, several promoter arrangements can lead to TI. However, the mechanisms of TI are still unclear. Based on published evidence, there have been five

possible mechanisms by which TI can occur (Figure 1-5). For convergent promoters, all five mechanisms are possible. When the promoters are arranged in tandem, all mechanisms except the collision (Figure 1-5d) can apply. For overlapping promoters divergently arranged promoters, only the promoter competition (Figure 1-5a) mechanism can apply (Batista and Chang, 2013; Mazo et al., 2007; Shearwin et al., 2005).

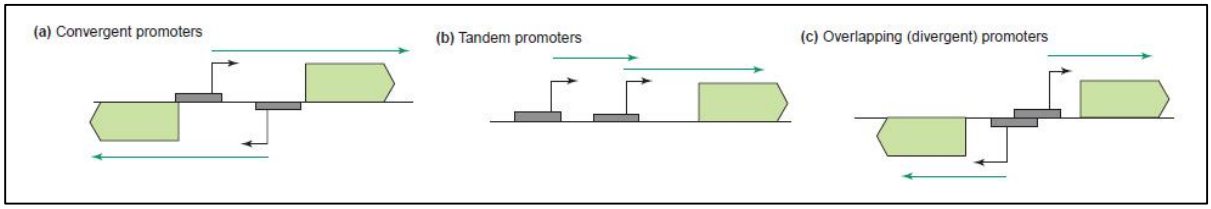

Figure 1-4 Promoter arrangements that can lead to transcriptional interference (TI).
TI can be triggered by several different promoter arrangements: (a) convergent promoters; (b) tandem promoters; (c) overlapping (divergent) promoters. RNA polymerase binding sites are indicated by grey boxes, the transcription start sites are shown as black arrows and transcripts as green arrows. (Adapted from Shearwin et al., 2005)

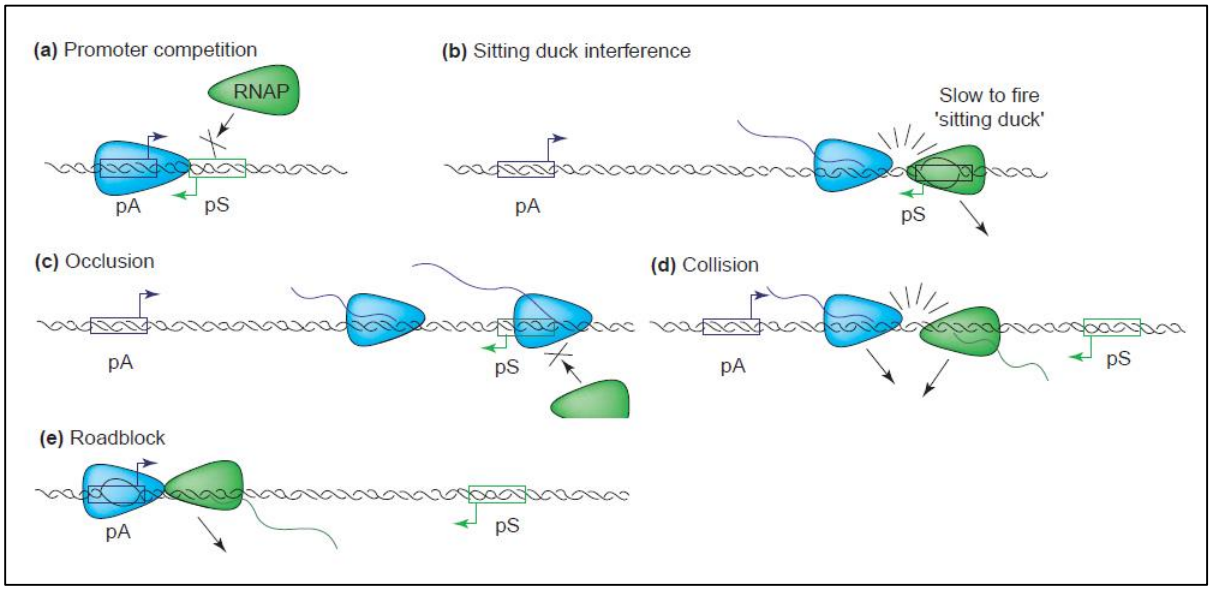

Figure 1-5 Mechanism of transcriptional interference.
Five possible mechanisms of TI: (a) promoter competition; (b) sitting duck interference; (c) occlusion; (d) collision; (e) roadblock. pA, a strong (aggressive) promoter; pS, a week (sensitive) promoter. (Adapted from Shearwin et al., 2005)

In addition, lncRNAs can interact with protein partners to acquire regulatory capacities. In spite of limited characterized examples, several mechanistic themes of lncRNAs' functions have emerged (Rinn and Chang, 2012). As shown in Figure 1-6, there are four types of mechanisms: I, as "Signals", lncRNAs expression can indicate specific gene regulation in space and time through reflecting the combinatorial actions of transcription factors or signaling pathways; II, as "Decoy", lncRNAs can titrate of the available transcription factors, protein factors, or miRNAs from their targets; III, as "Guide", lncRNAs can recruit chromatin-modifying enzyme to target genes *in cis* or *in trans*; IV, as "Scaffolds", lncRNAs can function as adaptors to bring multiple proteins together to form ribonucleoprotein complexes, which can act on chromatin to modify histone, or stabilize nuclear structures/ signaling complexes (Batista and Chang, 2013; Mercer et al., 2009; Nolan and Cogoni, 2004; Rinn and Chang, 2012; Wang and Chang, 2011).

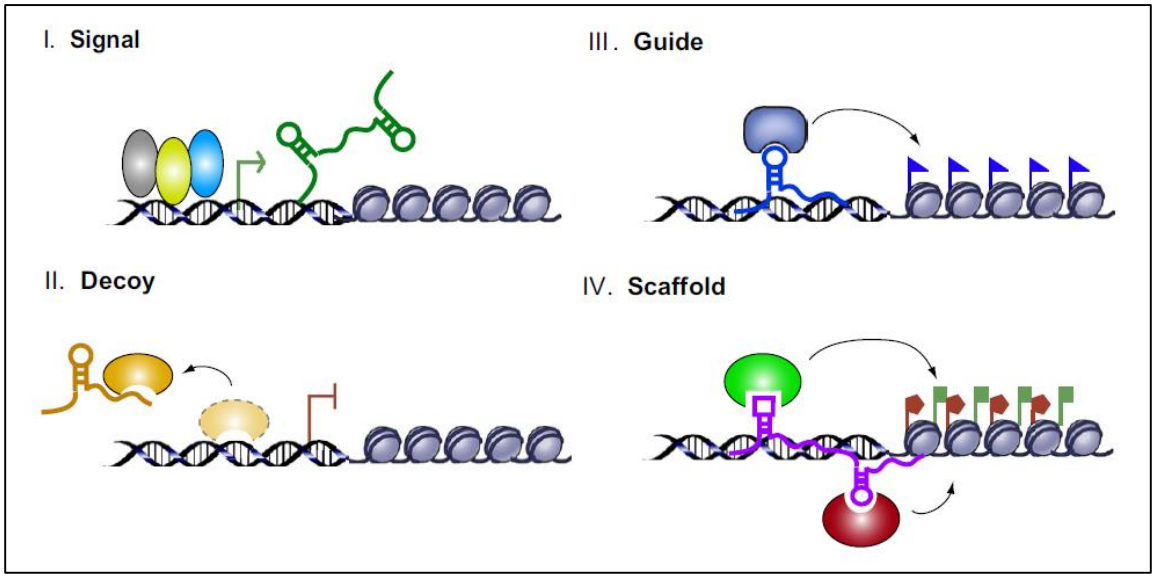

Figure 1-6 Models of lncRNA mechanisms of action.
Schematic diagram showing the four types of lncRNAs' function: I, Signal; II, Guide; III, Decoy; IV, Scaffold. (Adapted from Wang and Chang, 2011)

1.4 ncRNAs in *Neurospora crassa*

The filamentous fungus *Neurospora crassa* is one of the first model organisms used to study sRNAs-mediated gene silencing (Cogoni and Macino, 1999; Li et al., 2010; Romano and Macino, 1992). Due to its advantages in genetics and biochemistry studies, *Neurospora* has made fundamental contributions to the understanding of sRNAs-mediated gene silencing in eukaryotes. It has been known that sRNAs function in genomic surveillance, viral defense, and gene regulation (Dang et al., 2011) (Figure 1-7). In addition, natural antisense RNAs were found to be extensively expressed in *Neurospora* (unpublished data from N. Louise Glass Lab).

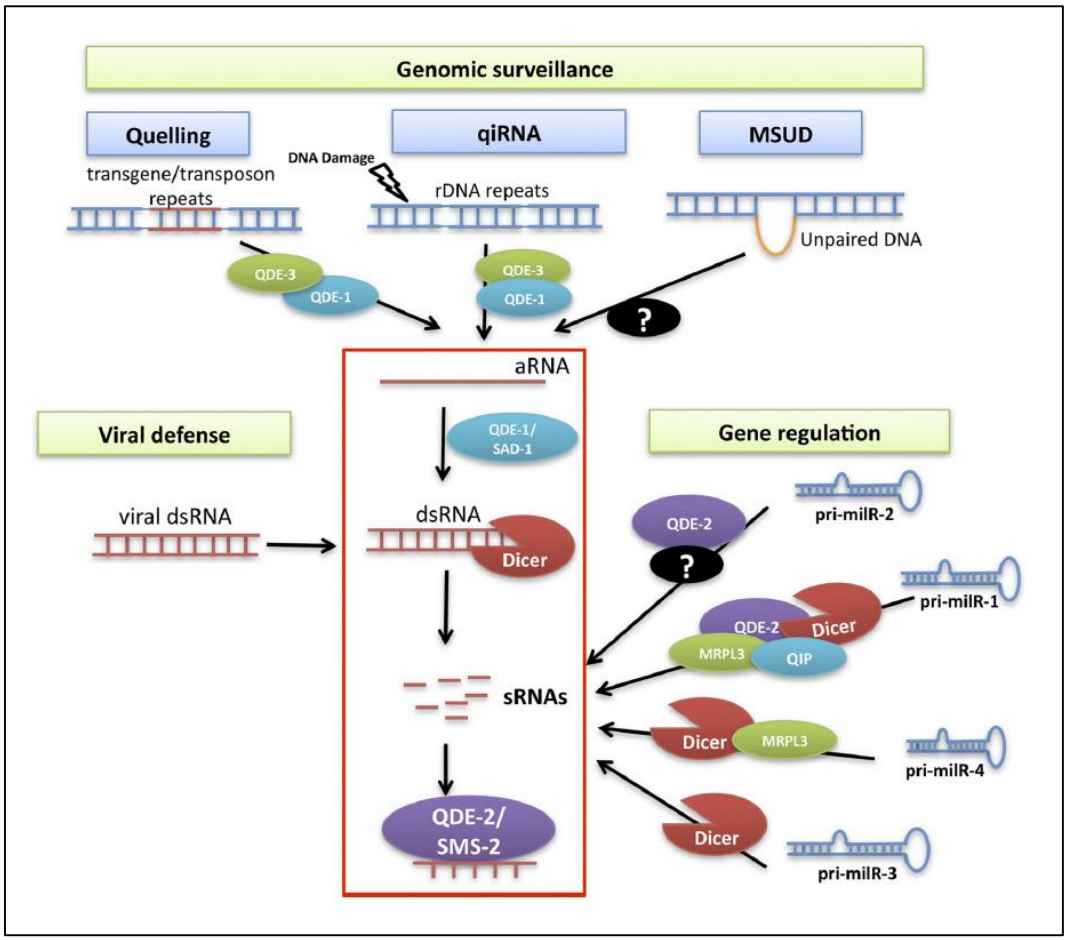

Figure 1-7 Biogenesis mechanisms and functions of sRNAs in *Neurospora*.
Schematic diagram showing the sRNAs' biogenesis mechanisms and functions in *Neurospora*. See text for details. (Adapted from Dang et al., 2011)

1.4.1 Quelling

In 1992, when Macino and his colleague transformed multiple copies of the gene responsible for the orange pigment biosynthesis into *Neurospora*, they obtained, unexpectedly, some pale yellow/ white transformants with decreased mRNA levels of the transformed gene. This phenomenon was named as quelling (Romano and Macino, 1992). Later, it was found that introduction of repetitive DNA sequences or dsRNAs triggers post-transcriptional gene silencing of all homologous genes. Forward and reverse genetic screenings identified several key genes required quelling: *quelling-deficient 1* (*qde-1*), *quelling-deficient 2* (*qde-2*), *quelling-deficient 3* (*qde-3*) and Dicer protein genes *dcl-1* and *dcl-2*. As shown in Figure 1-7, QDE-1 (a RdRP) and QDE-3 (a RecQ DNA helicase) function upstream of sRNAs biogenesis and are required for the generation of transgene/ transposon-specific aberrant RNAs (aRNAs). Afterwards, QDE1 uses single-stranded aRNAs as template to generate the dsRNAs, which are then recognized and processed by DCL-2/ DCL-1 (DCL-2 is responsible for 90% dicer activity) to produce the sRNAs. Subsequently, these sRNAs are loaded onto QDE-2 (an Argonaute protein) to mediate the post-transcriptional gene silencing (Borkovich et al., 2004; Fulci and Macino, 2007; Pickford and Cogoni, 2003).

1.4. 2 Meiotic silencing of unpaired DNA (MSUD)

MSUD is sRNAs-mediated gene silencing phenomenon that can silence unpaired DNA during the sexual cycle in *Neurospora* (Borkovich et al., 2004). Like quelling, aberrant RNAs from unpaired DNA are first generated by unknown mechanisms (Figure 1-7). Then, SAD-1 (a putative RdRP homologous to QDE-1) produces dsRNAs from these aRNAs. In MSUD, only DCL-1 can recognize and process the dsRNAs to generate the sRNAs. Finally, SMS-2 (an Argonaute protein homologous to QDE-2) binds these sRNAs to trigger posttranscriptional silencing of unpaired DNA regions (Borkovich et al., 2004; Li et al., 2010). The ability of MSUD to detect and silence transcription from unpaired DNA helps the genomic surveillance against genomic rearrangement, including deletions, duplications, and translocations in the sexual cycle (Dang et al., 2011).

1.4. 3 DNA damage-induced qiRNA

In 2009, our lab reported that DNA damage can induce the expression of QDE-2 and the production of small RNAs. Analyses of the QDE-2-associated sRNAs uncovered a new class of sRNAs, named as qiRNAs (QDE-2-interacting sRNAs). qiRNAs are about 20~21 nt in size with a strong preference of uridine at the 5' end. Interestingly, qiRNAs are mostly derived from ribosomal DNA locus. Genetic and biochemical analysis showed that the production of qiRNAs requires QDE-1, QDE-3, and DCL-1/2 (Figure 1-7). Similar to quelling, QDE-1 and QDE-3 are indispensable for the generation of DNA-damage-induced aRNAs, the precursors of qiRNAs. Furthermore, *qde-1* and *dcl* mutants showed increased sensitivity to DNA damage, indicating that qiRNAs may act to inhibit protein translation in response to DNA damage (Lee et al., 2009).

1.4. 4 miRNA-like sRNAs (milRNAs) and Dicer-independent small interfering RNAs (disiRNAs)

By analyzing QDE-2-associated sRNAs by deep sequencing, milRNAs and disiRNAs were identified from *Neurospora* in 2010 (Lee et al., 2010). Like canonical miRNAs, milRNAs predominantly originate from one strand of hairpin-like ssRNA precursors with strong preference of uridine at their 5' end. Surprisingly, milRNAs are generated with diverse biogenesis mechanisms. Studies of four most abundant milRNAs uncovered four different mechanisms, which use a distinct combination of factors, including Dicer, QDE-2, QIP (a putative exonuclease; interact with QDE-2) and MRPL3 (a putative RNaseIII domain-containing protein) (Figure 1-7) (Lee et al., 2010; Maiti et al., 2007). Additionally, the mRNA levels of the predicted milRNA target genes are up-regulated in *dcl* mutant, and QDE-2 was detected to specifically associate with the predicted milRNA target mRNAs (Lee et al., 2010). However, the physiological importance of milRNAs is still unclear. disiRNAs are about 22nt in size with a strong preference of uridine at 5' end, and are symmetrically arise from Watson and Crick strands of DNA. Importantly, disiRNAs' biogenesis was found to be independent of any known component for sRNAs production in *Neurospora*, including Dicers, indicating a completely unknown sRNA biogenesis pathway. disiRNAs appear to be derived from loci with overlapping sense and antisense transcripts (Lee et al., 2010). In addition, disiRNAs loci are associated with dynamic DNA methylation that is triggered by convergent transcription (Dang et al., 2013).

1.4. 5 Natural antisense RNAs

By analyzing polyadenylated ends of mRNAs from *Neurospora* with deep sequencing, 200 genes (accounted for about 2% of all mRNAs in *Neurospora* genome) were identified with antisense transcripts (unpublished data from N. Louise Glass Lab). In addition, a natural antisense transcript of *Neurospora frequency* (*frq*) gene (encodes a core component of the *Neurospora* circadian oscillator) was reported in 2003, named as *qrf* (Kramer et al., 2003). The transcript of *qrf*, a long non-coding RNA, is light induced and its levels oscillate in antiphase to *frq* sense RNA in the dark. In the mutant in which the light-induced *qrf* RNA is abolished, the time of the internal clock is delayed, and light-induced clock resetting is altered. In insects and mammals, *period* (*per*) genes encode for proteins with similar functions FRQ in circadian clocks. It was reported that both *per* of silkmoth and *mPer2* of mice also have an antisense RNA cycling in antiphase to the sense RNA (Koike et al., 2012; Sauman and Reppert, 1996; Vollmers et al., 2012). These results suggest that the regulation of the core clock protein expression by antisense RNA is a shared mechanism in eukaryotic circadian systems. But the function and the mechanism of the antisense RNA are unclear.

1.5 Summary

Argonaute proteins are required for the biogenesis of some sRNAs, including piRNAs and some miRNAs (Thomson and Lin, 2009; Yang and Lai, 2011). How Argonautes mediate maturation of sRNAs independent of their slicer activity is not clear. The maturation of milR-1 requires the Argonaute protein QDE-2, Dicer and QIP (Lee et al., 2010). In Chapter Two, I will describe our efforts to reconstitute *in vitro* the Argonaute-dependent milR-1 biogenesis

pathway from primary milR-1 precursor (pri-milR-1) to mature milR-1 using recombinant proteins. Our results establish the biochemical framework of an Argonaute-dependent sRNA biogenesis pathway.

Natural antisense RNAs are widely found in eukaryotic organisms and have been implicated in clock-gene regulation. The physiological importance of antisense RNAs and how they regulate sense RNAs are not clear. In Chapter Three, I will describe how the natural antisense RNA of *frq* regulates circadian rhythmicity. Our results demonstrate antisense transcription as an essential feature in a eukaryotic circadian system and shed light on the importance and mechanism of antisense RNA action.

CHAPTER TWO

BIOCHEMICAL RECONSTITUTION OF AN ARGONAUTE-DEPENDENT SMALL RNA BIOGENESIS PATHWAY

2.1 Introduction

RNA interference (RNAi) is a conserved regulatory mechanism from fungi to mammals in which sRNAs mediate post-transcriptional or transcriptional gene silencing (Ambros, 2004; Buhler and Moazed, 2007; Ghildiyal and Zamore, 2009; Hannon, 2002). A common theme among all known RNAi pathways is that the single-stranded sRNAs guide Argonaute family proteins to RNA targets to regulate gene expression. Argonaute proteins, the core component of all known RNAi pathways, function either by directly slicing their RNA targets or by mediating RNA degradation and translational repression. Since the discovery of the first small RNA in *C. elegans*, various types of sRNAs (with sizes ranging from 20-30 nt), including miRNAs, siRNAs, and piRNAs, have been discovered in animals, plants, and fungi (Ghildiyal and Zamore, 2009; Kim et al., 2009; Lee et al., 1993).

Although most known types of sRNAs are products of Dicer cleavage of double-stranded RNA precursors, piRNAs are produced independently of Dicer. Biogenesis of piRNAs is dependent on the PIWI proteins, and these sRNAs arise from long single-stranded RNA precursors. Although secondary piRNAs are known to be produced by a ping-pong amplification mechanism via the slicer activity of PIWI-related proteins

(Figure 1-1) (Brennecke et al., 2007; Gunawardane et al., 2007; Li et al., 2009; Malone et al., 2009), how primary piRNAs are produced from their RNA precursors and how PIWI proteins mediate such a process are not clear. Recently, a study using a cell-free system led to the proposal of a 3' end trimming model for piRNA maturation (Kawaoka et al., 2011). In this model, PIWI protein binds the single-stranded piRNA precursors which are then 3' to 5' trimmed into maturation by an exonuclease (Figure 2-1A). Whether this proposed mechanism occurs in vivo and the identity of the exonuclease are not known. Like piRNAs, the Dicer-independent primal RNAs in fission yeast are also dependent on an Argonaute protein for accumulation (Halic and Moazed, 2010).

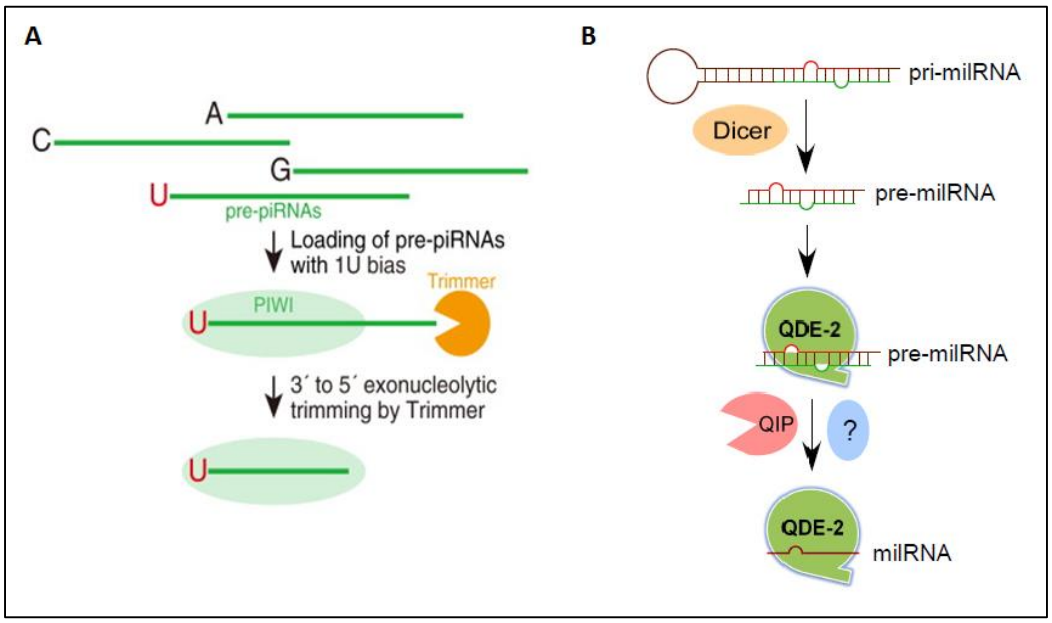

Figure 2-1 Models of piRNAs and milR-1 biogenesis pathway.

(A) A 3' end trimming model for piRNA maturation. Pre-piRNAs are first loaded onto Piwi protein with 1U bias, which are then trimmed to 27~28 nt by 3' to 5' exonucleolytic trimmer. (Adapted from Kawaoka et al., 2011) (B) A model of the milR-1 biogenesis pathway showing that the production of milR-1 requires Dicer, Argonaute protein QDE-2, and the putative exonuclease QIP.

As a filamentous fungus, Neurospora has a remarkable reservoir of sRNAs that are made by diverse biogenesis pathways (Li et al., 2010). We previously discovered the existence of milRNAs in this organism and found that milRNAs are produced through at least four different pathways (Lee et al., 2010). milR-1 is the most abundant milRNA-producing loci in the Neurospora genome; the maturation of milR-1 milRNAs requires the Argonaute protein QDE-2 but not its slicer activity. In addition, the production of milR-1 milRNAs also requires Dicer and a putative nuclease QIP. Dicer is required for the generation of milR-1 pre-milRNAs (pre-milR-1) from primary-milR-1 (pri-milR-1). In a *dicer* mutant, the pre-milR-1 and mature single-stranded milR-1 are not observed, and pri-milR-1 accumulates to high levels, suggesting that pri-milR-1 is cleaved by Dicer to generate double-stranded pre-milR-1. QIP was previously identified as a QDE-2-interacting protein and is important for siRNA RISC activation by removing the nicked siRNA passenger strand from the QDE-2-bound siRNA complex (Maiti et al., 2007). In the *qip* mutant, the mature milR-1 is abolished, but pre-milRNAs are maintained, indicating that QIP is required for the maturation of milR-1 milRNAs (Lee et al., 2010). These results led us to propose a model in which the QDE-2 Argonaute binds to pre-milRNAs and recruits one or more trimmer enzymes to process the pre-milRNAs into mature milRNAs by 3'-5' trimming (Figure 2-1B). This model is very similar to that of the recently proposed piRNA maturation model (Kawaoka et al., 2011).

In this study, we reconstituted in vitro the Argonaute-dependent milR-1 biogenesis pathway from pri-milRNA to mature milRNAs by using recombinant proteins. In addition to QIP, we identified the RNA exosome, a 3' to 5' exonuclease complex, as a

trimmer that is essential for milR-1 maturation. Together, our results establish the biochemical framework of an Argonaute-dependent sRNA biogenesis pathway and demonstrate the important roles of exosome in small RNA processing and degradation.

2.2 Materials and Methods

2.2.1 Strains and growth conditions

The wild-type strain (FGSC 4200) was used in this study. Mutant strains including *qde-2*^{RIP}, *qip*^{KO}, and *qde-2*^{RIP}*qip*^{KO} were generated in a previous study (Maiti et al., 2007). *qip*^{KO}, Myc-QDE-2 was generated by introducing a plasmid expressing Myc-QDE-2 into the *qip*^{KO} strain. The *qip*^{KO},QIP^{CD} and *qde-2*^{RIP}, *qip*^{KO},QIP^{CD} strains were generated by introduction of a plasmid expressing Myc-QIP (H504A;D509A) into *qip*^{KO} and *qde-2*^{RIP},*qip*^{KO} strains, respectively. The *rrp6*^{KO} mutant (FGSC# 16058, NCU02256.5) was obtained from the Fungal Genetic Stock Center (FGSC). The gene knockdown strains, including *dsfrh*, *dsrrp44*, *dsrrp4*, and *dsmtr3*, were generated as described in previous studies by introducing a construct that can inducibly express dsRNA specific for the gene of interest into a wild-type strain at the *his-3* locus (Cheng et al., 2005; Guo et al., 2009). The *qip*^{KO},*dsfrh* strain was generated previously by introduction of a plasmid expressing a *frh*-specific dsRNA into the *qip*^{KO} strain (Maiti et al., 2007). The *al-2* (quelled) *dsrrp44* strain was generated by co-transformation of plasmid containing *al-2* gene (kindly provided by Dr. Oded Yarden) and a plasmid containing hygromycin-resistant gene into a *dsrrp44* strain. The RRP46-TAP strain (YSB239, MATa *ade2-1 his3-11,5 leu2-3,112*

trp1-1 ura3-1 RRP46-TAP pep4::HIS3 rrp6::LEU2) was a generous gift from Dr. J. Scott Butler's laboratory.

Liquid cultures were grown in minimal medium (1x Vogel's, 2% glucose) at room temperature (Davis and deSerres, 1970). For liquid cultures containing quinic acid (QA), 0.01 M QA (pH 5.8) was added to the liquid culture medium containing 1x Vogel's, 0.1% glucose, and 0.17% arginine.

2.2.2 Purification of recombinant DCL-2, QIP, QDE-2 and exosome core complex

Polyhistidine-tagged recombinant proteins were expressed in *Sf9* insect cells using the BAC-to-BAC baculovirus expression system from Invitrogen. *Sf9* insect cells were infected with individual His-DCL-2, His-QIP, and His-QIPCD viruses. After 48 hours, the infected cells were harvested, washed in PBS, and resuspended in buffer A (10 mM potassium acetate, 10 mM HEPES (pH 7.4), 2 mM magnesium acetate, 5 mM β-mercaptoethanol) containing 10 mM imidazole. Cells were then lysed by sonication, and His-tag proteins were bound to TALON metal affinity resin according to the manufacturer's instructions (Clontech). After a 15 mM imidazole wash, the His-tagged proteins were eluted in buffer A containing 150 mM imidazole. His-QIP and His-QIPCD were further purified by Q-Sepharose chromatography. The His-tagged proteins were dialyzed in buffer A containing 20% glycerol, and then stored in aliquots at –80 degree.

To produce the MBP-QDE-2, full-length QDE-2 cDNA was subcloned into a pMAL-c2x expression vector (New England Biolabs). MBP-QDE-2 was expressed in BL21 (DE3) cells and purified using the pMAL™ Protein Fusion and Purification

System (NEB) according to the manufacturer's instructions. MBP-QDE-2 was further purified by Superdex-200 chromatography. After chromatography, MBP-QDE-2 was dialyzed in buffer A containing 20% glycerol, and then stored in aliquots at –80 degree.

The exosome core complex was purified as previously described (Callahan and Butler, 2010) except that the purified proteins were dialyzed in buffer A containing 20% glycerol, and then stored in aliquots at –80 degree.

2.2.3 Dicer assay

Uniformly radiolabeled dsRNA or pri-milR-1 substrates were prepared and the Dicer reactions carried out essentially as previously described (Bernstein et al., 2001; Elbashir et al., 2001). The *al-2* gene was used as the template for T7 in vitro transcription. Briefly, in a 10 μl reaction, 105 cpm [^{32}P]-labeled RNA substrate and 1 mM ATP were incubated with different amounts of His-DCL-2 in buffer (100 mM potassium acetate, 10 mM HEPES (pH 7.4), 1 mM magnesium acetate) for 30 minutes at 30 ℃. For dsRNA substrates, 14 ng, 54 ng, 136 ng, and 1.36 μg His-DCL-2 was used. For pri-milR-1a substrates, 0.68 μg, 1.36 μg, and 4.98 μg His-DCL-2 was used. The products were resolved on 16% denaturing or native polyacrylamide gels, and gels were exposed to X-ray film.

2.2.4 Northern blot analysis

Small RNAs were separated on 16% denaturing or native polyacrylamide gels and transferred onto a Hybond-NX membrane (GE Healthcare). Crosslinking of RNA to

Hybond-NX was performed as described (Pall et al., 2007). Northern blots were carried out as previously described (Lee et al., 2010).

2.2.5 Exonuclease processing assay

Single-stranded RNA oligos were synthesized by Sigma and radiolabeled at their 5' ends by T4 polynucleotide kinase (New England Biolabs). For 3' end labeling, RNA oligos were radiolabled at their 3'ends by T4 RNA ligase with ^{32}pCp (New England Biolabs). The sequences of RNA oligos are as follows:

let-7	UGAGGUAGUAGGUUGUAUAGUU
let-7 antisense	CUAUACAACCUACUACCUCAUU
let-7 star	CUAUACAAUCUACUGUCUUUC
pre-milR-1	UAAGCCGCGAGUACGCCUCCGGACUGUAACUUU
pre-milR-1 30	UAAGCCGCGAGUACGCCUCCGGACUGUAAC
pre-milR-1 27	UAAGCCGCGAGUACGCCUCCGGACUGU
pre-milR-1 25	UAAGCCGCGAGUACGCCUCCGGACU
pre-milR-1 22	UAAGCCGCGAGUACGCCUCCGGACUGUAACUUU
pre-milR-1 star	GGUUACAGCCCCCGGGACGCACUACGGUUUAUA

In a 10 μl reaction, 105 cpm [32P]-labeled RNA substrate and 1 mM ATP were incubated with 0.5 μg His-QIP or His-QIPCD in buffer X1 (10 mM Tris-HCl (pH 7.4), 12.5 mM potassium acetate, 5 mM magnesium acetate, 1 mM DTT) for 30 minutes at 30℃. The reaction was stopped as described (Bernstein et al., 2001; Elbashir et al., 2001). The products were resolved on 20% denaturing polyacrylamide gels, and gels were exposed to X-ray film.

2.2.6 Small RNA immunoprecipitation

Immunopurification of the Myc-QDE-2 ribonucleoprotein complex was performed as previously described (Maiti et al., 2007) except that beads were washed with buffer X1 instead of the extraction buffer.

2.2.7 Co-Immunoprecipitation

Co-immunoprecipitation was performed as previously described (Cheng et al., 2005) with the following modifications: Before adding FRH antibody into the protein solution, 100 μl 20 mM DTSSP solution (Thermo #21578) was added to 1 ml protein solution (at 1 mg/ml). The reaction was quenched with 20 μl 1 M Tris solution after a 4-hour incubation at 4 ℃.

2.2.8 siRNA-initiated RISC assay

The single-stranded let-7 was used as the guide strand to perform the siRNA-initiated RISC assay previously described (Liu et al., 2003). The mRNA substrate containing one let-7 target site was prepared as described (Liu et al., 2003). The template for mRNA substrate T7 in vitro transcription was kindly provided by Dr. Qinghua Liu.

2.2.9 Exosome processing assay

The exosome processing assay was performed using the procedure described for the exonuclease processing assay except that MBP-QDE-2 was incubated with [^{32}P]-labeled RNA substrate and 1 mM ATP in buffer X1 for 30 minutes at 30 ℃, and then exosome was added to the reaction for 30 minutes at 30 ℃.

2.3 Results

2.3.1 The Neurospora Dicer-2 generates pre-milR-1 from pri-milRNA

The QDE-2-dependent milR-1 milRNAs are the most abundant milRNAs in *Neurospora* under normal growth conditions (Lee et al., 2010). The production of mature single-stranded milR-1 milRNAs requires Dicer, QDE-2, and the putative exonuclease QIP (Figure 2-1A). The 170-nt pri-milRNA of milR-1 is predicted to form a long stem-loop structure with milR-1 and milR-1* sequences located near the bottom of the stem structure. In the dicer (*dcl-1/dcl-2*) double mutant, the milR-1 pri-milRNA accumulates to high levels and the production of pre-milRNAs and the milRNAs is completely abolished (Lee et al., 2010), suggesting that Dicer is responsible for the generation of pre-milRNAs from pri-miRNAs. To demonstrate that Dicer can directly produce pre-milRNA of milR-1 from pri-milRNA, we expressed and purified the full-length recombinant *Neurospora* DCL-2 (His-DCL-2), which is responsible for more than 90% of the Neurospora Dicer activity (Catalanotto et al., 2004), from *Sf9* cells (Figure 2-2A). As expected, the recombinant DCL-2 generated siRNAs around 24-25nt from a long double-stranded RNA substrate (Figure 2-2B), consistent with the previous result using *Neurospora* extracts (Catalanotto et al., 2004). To examine the activity of the recombinant DCL-2 on milR-1 pri-milRNA, we synthesized the full-length pri-milRNA *in vitro*. As shown in Figure 2-2C, the treatment of pri-milRNA with DCL-2 resulted in the production of small RNAs of the same size as the synthesized 33-nt pre-milR-1, the precursor of mature milRNAs. The DCL-2 generated pre-milRNA is double stranded as

indicated by its mobility in a native gel (Figure 2-2C, the bottom panel). This result demonstrates that DCL-2 can directly generate the precursor of milRNA by cleaving the loop structure from the milR-1 pri-milRNA.

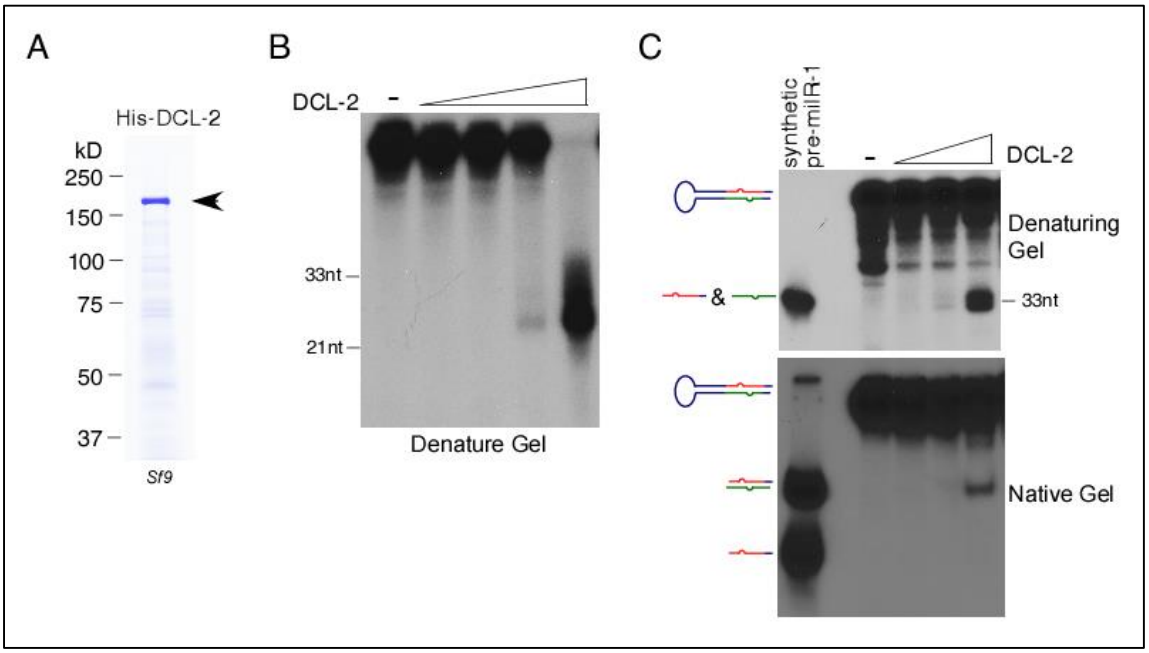

Figure 2-2 Recombinant DCL-2 processes pri-milR-1 into pre-milR-1 *in vitro*.
(A) The coomassie blue stained SDS-PAGE gel showing the purified His-DCL-2 from *Sf9* cells; (B) Dicer assay using radiolabeled dsRNA as the substrate; (C) Dicer assay using radiolabeled pri-milR-1 as the substrate.

2.3.2 QIP is a 3'-5' exonuclease in vitro

Northern blot analysis using a probe specific for milR-1 milRNAs previously showed that there are two double-stranded pre-milR-1 species (pre-milR-1 and pre-milR-1') (Lee et al., 2010). In agreement with our previous results, the mature single-stranded milRNA species, but not the pre-milR-1, are abolished in the *qde-2*^{RIP} and *qip*^{KO} mutants (Figure 2-3A), indicating that both QDE-2 and QIP function downstream of the pre-miRNA generation and are required for milRNA maturation. In addition, the levels of

pre-milR-1, but not pre-milR-1', were increased in both *qde-2* and *qip* mutants, suggesting that pre-milR-1 is processed by QDE-2 and QIP to generate mature milRNAs. Consistent with this notion, pre-milR-1, but not pre-milR-1', specifically associates with QDE-2 (Lee et al., 2010).

Our previous bioinformatics analysis showed that QIP contains a putative 3'-5' exonuclease domain that belongs to the DEDDh superfamily of 3'-5' exonucleases (Maiti et al., 2007). The role of QIP in milR-1 maturation and its interaction with QDE-2 are consistent with its role as an exonuclease that trims the pre-milR-1 from the 3'ends. To directly test this hypothesis, we expressed and purified the recombinant, His-tagged wild-type QIP and QIP with its predicted catalytic sites mutated (QIP^{CD}) from *Sf9* cells (Figure 2-3B). Using various 21-nt, 5' end labeled, single-stranded human let-7 miRNAs as substrates, we showed that the recombinant QIP could generate a ladder of smaller RNA products (Figure 2-3C). This activity was not observed with the catalytically dead QIP. These results demonstrate that QIP is indeed a nuclease that cleaves short single-stranded sRNAs.

To demonstrate that QIP is a 3' to 5' exonuclease and to understand its substrate requirement for 3'end nucleotide modification, we labeled the single-stranded let-7* RNA at the 3' end by ^{32}pCp to remove its 3'end hydroxyl group. As shown in Figure 2-3D, QIP could efficiently cleave the alkaline phosphatase treated RNA (to create 3' hydroxyl group) but not the untreated RNA. This result indicates that QIP is a 3' to 5' exonuclease that requires 3' hydroxyl group on its RNA substrate.

We then examined the effect of recombinant QIP on the synthetic 33-nt single-stranded pre-milR-1 and pre-milR-1*. Surprisingly, we found that QIP could not efficiently process the pre-milR-1 RNAs in vitro (Figure 2-4A). This result raises the possibility that QIP may prefer short RNA substrates. To test this, we synthesized a series of single-stranded pre-milR-1 of different lengths with 3' end deletions. Although QIP could not efficiently cleave the pre-milR-1 that is larger than 30 nt, it cleaved 22-27 nt pre-milR-1 RNAs efficiently into RNA fragments between 9-15 nt (Figure 2-4B). In addition, the cleavage by QIP was more complete for the 22 and 25 nt pre-milR-1 RNAs than that for the 27 nt RNA. This result suggests QIP prefers shorter RNA substrates. Therefore, if QIP is a nuclease that results in the maturation of milR-1, a hand-over mechanism exists and another nuclease is required for generating shorter pre-milR-1 RNAs as substrates for QIP. In addition, because QIP cleaves RNA substrates into fragments that are much smaller than the mature milR-1, a mechanism must also exist to determine the milR-1sizes.

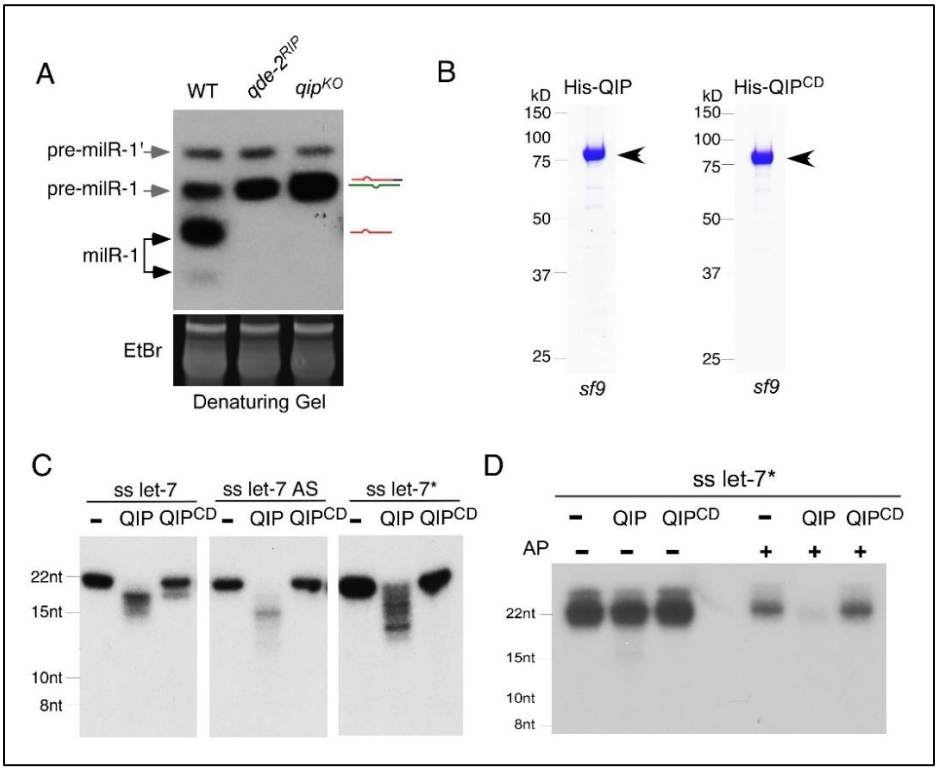

Figure 2-3 QIP is a 3'-5' exonuclease.
(A) Northern blot analysis showing the level of pre-milR-1 and milRNAs in the indicated strains in denaturing gels. The ethidium bromide-stained gel in the bottom panel shows equal loading of RNA samples. (B) The coomassie blue stained SDS-PAGE gel showing purified His-QIP and His-QIP^{CD} from *Sf9* cells. (C) Indicated 5' [^{32}P] radiolabeled synthetic small RNAs incubated with buffer and His-QIP. The products were separated by a denaturing gel. (D) Indicated 3' [^{32}P] radiolabeled synthetic small RNAs were treated with/without alkaline phosphatase (AP) before they were incubated with buffer and His-QIP. The products were separated by a denaturing gel.

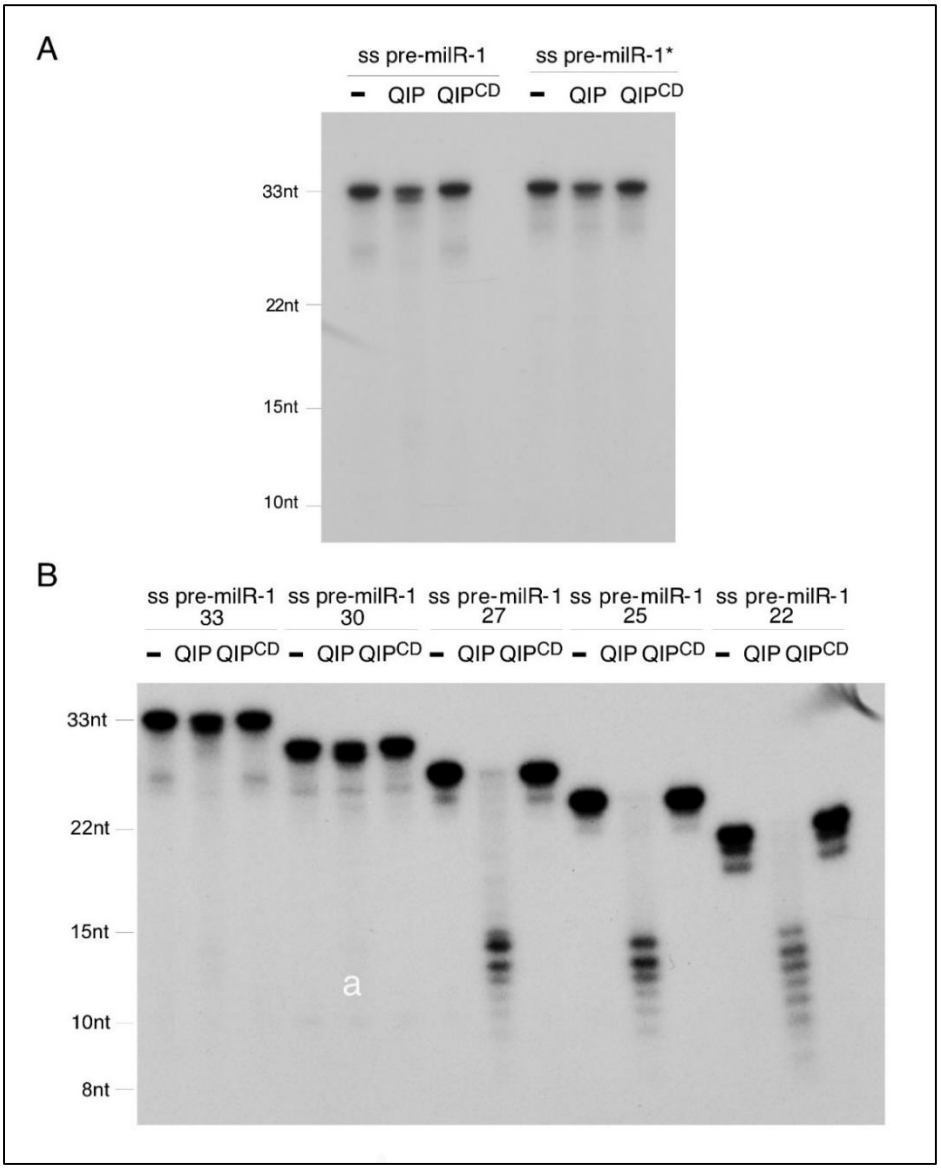

Figure 2-4 QIP prefers short pre-milR-1 as substrates *in vitro*.
(A) Indicated 5' [^{32}P] radiolabeled synthetic small RNAs incubated with buffer and His-QIP. The products were separated by a denaturing gel. (B) Indicated 5' [^{32}P] radiolabeled synthetic pre-milR-1 RNAs were incubated with buffer and His-QIP. The products were separated by a denaturing gel.

2.3.3 Another nuclease can progressively process pre-milR-1 via 3'-5' trimming

To examine whether there is another nuclease that processes pre-milR-1, we compared the milR-1 profile of the wild-type strain and the *qip* mutants. As shown in Figure 2-5A, a faint ladder of sRNAs was observed between the mature milR-1 and the pre-milR-1 in the qip^{KO} and qip^{CD} mutants but not in the wild-type sRNA sample. In addition, the levels of the sRNA ladder and pre-milR-1 were further increased in the qip^{CD} mutant (Figure 2-5A and 2-5B). This ladder of sRNAs was singled-stranded because its gel mobilities did not change after the RNA samples were heat denatured. These results indicate that another *Neurospora* nuclease can progressively processes pre-milR-1 into mature milR-1 independent of QIP, albeit very inefficiently. The accumulation of this small RNA ladder in the *qip* mutants suggests that these sRNAs are substrates of QIP, which prefers smaller RNA substrates. The fact that the ladder of sRNAs accumulated to a higher level in the qip^{CD} mutant than the qip^{CD} mutant suggest that the catalytically dead QIP can protect these small RNAs from being degraded.

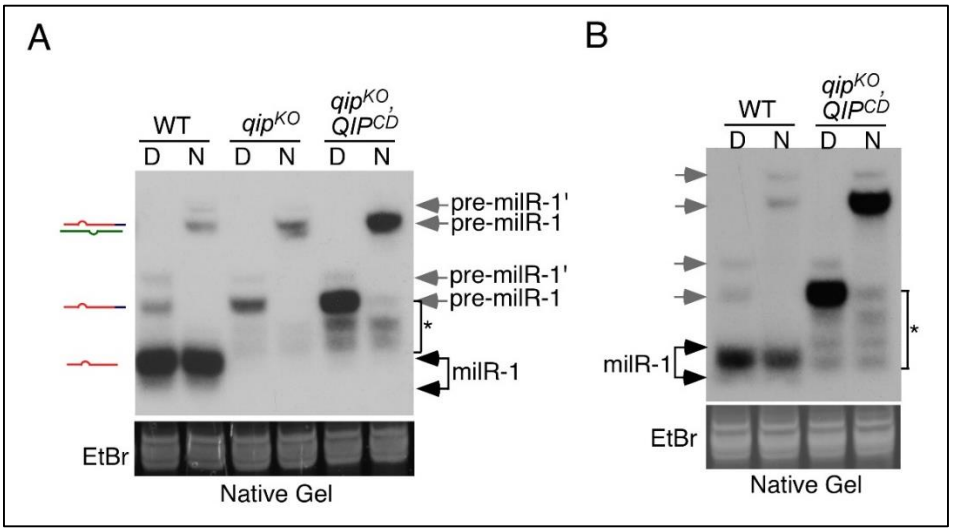

Figure 2-5 A ladder of processed pre-milR-1 is produced independent of QIP.

(A, B) Northern blot analysis of small RNA samples separated on native gels showing the levels of milR-1 pre-milRNAs and milRNAs in the indicated strains. “D” indicates that RNA samples were denatured by boiling. “N” represents native RNA samples.

The generation of the sRNA ladder requires the QDE-2 Argonaute since it was completely absent in the *qde-2*^{RIP} mutant (Figure 2-6A). Furthermore, the sRNA ladder was also abolished in the *qde-2*^{RIP}, *qip*^{KO} double mutants with or without the expression of the catalytic dead form of QIP (Figure 2-6B). These results suggest that in addition to QIP, QDE-2 may recruit another nuclease to progressively process pre-milR-1 to generate the substrates for QIP.

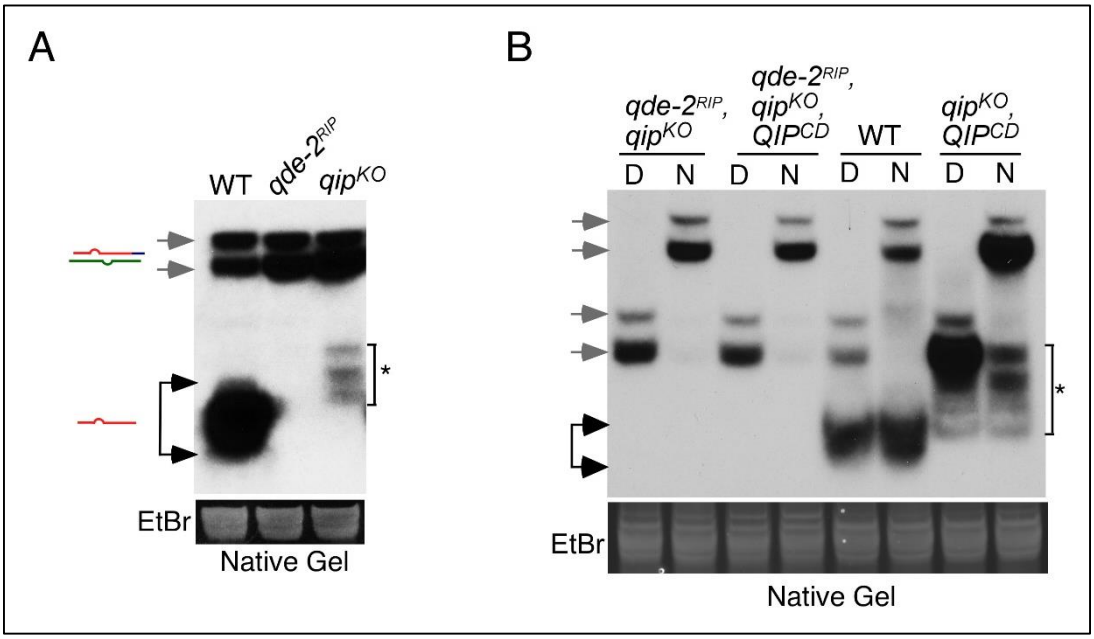

Figure 2-6 QDE-2 is required for the generation of sRNA ladder.
(A, B) Northern blot analysis of small RNA samples separated on native gels showing the levels of milR-1 pre-milRNAs and milRNAs in the indicated strains. “D” indicates that RNA samples were denatured by boiling. “N” represents native RNA samples.

2.3.4 Exosome is required for the maturation of milR-1 milRNAs

To identify the nuclease, we screened various nuclease knock-out mutants available in the Neurospora knock-out library for genes involved in milR-1 production (Colot et al., 2006). Among these mutants, the *rrp6*^{KO} mutant showed a reduced level of mature milR-1 (Figure 2-7A). *rrp6* (NCU02256) encodes the *Neurospora* sequence homolog of the yeast RRP6, which is a component of the exosome complex. The RNA exosome, a highly conserved large complex consisting of several 3' to 5' exonucleases, is a major regulator of RNA (rRNA, mRNA, and noncoding RNA) metabolism as it mediates 3' to 5' RNA processing and degradation (Houseley et al., 2006; LaCava et al., 2005; Vanacova et al., 2005). In the budding yeast, the exosome functions require Mtr4p, which is an essential co-factor of the exosome and part of the TRAMP (Trf4/Air2/Mtr4p Polyadenylation) complex that polyadenylates RNA substrates (Houseley and Tollervey, 2006; LaCava et al., 2005; Vanacova et al., 2005). As in yeast, the knock-out of *rrp6* is not lethal in *Neurospora*, indicating that RRP6 is not essential for exosome functions.

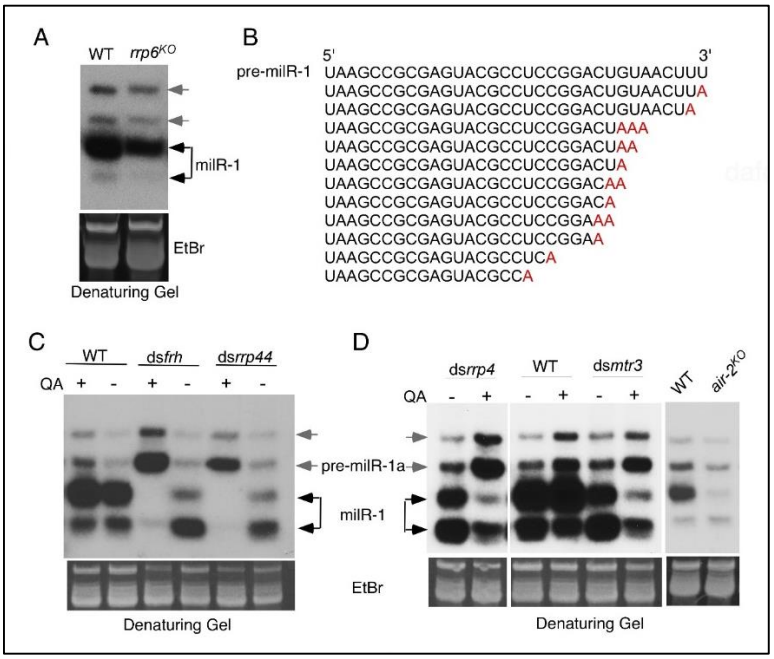

Figure 2-7 The exosome complex is required for milR-1 maturation.
(A) Northern blot analysis of small RNA samples separated in denaturing gels showing the levels of milR-1 pre-milRNAs and milRNAs in the indicated strains. (B) Representative small RNA species with untemplated adenosines identified by Solexa deep sequencing analysis. (C) & (D) Northern blot analysis of small RNA samples separated in denaturing gels showing the levels of milR-1 pre-milRNAs and milRNAs in the indicated strains. *dsfrh* and *dsrrp44* are the dsRNA knockdown strains in which *frh* or *rrp44* dsRNA expression is induced by QA.

We previously performed deep sequencing and 5' RACE experiments on the QDE-2-associated sRNAs (Lee et al., 2010). In our analysis of the milR-1-related sRNA reads, we found that almost all pre-milR-1 and mature milRNA reads shared the same 5' U position, but that their 3'ends were heterogeneous with sizes ranging from ~17 to 33 nt. This observation suggests that pre-milR-1 is subjected to 3'-5' enzymatic trimming. In addition, some of pre-milR-1 and mature milRNA reads had one to three 3' untemplated adenosines (Figure 2-7B). The presence of these untemplated adenosines in the milR-1 pre-milRNA and mature milR-1 reads also suggests that they are exosome substrates.

To demonstrate the role of exosome in milR-1 production, we examined the strains in which the essential Neurospora exosome components were inducibly knocked-down by expression of dsRNA specific for the gene of interest. RRP44 (also called Dis3), a member of the RNase II family, is the core catalytic subunit of the yeast and *Neurospora* exosome complex (Dziembowski et al., 2007; Guo et al., 2009; Schneider et al., 2007). FRH (FRQ-interacting RNA helicase) is the *Neurospora* sequence and functional homolog of the yeast Mtr4p (Cheng et al., 2005; Guo et al., 2009). Long inverted repeats specific for these genes were under the control of quinic acid (QA)-inducible promoter, so that in the presence of QA, the gene of interest was specifically silenced by the

expression of dsRNA (Cheng et al., 2005). As shown in Figure 2-8, the additional QA resulted in dramatic reduction of cell growth of both *dsrrp44* and *dsfrh* strains, indicating the essential roles *rrp44* and *frh* in cell growth. Northern blot analysis showed that the addition of QA resulted in a near complete disappearance of mature milR-1 and a dramatic increase of pre-milR-1 levels in both dsrrp44 and *dsfrh* strains (Figure 2-7C). To further confirm this result, we created two additional strains, *dsrrp4* and *dsmtr3*, in which two other exosome components, *rrp4* and *mtr3*, respectively, can be inducibly knocked-down. As expected, the silencing of *rrp4* and *mtr3* also resulted in the decrease of mature milR-1 and increase of pre-milR-1 levels (Figure 2-7D). In addition, deletion of one of the two of the Neurospora homolog of *air2* (NCU04617) also resulted in a significant reduction of mature milR-1 (Figure 2-7D). Together, these results indicate that exosome is essential for the maturation of milR-1 milRNAs.

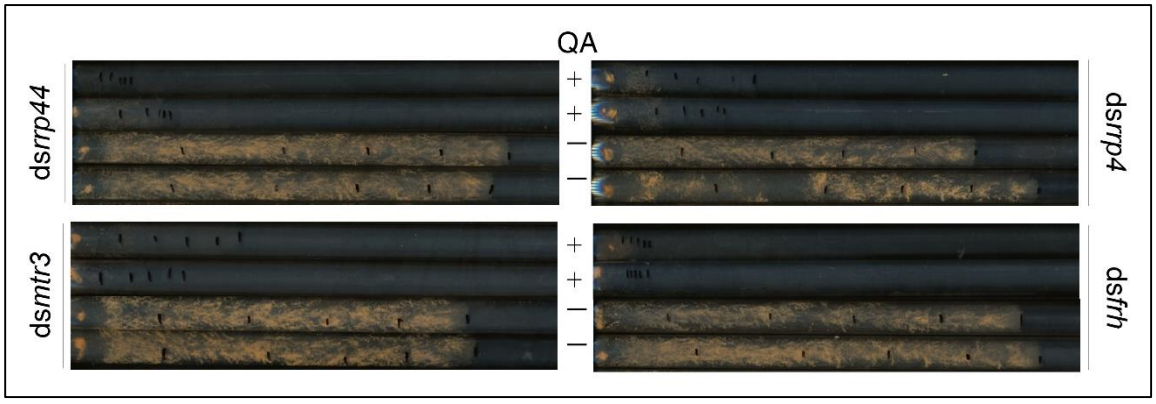

Figure 2-8 Inducible silence of exosome complex components.
Racetube assays showing the growth rates of the indicated strains in the presence or absence of quinic acid (QA).

To examine whether the RNA exosome is responsible for the generation of the single-stranded small RNA ladder seen in the qip^{KO} strains, we compared the milR-1

profiles in the wild-type, *dsfrh*, *dsrrp44*, *qip*^{KO}, and *qip*^{CD} strains. In addition, we also created a *qip*^{KO} strain (*qip*^{KO}, *dsfrh*) in which frh can be inducibly silenced. As shown in Figure 2-9, the silencing of *frh* or *rrp44* abolished the production of the sRNA ladder in the wild-type and *qip*^{KO} strains. These results indicate that exosome is required for processing pre-milR-1 into the single-stranded small RNA ladder seen in the qip mutants.

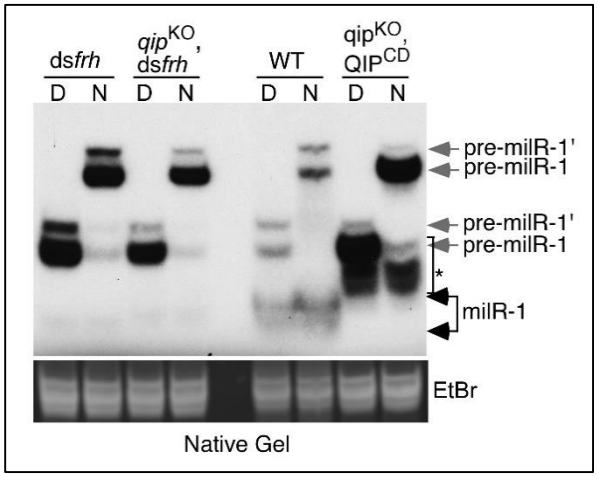

Figure 2-9 The exosome complex is responsible for the generation of the single-stranded pre-milR-1 ladder in the *qip* mutants.
Northern blot analysis of small RNA samples separated in native gels showing the levels of milR-1 pre-milRNAs and milRNAs in the indicated strains. "D" indicates that RNA samples were denatured by boiling. "N" represents native RNA samples.

2.3.5 QDE-2 mediates the processing pre-milR-1 by the exosome

Because of the essential role of the exosome in mediating the QDE-2-dependent milR-1 maturation, we tested whether QDE-2 interacts with exosome *in vivo*. An immunoprecipitation assay using an anti-FRH antibody showed that Myc-QDE-2 co-precipitated with FRH in an RNA-independent manner (Figure 2-10). In addition, we have previously shown that FRH associates with the core exosome components (Guo et al., 2009). These results suggest that QDE-2 recruits the exosome to process pre-milR-1.

To demonstrate the role of exosome in mediating the QDE-2-dependent milR-1 maturation, we expressed and purified the full-length MBP-tagged QDE-2 in *E. coli*

(Figure 2-11A). The budding yeast exosome homoenzyme is currently the only active eukaryotic exosome complex that can be reconstituted *in vitro* (Liu et al., 2006). Therefore, to obtain a functional exosome complex, we purified the budding yeast core exosome complex by tandem-affinity purification using a TAP-tagged RRP46 strain (Callahan and Butler, 2010). To examine whether the recombinant QDE-2 is functional, we performed a RISC assay to examine whether MBP-QDE-2 was able to mediate single-stranded siRNA-dependent RNA cleavage. As shown in Figure 2-11B, like the human Ago2 protein, MBP-QDE-2 sliced the RNA target into the expected size, indicating that MBP-QDE-2 is functional.

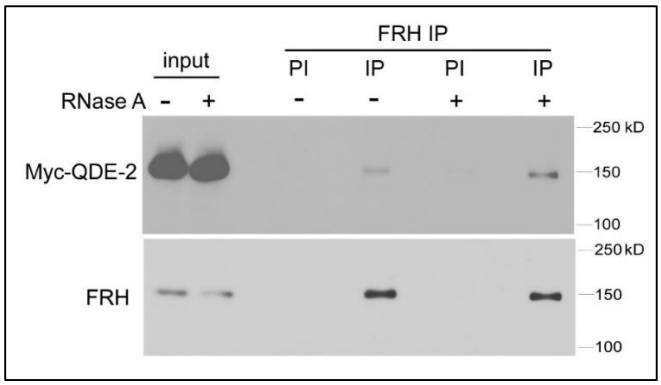

Figure 2-10 QDE-2 interacts with an exosome component. Western blot analysis showing the result of IP with the anti-FRH antibody in the Myc-QDE-2 strain. IP with the FRH pre-immune (PI) serum was used as the negative control.

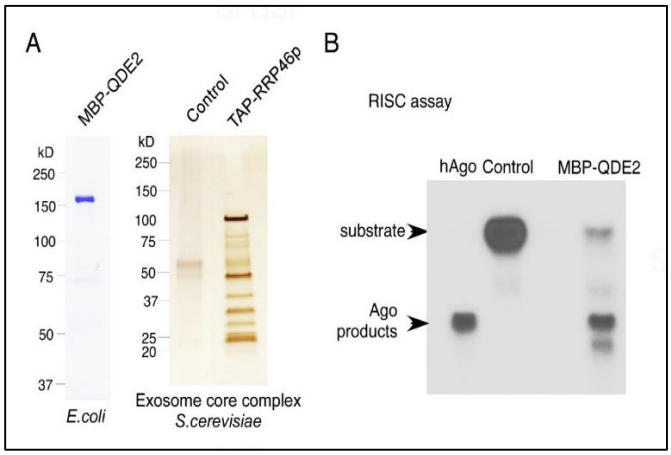

Figure 2-11 QDE-2 mediates single-stranded siRNA-dependent RNA cleavage *in vitro*. (A) The coomassie blue stained SDS-PAGE gel showing purified MBP-QDE-2 from *E. coli*, and the silver stained SDS-PAGE gel showing purified core exosome complex from *S. cerevisiae*. (B) siRNA-initiated RISC assays performed with human Ago2 (hAgo) or MBP-QDE-2.

We then examined whether MBP-QDE-2 facilitated the processing of the single-stranded pre-milR-1 by the exosome. As shown in Figure 2-12, although exosome alone only showed weak processing activity towards the synthetic single-stranded pre-milR-1, the addition of MBP-QDE-2 but not MBP to the exosome dramatically increased the 3'-5' trimming of the pre-milR-1, resulting in a small RNA ladder similar to what we observed in the *qip* mutants. Although the optimal activity of exosome requires is known to require the TRAMP complex (LaCava et al., 2005), this result indicates that QDE-2 can promote the activity of exosome to pre-milR-1. In addition, exosome could not process double-stranded pre-milR-1 with or without QDE-2 (Figure 2-13), consistent with its known activity only on single-stranded RNAs. Together, these results suggest that QDE-2 recruits the exosome and promotes its trimming of the single-stranded pre-milRNAs. However, the double-stranded pre-milR-1 needs to be unwound into single-stranded to allow exosome-mediated processing.

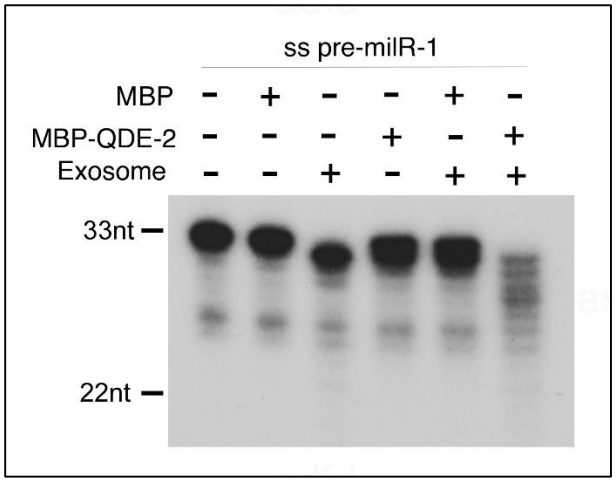

Figure 2-12 QDE-2 promotes the trimming of single-stranded pre-milR-1 by the exosome *in vitro*.
5' [^{32}P] radiolabeled single-stranded pre-milR-1 incubated with the indicated purified proteins. The products were separated by a denaturing gel.

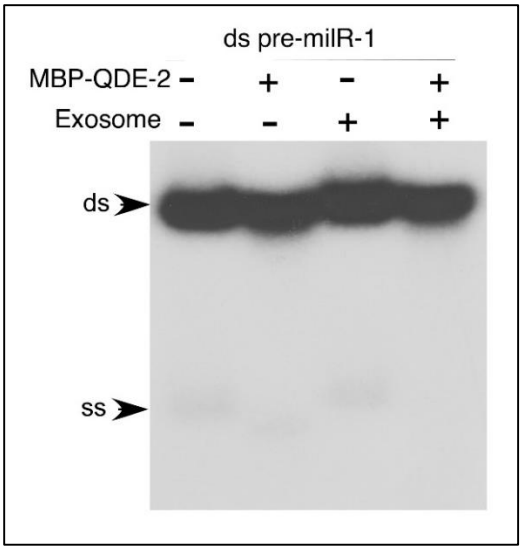

Figure 2-13 Exosome alone could not process double-stranded pre-milR-1 *in vitro*.
Nuclease assay showing that the core exosome has no activity towards double-stranded pre-milR-1 in the presence or absence of QDE-2.

2.3.6 QIP is an exonuclease required for the QDE-2-dependent milR-1 maturation in vitro

Because pre-milR-1 is associated with QDE-2 and QDE-2 associates with exosome factors in Neurospora, we then examined whether QIP can process the QDE-2-bound pre-milR-1 purified from *Neurospora* into mature milR-1. In a wild-type strain, immunoprecipitation of QDE-2 pulled down both the mature single-stranded milR-1 and the double-stranded pre-milR-1 (Figure 2-14). The QDE-2-bound pre-milR-1 is double-stranded because the denatured (boiled) RNA sample exhibited significantly increased the mobility relative to a sample that was not denatured.

To specifically obtain the QDE-2-pre-milR-1 complex, we immunoprecipitated QDE-2 from the qip^{KO} mutant extracts and used the immunoprecipitates as substrates for the QIP nuclease assays (Figure 2-15A). The use of QDE-2-bound sRNA from the qip^{KO} mutant ensured that only pre-milR-1 but not the mature milR-1 was immunoprecipitated. The resulting sRNAs were extracted, separated on a native gel, and analyzed by northern

blot analysis with a probe specific for milR-1. As shown in Figure 2-15B, immunoprecipitation of QDE-2 in the *qip*^{KO} mutant indeed only pulled down pre-milR-1, supporting the notion that pre-milR-1 is the precursor of mature milR-1. The addition of recombinant QIP, but not QIP^{CD}, to the reaction resulted in the complete disappearance of the double-stranded pre-milR-1 and the appearance of single-stranded sRNA species similar to the mature milR-1 milRNAs in size. This *in vitro* complementation result indicates that QIP is an exonuclease that directly processes the QDE-2-bound pre-milR-1 into mature milRNAs.

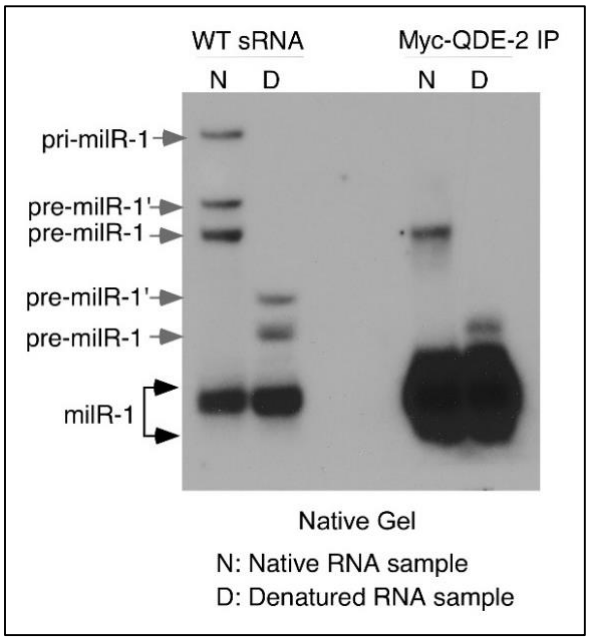

Figure 2-14 QDE-2-associated milR-1 species in wild-type strain.
Pre-milRNA unwinding assay using synthetic double strand pre-milR-1 and indicated recombinant proteins. Pre-milR-1 sense strand was 3' labeled with ^{32}pCp. The products were separated by a native gel.

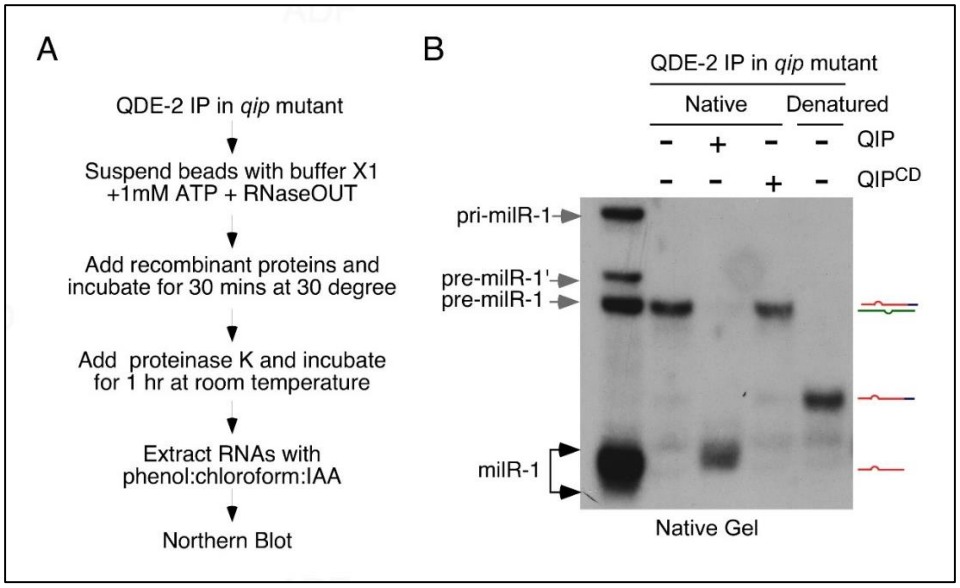

Figure 2-15 QIP is an exonuclease required for the QDE-2-dependent milR-1 maturation *in vitro*.
(A) Northern bot analysis of the QDE-2-associated sRNA sample showing that the single-stranded pre-milR-1* strand is not associate with QDE-2.(B) Myc-QDE-2 immunoprecipitated RNAs from the *qip*^{KO} strain was incubated with the QIP recombinant proteins. The products were separated by a native gel, and northern blot was probed with a milR-1 specific star-fire probe.

2.3.7 QIP separates the QDE-2-associated double-stranded pre-milR-1 and collaborates with exosome to process pre-milRNA into milRNAs

Because exosome cannot process double-stranded pre-milRNAs, a factor is required to separate the pre-milR-1 duplex or remove the pre-milR-1* strand to generate single-stranded substrates for exosome. It has been long hypothesized that factors may exist that unwind the siRNA and miRNA duplexes loaded onto Argonaute proteins, but no such factor with dsRNA strand separation activity has yet been identified (Haley and Zamore, 2004; Matranga et al., 2005). We initially identified QIP as a QDE-2-interacting protein that is required for the removal of passenger strands of siRNA from the QDE-2

associated siRNA duplex (Maiti et al., 2007). Although a small amount of exosome-processed single-stranded RNAs was observed in the *qip* mutants (Figure 2-5), which is likely due to spontaneous strand separation of the QDE-2-bound pre-milR-1, the vast majority of the pre-milR-1 is in duplex form. In addition, the levels of the pre-milR-1 duplex are dramatically increased in the *qip* mutants (Figures 2-3A and 2-5). These observations raised the possibility that QIP has the ability to separate the QDE-2-bound pre-milR-1 duplex into single-strands. Interestingly, the budding yeast sequence homolog of QIP, Gfd2p, was previously identified as a high-copy suppressor of a DEAD-box RNA helicase mutant (Estruch and Cole, 2003).

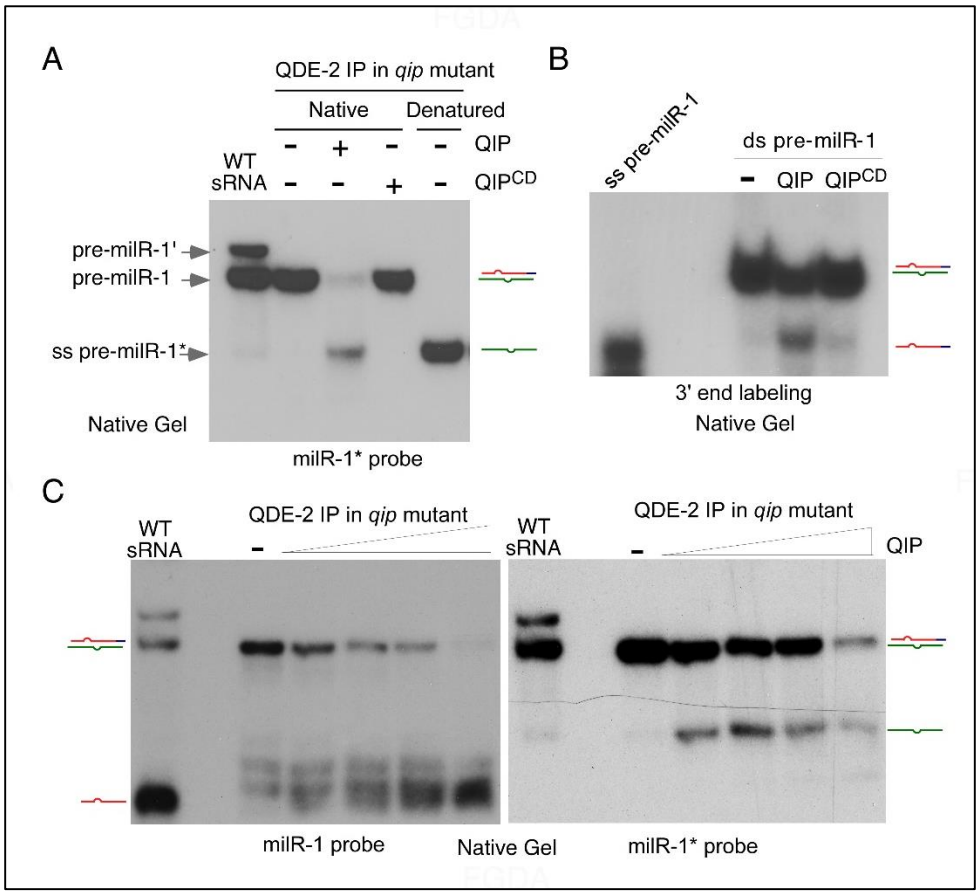

Figure 2-16 QIP unwinds the QDE-2-bound pre-milR-1 duplex and then processes it to maturation.
(A-C) Pre-milRNA processing assays using QDE-2 immunoprecipitates from the *qip*^{KO} strain and the indicated recombinant proteins. The reaction products were separated by native gels (A-C), and the northern blot was probed with a milR-1* or milR-1 specific probe (A, C). For the experiment in (A & B), 0.5μg His-QIP or His-QIPCD was used. For the experiment in (C), 0.25μg, 0.5μg, 1μg, 2μg His-QIP were used. Independent QDE-2 immunoprecipitation products from the *qip*^{KO} strain were used in these experiments.

To test this hypothesis, we examined whether the recombinant QIP could separate the QDE-2-bound pre-milR-1 into single strands. The immunoprecipitates of QDE-2 from the *qip*^{KO} strain was used in the assay, so that most of pre-milR-1 was in duplex form. Because the milRNA strand of the pre-milR-1 is rapidly converted into smaller RNA species (Figure 2-15B), we performed northern blot analysis specific for the milRNA* strand. As shown in Figure 2-16A, the addition of QIP in the reaction resulted in the disappearance of the pre-milR-1 duplex and the appearance of a small RNA band that was identical in size as the single-stranded full-length pre-milR-1*, indicating the separation of the QDE-2-bound double-stranded pre-milR-1. In addition, the recombinant QIP is also able to convert the synthesized double-stranded pre-milR-1 *in vitro* into single-stranded (Figure 2-16B). Together, these results indicate that QIP is a factor that can separate sRNA duplex and can also degrade single-stranded sRNA. It should be noted that the duplex separation ability of QIP also require QDE-2 in vivo, since pre-milR-1 and siRNA are maintained in duplex forms in the qde-2 mutant (Figure 2-3) (Maiti et al., 2007). It is likely that QIP requires QDE-2 to recruit double-stranded RNA substrates.

Titration of the recombinant QIP in the assay using QDE-2-bound pre-milR-1showed that as the concentration of QIP increased, the levels of the single-stranded pre-milR-1* first increased and then decreased at high QIP concentrations (Figure 2-16C, right panel). This result indicates that the duplex pre-milRNAs were first separated into single strands before being processed. We failed to detect a significant amount of smaller processed pre-milR-1* products, suggesting that the pre-milRNA* strand was processed into very small sizes that could not be detected by our northern blot analysis. In contrast, when we analyzed the milR-1 strand products, an increasing concentration of QIP resulted in increases in levels of single-stranded sRNAs similar in sizes as the mature milRNAs, and the full-length single-stranded pre-milR-1 was not easily detected (Figure 2-16C, left panel). These experiments indicate that after strand separation, the milR-1 strand of pre-milRNA is immediately and progressively processed by QIP and exosome to maturation. As many miRNAs in animal and plants, milR-1 is the predominant species and that little milR-1* milRNA is produced in vivo (Lee et al., 2010). Thus, our in vitro reconstitution results recapitulate this highly selective processing and maturation step.

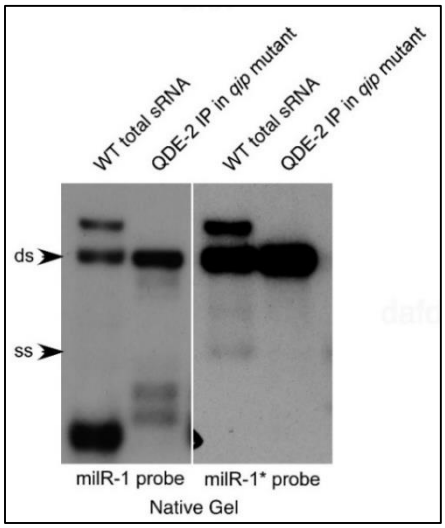

Figure 2-17 QDE-2-associated milR-1 species in *qip* mutant.
Northern bot analysis of the QDE-2-associated sRNA sample showing that the single-stranded pre-milR-1* strand is not associate with QDE-2.

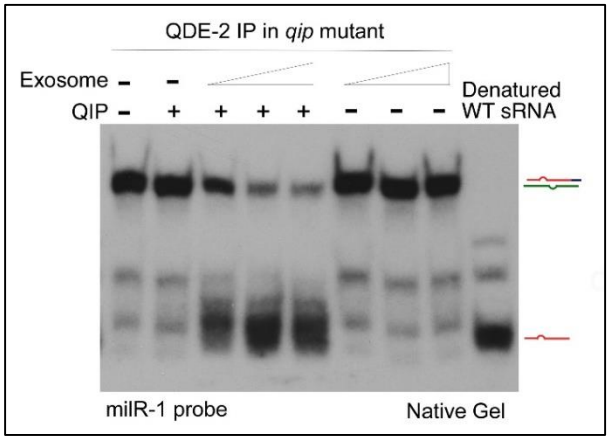

Figure 2-18 Exosome promotes the QIP-dependent maturation of milR-1 *in vitro*.
Exosome promotes the QIP-dependent maturation of milR-1 *in vitro*. Pre-milRNA processing assays were performed by using QDE-2 immunoprecipitates from the qip^{KO} strain and different concentrations of exosome (87ng, 175ng, or 0.7µg). For reactions containing QIP, 60ng His-QIP was used. The reaction products were separated by a native gel. Northern blot was probed with a milR-1 specific probe.

Why is pre-milR-1 processed to maturation and pre-milR-1* degraded away? What determines the sizes of mature milR-1 milRNAs? The differences in QIP processing efficiency and end products between the milR-1 and milR-1* strands of pre-milRNA indicate that the same nucleases act on them differently. The much slower degradation rate of the full-length pre-milR-1* strand in the *in vitro* reactions suggests that it dissociates from the QDE-2-pre-milRNA complex after duplex separation, making it less accessible to QIP and exosome. Supporting this notion, we found that in *Neurospora*, while QDE-2 is associated with single-stranded processed pre-milR-1 species, no QDE-2-bound single-stranded pre-milR-1* species could be detected (Figure 2-17). Thus, the

different outcomes of pre-milR-1 and pre-milR-1* should be due to the binding of pre-milR-1 by QDE-2. Together, these results suggest that upon strand separation, pre-milR-1* dissociates from QDE-2 and is degraded away, while pre-milR-1 remains associated with QDE-2 and is progressively processed by QIP and exosome. Thus, the sizes of the mature milR-1 are determined by the region of pre-milRNA that is protected by QDE-2 from nuclease processing.

Because of the association of between QDE-2 and FRH, which is known to associate with RRP44 in Neurospora (Guo et al., 2009), a small amount of exosome should exist in the QDE-2 immunoprecipitates used in the QIP nuclease assays. To determine the role of exosome in milR-1 maturation, we performed the assay using a limiting amount of QIP and different concentrations of purified core exosome complex. As shown in Figure 2-18, although this concentration of QIP could only modestly increase the level of mature milR-1, the addition of exosome led to a dramatic increase of mature milR-1 levels. In contrast, exosome alone had little effects on pre-milR-1 processing in the absence of QIP. This *in vitro* result is consistent with our genetic results and indicates that the maturation of milR-1 is a collaborative process requires QDE-2, QIP and exosome. QDE-2 recruits both QIP and exosome to pre-milRNA-1. The processing of pre-milR-1 by the exosome requires the strand-separation of pre-milRNA duplex by QIP. On the other hand, exosome can generate substrates for QIP. Afterwards, both exosome and QIP contribute to the processing and maturation of milR-1. Together, our results present above establish the biochemical basis for an Argonaute-dependent sRNA biogenesis pathway.

2.3.8 The role of exosome in degrading other milRNAs and siRNAs

The essential role of exosome in milR-1 production also prompted us to examine whether it regulates other *Neurospora* milRNAs and siRNA. Like milR-1, the production of milR-2 milRNAs also requires QDE-2, but milR-2 biogenesis requires the catalytic activity of QDE-2 and is produced independent of Dicer (Lee et al., 2010). On the other hand, milR-3, like most plant and animal miRNAs, requires only Dicer for its biogenesis. Except for milR-1, no other known milRNAs requires QIP for biogenesis. As shown in Figure 2-19A, the silencing of either *rrp44* or *frh* in *Neurospora* resulted in significant increases in levels of milR-2 and milR-3 milRNAs. Similarly, silencing of *rrp44* in an *albino-2* (*al-2*) quelled strain also resulted in an increase of the *al-2*-specific siRNA (Figure 2-19B). These results suggest that exosome is important for the decay of siRNAs and these two milRNAs and is not required for their maturation. Together, our results indicate that the exosome has at least two different roles in sRNA regulation in *Neurospora*: It mediates sRNA degradation and, in the case of milR-1 and perhaps other small RNAs, is directly involved in the maturation by 3'-5' processing.

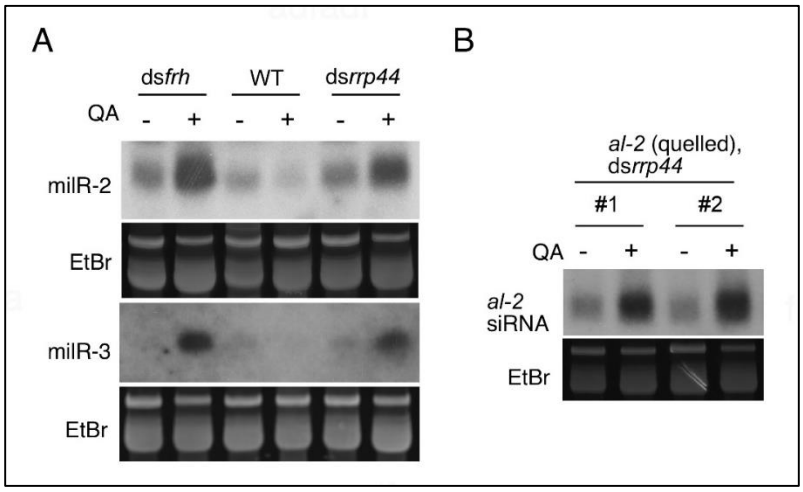

Figure 2-19 Exosome is important for the decay of other milRNAs and siRNAs.
(A) Northern blot analysis of small RNA samples separated in a denaturing gel showing the levels of milR-2 and milR-3 in the indicated strains. (B) Northern blot analysis of small RNA samples separated in a denaturing gel showing the level of *al-2* siRNA in the indicated strains.

CHAPTER THREE

TRANSCRIPTIONAL INTERFERENCE BY SENSE AND ANTISENSE OF *frequency* FORMS A DOUBLE NEGATIVE FEEDBACK LOOP THAT IS REQUIRED FOR CIRCADIAN GENE EXPRESSION

3.1 Introduction

Circadian clocks coordinate diverse molecular and physiological activities in most eukaryotic and some prokaryotic organisms. The core eukaryotic circadian oscillators consist of autoregulatory circadian negative feedback loops (Bell-Pedersen et al., 2005; Dunlap, 1999; Young and Kay, 2001) (Figure 3-1A). Despite the evolutionary distance between the filamentous fungus *Neurospora crassa* and higher eukaryotes, their circadian oscillator mechanisms share remarkable similarities (Baker et al., 2012; Heintzen and Liu, 2007; Liu and Bell-Pedersen, 2006). In the core *Neurospora* circadian oscillator (Figure 3-1B), FREQUENCY (FRQ) protein functions as the circadian negative element with its protein partner FRH (Aronson et al., 1994a; Cheng et al., 2005). Two PER-ARNT-SIM (PAS) domain transcription factors, the WHITE COLLAR (WC) proteins 1 and 2 form a heterodimeric complex that activates *frq* transcription (Cheng et al., 2001; Choudhary et al., 2007). To close the negative feedback loop, the FRQ-FRH complex inhibits WC complex activity by interacting with the WCs (Cheng et al., 2001; Denault et

al., 2001; He et al., 2006; Schafmeier et al., 2005). The WC complex also mediates light-induced *frq* transcription for light-resetting of the clock by binding to the light-responsive elements (LREs) on the *frq* promoter (Crosthwaite et al., 1995; Froehlich et al., 2002; He et al., 2002)

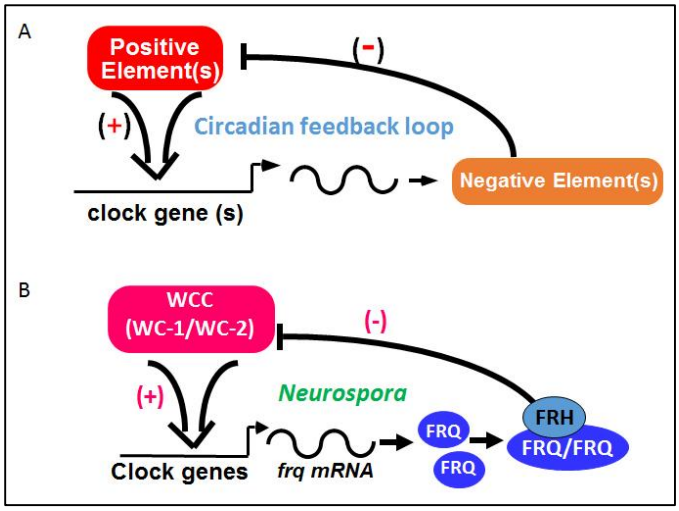

Figure 3-1 Model of circadian negative feedback loop. The model of eukaryotic (A) or *Neurospora* (B) circadian negative feedback loop.

Natural antisense RNAs, which are mostly long non-coding RNAs, overlap with and are transcribed independently from the sense RNAs. Recent studies showed that antisense RNA is a common phenomenon in the eukaryotic transcriptome (Berretta and Morillon, 2009; Osato et al., 2007; Xu et al., 2009). Even though only few antisense RNAs have demonstrated physiological functions, they appear to be involved in diverse physiological processes, such as the circadian clock, X chromosome inactivation, imprinting and cell fate determination in fungi, plants and animals (Deuve and Avner, 2011; Kramer et al., 2003; Nagano et al., 2008; Osato et al., 2007). Antisense RNAs may inhibit the expression of sense RNA by epigenetic silencing due to chromatin modifications or by formation of double-stranded RNA or small non-coding RNAs that function through the

RNA interference (RNAi) pathway (Camblong et al., 2007; Ogawa et al., 2008). Overlapping convergent transcription has been proposed to cause collision of RNA polymerase II that may disrupt gene expression (Hobson et al., 2012; Osato et al., 2007; Prescott and Proudfoot, 2002), but the physiological relevance of this mechanism is not clear.

In the *Neurospora frq* locus, a long non-coding antisense RNA named *qrf* overlaps with the sense *frq* transcript (Kramer et al., 2003). Like *frq*, the transcription of *qrf* is light-induced and the levels of *qrf* exhibit a circadian rhythm. However, the rhythms of *frq* and *qrf* transcripts are antiphase to each other. The deletion of the putative *qrf* promoter abolishes light-induced qrf transcription and affects the light-induced phase resetting of the clock (Kramer et al., 2003). The interpretation of this study, however, is complicated by the fact that the deletion made in the *qrf* promoter region did not completely abolish *qrf* expression and might have had unintended effects on *frq* expression because the deleted fragment includes part of the *frq* 3'UTR. The protein encoded by period (*per*) in insects and its homologs in mammals has a role similar to FRQ in animal circadian systems. In the silkmoth *Antheraea pernyi*, an antisense RNA to the *per* RNA oscillates with a phase that is antiphase to that of the per mRNA (Sauman and Reppert, 1996). Recently, RNA-sequencing studies in mice liver identified mPer2 antisense RNA that oscillates in antiphase to that of the mPer2 mRNA (Koike et al., 2012; Vollmers et al., 2012). These results suggest that the regulation of the core clock protein expression by antisense RNA is a shared mechanism in eukaryotic circadian systems.

3.2 Materials and Methods

3.2.1 strains, plasmid constructs and growth conditions

The wild-type strain used in this study is 87-3 (*ras-1*^{bd}, a). The *frq*^{10} strain is a *frq* null mutant (Aronson et al., 1994b). The *frq*^{9} strain bears a frame-shift mutation in the *frq* ORF (Aronson et al., 1994b). The mutants *wc-1*^{RIP}, *wc-2*^{KO}, *wcc*^{DKO} (*wc-1*^{RIP}, *wc-2*^{KO}), *dcl*^{DKO} (*dcl-1*^{RIP}, *dcl-2*^{KO}), *qde-1*^{KO}, *qde-2*^{RIP}, *qde-3*^{KO} were generated in previous studies (Choudhary et al., 2007; He et al., 2002). The *dim-2*^{KO} and *dim-5*^{KO} strains were generously provided by Dr. Qun He (Zhao et al., 2010). The *set-2*^{KO} (FGSC #15505) strain was from Fungal Genetic Stock Center (FGSC). The *set-2*^{KO}*;frq*^{9} double mutant was created in this study by crossing *set-2*^{KO} and *frq*^{9}. The *dsrrp44* strain was generated by introduction of a plasmid expressing quinic acid-driven *rrp44*-specific RNA hairpin into a wild-type strain (Guo et al., 2009). The *frq*$^{KI(WT)}$ and *frq*$^{KI(qLRE\ mut)}$ strains were created in this study (Figure 3-2A,C). The *frq*$^{KI(qLRE\ mut)}$; *dsrrp44* strain was created by crossing *frq*$^{KI(qLRE\ mut)}$ and *dsrrp44* in this study. The *frq*^{10};frq^{WT}, *frq*^{10};frq^{qLREmut}, *frq*^{10};frq.aq strains were obtained by targeting plasmids pKAJ120, pKAJ120$^{qLRE\ mut}$, and pKAJ120.aq, respectively, into *his-3* locus of the *frq*^{10} mutant as previously described (Aronson et al., 1994a) (Figure 3-2B). The *frq*^{10};frq$^{qLRE\ mut}$;qrf strain was generated by targeting the plasmid pCSR1.qrf into *csr-1* locus of the *frq*^{10};frq$^{qLRE\ mut}$ mutant as previously described (Figure 3-2D) (Bardiya and Shiu, 2007).

The pKAJ120 that contains the entire wild-type *frq* gene including its promoter and a *his-3* targeting sequence was used as the parental plasmid (Aronson et al., 1994b). The

qLRE in pKAJ120 was mutated as described (Figure 3-2A) by site-directed mutagenesis to create pKAJ120$^{qLRE\ mut}$. The fragment between *BssHII* and *SapI* sites of pKAJ120 was replaced with inverted *Neurospora qa-2* promoter (Giles et al., 1985) to create pKAJ120.aq. The PCR fragment containing entire wild-type *qrf* and its promoter (primer: 5'-TTCATTAAGGTGGGGCAGG-3', 5'-TTTCCACGCCGGCCCCAGTC-3') was inserted into vector pCSR1 between *NotI* and *PstI* sites to generate pCSR1.qrf (Bardiya and Shiu, 2007).

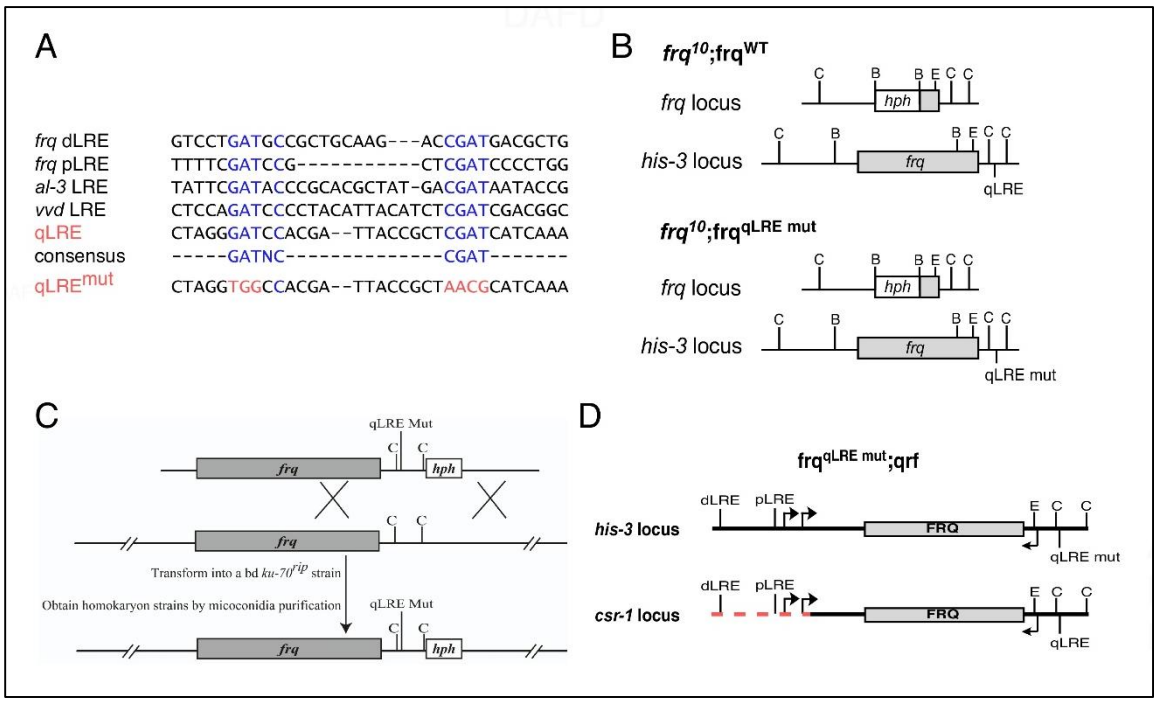

Figure 3-2 Diagrams of chromosomal modifications in *qrf* mutants.
(A) Sequence alignment of known LRE elements. The qLRE and the mutated regions in the *qrf* promoter are shown. (B) Diagrams showing the chromosomal modifications in the indicated loci in the *frq*^{10};frq^{WT} and *frq*^{10};frq^{qLRE} mutant strains. (C) Diagram describes the strategy used to obtain the knock-in strains by homologous recombination. (D) Diagram showing the chromosomal modifications in the frq$^{qLRE\ mut}$;qrf strains that allow the expression of *qrf in trans*. The frq$^{qLRE\ mut}$ construct is at *his-3* locus, and *qrf* is expressed only from the *csr-1* locus. The red dashed line indicates that the *frq* promoter region is deleted in the *qrf* construct to abolish *frq* expression.

Growth conditions have been described previously (Aronson et al., 1994b). Liquid cultures were grown in minimal medium (1xVogel's, 2% glucose). When quinic acid (QA) was used, liquid cultures were grown in low glucose medium (1xVogel's, 0.1% glucose, 0.17% arginine) with indicated concentrations of QA. For *rrp44* knockdown assay, *Neurospora* was cultured into mats in low glucose medium with 10^{-2} M QA for 2 days. Afterwards, *Neurospora* mats were cut into discs and cultured in flasks in same medium with shaking. After 2 days, the tissues were harvested. For mRNA decay assay, the cultured condition has been described previously (Guo et al., 2009). For rhythmic experiments, the *Neurospora* cultures were transferred from LL to DD at time 0 and were collected in DD at the indicated time (hours). For light induction assay, *Neurospora* cultures were grown in DD for 24 hrs with shaking, and then treated with 2mins 1750 lux light pulse. Afterwards, *Neurospora* cultures were transferred back to DD and collected at the indicated time (minutes). For race tube assay, the medium contains 1xVogel's, 0.1% glucose, 0.17% arginine, 50ng/ml biotin, and 1.5% agar with indicated concentrations of QA. Strains were inoculated and grown in constant light at 25℃for 24hrs before being transferred to DD at 25℃. Calculations of period length and phase were performed as described (Liu et al., 1997).

3.2.2 Analysis of light-resetting of circadian clock

The assay was performed on race tubes containing acetate/casamino acid medium (1X Vogel's, 1.2% sodium acetate, 0.05% casamino acid hydrolysate, and 1.5% agar)(Dharmananda, 1980). Race tubes were first grown in LL at 25℃for 48 hrs before

being transferred to DD. Cultures were then grown in DD at 25℃for 25 hrs, and different individual cultures were given a 2-min light pulse (1750lux) at different times (2 hrs intervals) to cover an entire circadian cycle. The amount of phase shifts was determined by comparing light-treated cultures (6 replicas for each time point) with those of the control cultures (kept in DD). The initial LL to DD transition was defined as circadian time (CT) 12. The phases of the cultures were calculated as the average phase for 2 consecutive days after the light treatment.

3.2.3 Protein and RNA analysis

Tissue harvest, protein extraction and western blot were performed as previously described (Cheng et al., 2001). 40μg total proteins were loaded in each lane of SDS-PAGE (7.5%). Total RNA was extracted with Trizol in accordance with the manufacturer's protocol, and then further purified by 2.5M LiCl as previously described (Barlow et al., 1963). Northern blot analyses were performed as previously described (Aronson et al., 1994b) using [^{32}P]UTP-labelled riboprobes. Riboprobes were transcribed *in vitro* from PCR products by T3 or T7 RNA polymerase (Ambion) with the manufacturer's protocol. The primer sequences used for the template amplification were frq-N term (5'-TAATACGACTCACTATAGGG (T7) GGCAGGGTTACGATTGGATT-3', 5'-GGGTAGTCGTGTACTTTGTCAG-3'), frq-C term (5'-TAATACGACTCACTATAGGG (T7) CCTTCGTTGGATATCCATCATG-3', 5'-GAA TTCTTGCAGGGAAGCCGG-3'),and qrf-N term(5'-AATTAACCCTCACTAAAGGG (T3)GAATTCTTGCAGGGAAGCCGG-3',5'-CCTTCGTTGGATATCCATCATG-3').

Except Figure 3-23, riboprobes of frq-C term and qrf-N term were mostly used for detecting *frq* and *qrf*, respectively. For Figure 3-23, the riboprobes were hydrolyzed for 25mins in the buffer (40mM Na2CO3, 60mM NaHCO3, 10mM 2-mercaptoethanol), and then the reaction was stopped by equal volume of the buffer (0.2M NaOAC, pH6.0, 1% HOAC, 10mM DTT). For western blot and northern blot, densitometry of the signal as performed using Image J.

Quantitative PCR (qPCR) and quantitative reverse transcriptase PCR (qRT-PCR) were performed as previously described (Choudhary et al., 2007). For strand-specific qRT-PCR, several modifications of the protocol were made. The primer sequences for strand-specific RT reactions were as follows.

frq GCTAGCTTCAGCTAGGCATCCGTTGCCTCCAACTCACGTTTCTT
qrf
CCTCAGCTCGTACGAGTCGTACGTCATGGAGCCCTCTGGTCTTGG
frq pre-mRNA GCTAGCTTCAGCTAGGCATCTTGAACGGTAGGGAGGAGGAGAG
β-tubulin CTCGTTGTCAATGCAGAAGGTC

The RT reaction was performed by mixing the primers of specific strand and *β-tubulin*. *β-tubulin* was used for internal control. The primer sequences for the qPCR step of qRT-PCR assay were as follows.

frq	AGCTTCAGCTAGGCATCCGTT
	GCAGTTTGGTTCCGACGTGATG
qrf	CAGCTCGTACGAGTCGTACGTC
	ATCTTCCGATGTTGTCGAGCGT
frq pre-mRNA	AGCTTCAGCTAGGCATCTTGAACG
	ACGGCATCTCATCCATTCTCACCA
β-tubulin	ATAACTTCGTCTTCGGCCAG
	ACATCGAGAACCTGGTCAAC

3.2.4 Chromatin immunoprecipitation (ChIP) assay

The ChIP assay was performed as previously described (He and Liu, 2005) with several modifications. 500 µg total cell lysis was used for each immunoprecipitation assay. The antibodies used in this study were WC-2 (Cheng et al., 2001) (home-made, 2 µl/assay), Pol II S2P-CTD (abcam #ab5095, 2 µl/assay), Pol II S5P-CTD (abcam #ab5095, 2 µl/assay), and H3K36me3 (abcam #ab9050, 2 µl/assay). Each experiment was independently performed three times, and immuoprecipitation with IgG or *wcc*^{DKO} extract was used as the negative control. qPCR was used for measuring the immunoprecipitated DNA. Primer sequences for qPCR were as follows.

frq dLRE	AGAGTTTGGCCGGACAACCAGTA
	GCTTCGACCGAAAGTATCTTGAGCCT
frq pLRE	GTCGCAGAGGACCCTGAACTTT
	TCCCACAGATGCACAGGAATCG
qrf qLRE	ATCGATCACTAGTCCCGGTTCGTT
	TTGCTGATAATGCGCTGAGGGTCT
1	AGAGTTTGGCCGGACAACCAGTA
	GCTTCGACCGAAAGTATCTTGAGCCT
2	GGGTAGTCGTGTACTTTGTCAG
	ACCGGACTTTAGGTTGTGTG
3	ACGGCCTTTCTCTGTTTACC
	GCAGAGTTGGGTCGGATTTA
4	CCGTTCTAGCGTGCTTCTT
	GGCACTAATGAGGTTCGAGATT
5	TTACTTCATCTTCCGCACTGG
	GGCAGGGTTACGATTGGATT
6	ACTGTTCACCGGAAAGATCAG
	GGGCCATGTTGGTTCCTT
7	TTGCACCGATCTTTCAGGAG
	CTGCAGCACATGTTCAACTTC
8	GGGCAGAGAGTGGCTATAGTA
	CCGCGTCTTCTTCTCACATAG
9	CCGATCCAGTGAAGCACATA
	CCCGCGTACAGTACAATTCA

3.2.5 Luciferase reporter assay

The luciferase reporter assay was performed as previously described (Gooch et al., 2008). The reporter construct in Figure 3-9A (P*frq-luc*) was generated by inserting *BamHI-NotI* fragment of P*frq-luc*-I (a generous gift from J.Dunlap) into corresponding sites of pBARKS1 (Barlow et al., 1963). The reporter construct in Figure 3-9A (P*qrf-luc*) was generated by inserting the PCR fragment containing *qrf* promoter and luciferase gene into *NotI-EcoRI* sites of pBARKS1. For the PCR fragment, *qrf* promoter was directly fused with luciferase gene ORF. The primer sequences were *qrf* promoter (5'-ATCGATTTCATTAAGGTGGGG-3',5'-GGTGGTGGGTGGTGGGTGGAG), and luciferase gene (5'-ATGGAGGACGCCAAGAA CATCAAG-3',5'-TCAGAGCTTGGACTTGCCGCC-3'). The plasmids P*frq-luc* and P*qrf-luc* were transformed into wild-type or frq^{10};frq.aq strains with Ignite selection as previously described (Pall, 1993). The plasmid P*min.luc* was generated by inserting the luciferase gene ORF into *XmaI* site of pDE3dBH. The plasmid P*min.luc*.P*frq* was generated by inserting inverted *frq* promoter (the same as P*frq-luc*-I) into downstream of luciferase gene ORF of P*min.luc*. The non-regulated basal promoter in pDE3dBH (upstream of *EcoRI* site) was used as the minimal promoter to control the expression of luciferase gene in P*min.luc* and P*min.luc*.P*frq* as previously described (Bell-Pedersen et al., 2005). For 3-12, the plasmids P*frq-luc*-I, P*min.luc*.P*frq*, and P*min.luc* were transformed into wild-type strain respectively by targeting *his-3* locus.

3.2.6 Mathmatic modeling

The mathematic simulation of relative *frq* and *qrf* RNA levels in DD was performed based on previously described (Hong et al., 2008; Ruoff et al., 2005; Ruoff et al., 1999; Yu et al., 2007) with several modifications. The equations are described in Figure 3-13. The ordinary differential equations (1)-(8) were solved numerically by Gear method (Gear, 1971) and XPPAUT (Ermentrout, 2007). The values of parameters for Figure 3-14 are described in Figure 3-13. The values of k_2, k_3, k_6, k_7, k_8, k_9, k_{11}, k_{12}, k_{13}, k^{14}, k_{15}, K, K_2, k_{01} were from previous study (Hong et al., 2008). The values of k_4 and k_5 were from previous study (Ruoff et al., 2005; Ruoff et al., 1999). The values of k10 was from previous study (Yu et al., 2007). The values of other parameters were for this study. For Figure 3-14B, k_{19} was set to 0; For Figure 3-14D, k_{16} was increased to 0.91.

3.3 Results

3.3.1 WC-dependent and WC-independent qrf transcription

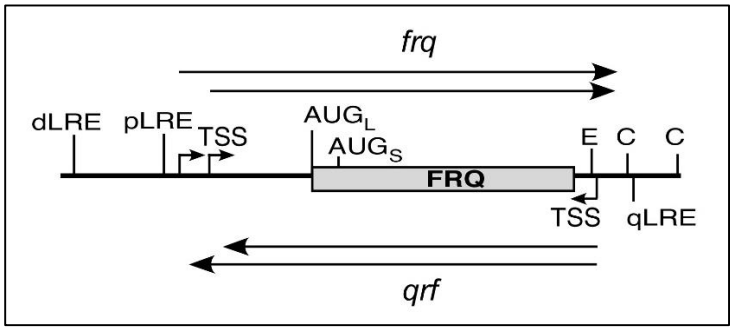

Figure 3-3 The diagram of *frq* locus.
A diagram showing the *frq* locus. The LRE are the light response elements in the *frq* and *qrf* promoters. E: *EcoR V* site. C: *ClaI* site.

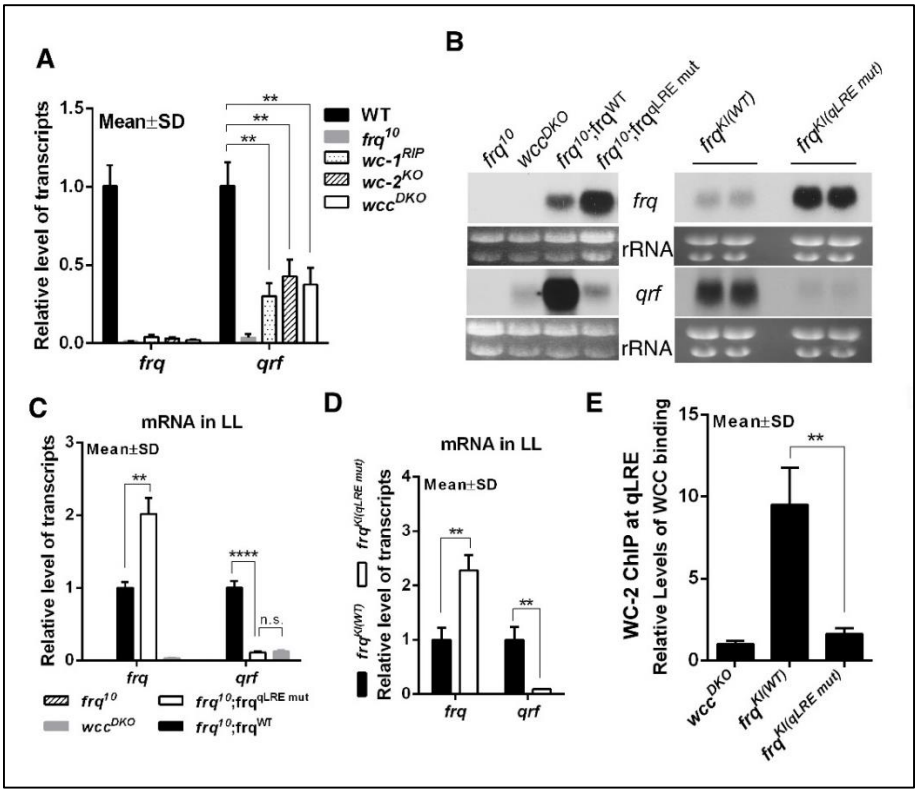

Figure 3-4 WC-mediated expression of *frq* and *qrf*.
(A) Strand-specific RT-qPCR analyses showing the levels of *frq* and *qrf* in the indicated strains in LL. The error bars are standard deviations (n=3). The asterisks indicate P value < 0.01. (B) Northern blot analyses showing the expression of *frq* and *qrf* in the indicated strains. (C, D) Strand-specific RT-qPCR results showing the expression levels of *frq* and *qrf* in indicated strains in LL. Error bars are standard deviations (n=3). Asterisks indicate P value < 0.01. n.s. indicates that the difference is not statistically significant. (E) WC-2 ChIP assays showing the WC binding levels at the qLRE of *qrf* promoter.

To determine the physiological role of *qrf*, we mapped the ends of the both *frq* and *qrf* transcripts by 3' RACE and strand-specific RNA sequencing and found that *frq* and *qrf* transcripts almost completely overlap with each other (Figure 3-3). Expression of both *frq* and *qrf* is light induced (Kramer et al., 2003). To determine whether the transcription of *qrf* is completely dependent on the WC complex, we compared the levels of *frq* and *qrf* transcripts in wild-type, *frq*-null (frq^{10}), and *wc* single and double mutants in constant light (LL) by strand-specific RT-qPCR. As shown Figure 3-4A, *frq*

expression was nearly completely abolished in the *wc* mutants. In contrast, *qrf* transcription was observed at ~25% of wild-type levels in the *wc* mutants, indicating that the transcription of *qrf* is mediated by both WC-dependent and WC-independent mechanisms. The WC complex was previously shown to bind to the *qrf* promoter region (Smith et al., 2010), and sequence analysis of the *qrf* promoter uncovered five putative WC complex binding sites. Point mutations were introduced into each of these possible binding sites, and the *frq* constructs with the mutations were individually introduced at the *his-3* locus of a frq^{10} strain (Aronson et al., 1994a). Northern blot and strand-specific qRT-PCR analyses showed that mutation of one of these sites in the qrf promoter, the qrf light response element (qLRE), dramatically reduced the level of qrf (Figure 3-2A and 3-4B, C). In the $frq^{qLREmut}$ strain, the level of *qrf* was comparable to that in the *wc* double mutant (wcc^{DKO}). To further confirm our result, we created a knock-in strain ($frq^{KI(qLREmut)}$) by homologous recombination in which the qLRE was mutated at the endogenous *frq* locus (Figure 3-2A). *qrf* levels in the $frq^{KI(qLREmut)}$ mutant were much lower than those in the control strain (Figure 3-4B, D). A chromatin immunoprecipitation (ChIP) assay using WC-2 antibody showed that WC complex binding at the *qrf* promoter was completely abolished in the $frq^{KI(qLREmut)}$ mutant (Figure 3-4E), indicating that the qLRE is the only WC binding site in the *qrf* promoter that mediates light-induced *qrf* expression.

3.3.2 qrf represses frq transcription to regulate light-induced resetting of the clock

In contrast to the reduction of *qrf* levels in the qLRE mutants, higher than wild-type levels of *frq* mRNA were observed (Figure 3-4B, D). In addition, levels of FRQ protein were also higher in the qLRE mutant than in the WT strain (Figure 3-5). These results suggest that expression of *qrf* represses *frq* transcription. Light rapidly induces *frq* transcription, a mechanism that is responsible for the light resetting of the clock (Crosthwaite et al., 1995). To further examine the role of *qrf* on *frq* transcription, we compared *frq* and *qrf* expression after a 2-min light pulse in constant darkness (DD). As previously reported (Crosthwaite et al., 1995; Kramer et al., 2003), the light pulse resulted in rapid induction of both *frq* and *qrf* mRNA in the wild-type strain with similar kinetics (Figure 3-6A). As expected, the light induction of qrf was completely abolished in the frq^{10};$frq^{qLREmut}$ strain (Figure 3-6B). The light-induction of *frq*, however, was significantly elevated compared to that in the control strain, further indicating that light induction of *qrf* transcription represses the light-induced *frq* transcription. The circadian conidiation rhythm of qLRE mutant strains in the dark were similar to that of the frq^{10},frq^{WT} strain (data not shown), indicating that light-induced *qrf* transcription is not required for the circadian clock function in DD. However, phase response curves after a 2-min light pulse at different time points in DD showed that same light pulse resulted in significantly greater phase-shifts from ~circadian time (CT) 10 to 20 in the frq^{10},$frq^{qLREmut}$ and $frq^{KI(qLRE\ mut)}$ strains than in control strain (Figure 3-6C, D). These results are consistent with a previous report that the deletion of the *qrf* promoter region enhances light resetting of the clock (Kramer et al., 2003) and indicate that the light-

induction of *qrf* regulates light resetting of the clock by repressing light-induced *frq* transcription.

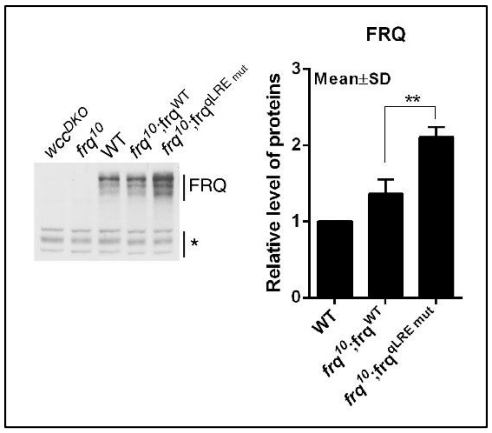

Figure 3-5 *qrf* represses the level of FRQ. Western blot results showing the FRQ expression levels in the indicated strains in LL. The densitometric analysis of western blot results from three independent experiments is shown at right. Error bars are standard deviations. Asterisks indicate P value < 0.01.

3.3.3 qrf expression is required for circadian clock function in the dark

Significant amounts of *qrf* are expressed in the qLRE mutant strains independently of the WC proteins (Figure 3-4A, B), indicating that unlike *frq* transcription, a separate mechanism mediates light-independent *qrf* transcription. Consistent with this notion, similar levels of *qrf* transcripts were seen in the $frq^{KI(WT)}$ and $frq^{KI(qLRE\ mut)}$ strains at DD24, (Figure 3-7A), indicating that the qLRE is not involved in *qrf* expression in the dark. To determine the function of *qrf* in the dark, we created a construct in which the promoter of *qrf* was replaced with the *qa-2* promoter, which is inducible with quinic acid (QA) (Aronson et al., 1994a), and introduced it at the *his-3* locus of the *frq*-null strain. In the resulting frq^{10};frq.aq strain, *qrf* expression can be induced to different levels in a QA concentration-dependent manner. As shown in Figure 3-8A, *qrf* expression was completely abolished in the absence of QA in the frq^{10};frq.aq strain. The addition of QA ($1x10^{-3}$ M) led to a dramatic induction of *qrf* expression. As a result of *qrf* expression, the

levels of *frq* were significantly reduced, further indicating the repression of *frq* expression by *qrf*.

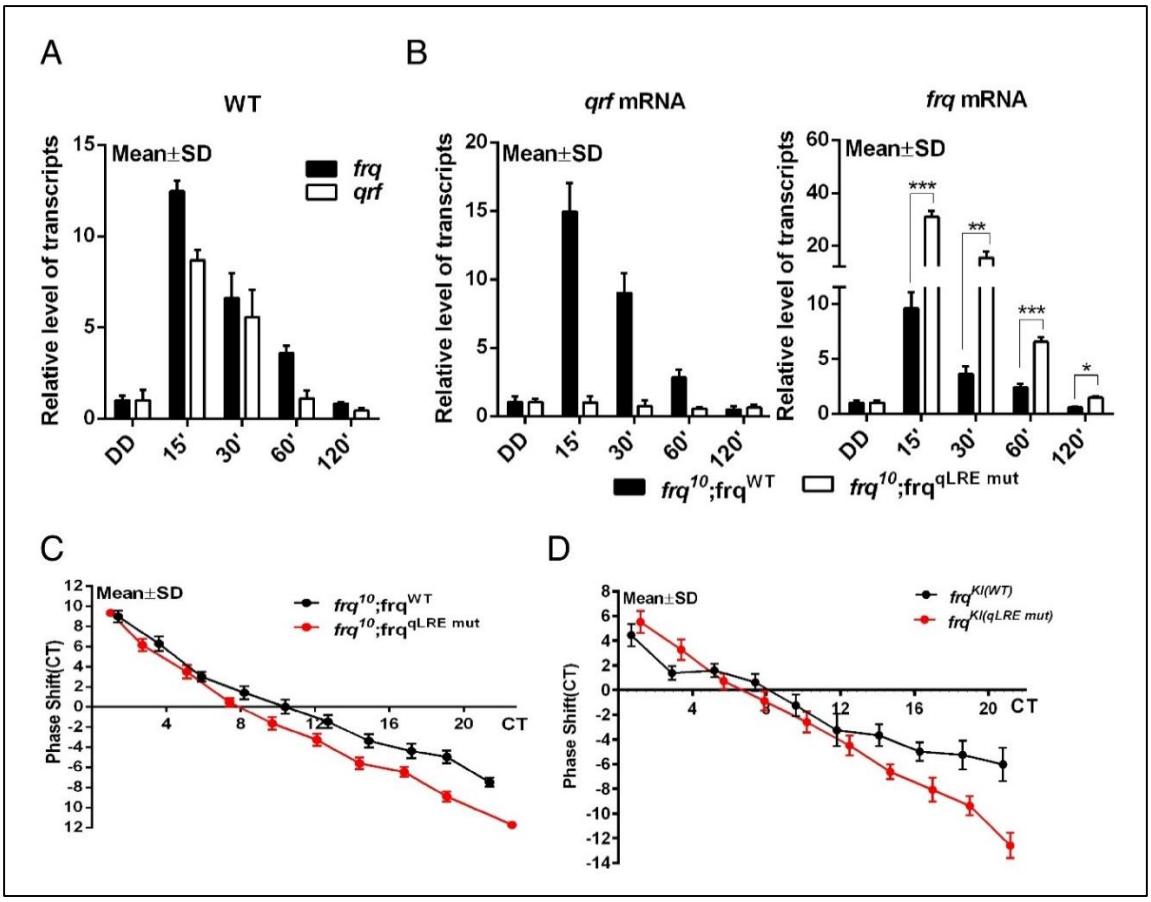

Figure 3-6 Light-induced *qrf* expression represses *frq* transcription and regulates light resetting of the clock.

(A, B) Strand-specific RT-qPCR analyses showing the levels of *frq* and *qrf* after a 2 min of light induction at DD24 in the indicated strains. (C, D) Phase response curves of circadian conidiation rhythms of the indicated strains after 2 min of light pulse at different circadian time (CT) points.

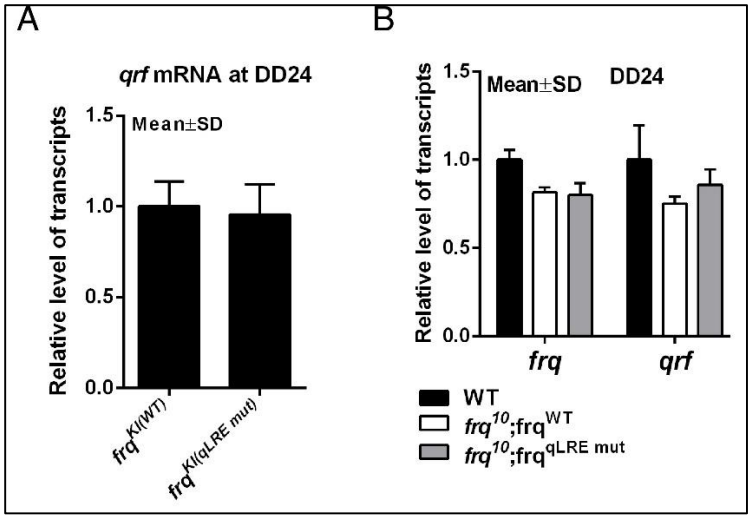

Figure 3-7 The expression levels of *frq* and *qrf* at DD24. Strand-specific RT-qPCR results showing the expression levels of *frq* and *qrf* in the indicated strains at DD24.

Race tube assays showed that in the absence of QA, the *frq*^{10};frq.aq strain exhibited a low amplitude conidiation rhythm for the first 1-2 days and became arrhythmic thereafter (Figure 3-8B, C). To confirm these results at the molecular level, we introduced a *frq* promoter driven luciferase reporter construct (P*frq-luc*) (Gooch et al., 2008) into the *frq*^{10};frq.aq strain. The robust circadian luciferase activity seen in the control strain was completely abolished in the *frq*^{10};frq.aq strain in the absence of QA, indicating that qrf expression is required for rhythmic *frq* promoter activity (Figure 3-9A). As the concentration of QA was increased, the circadian conidiation rhythms were gradually restored in the *frq*^{10};frq.aq strain and at 10^{-5} -10^{-4} M QA, the rhythms were as robust as the strain carrying the wild-type *frq* construct (*frq*^{10};frqWT) (Figure 3-8B). When QA was increased to higher concentrations, however, the amplitudes of the conidiation rhythms were reduced (Figure 3-8B) or became arrhythmic (Figure 3-8C).

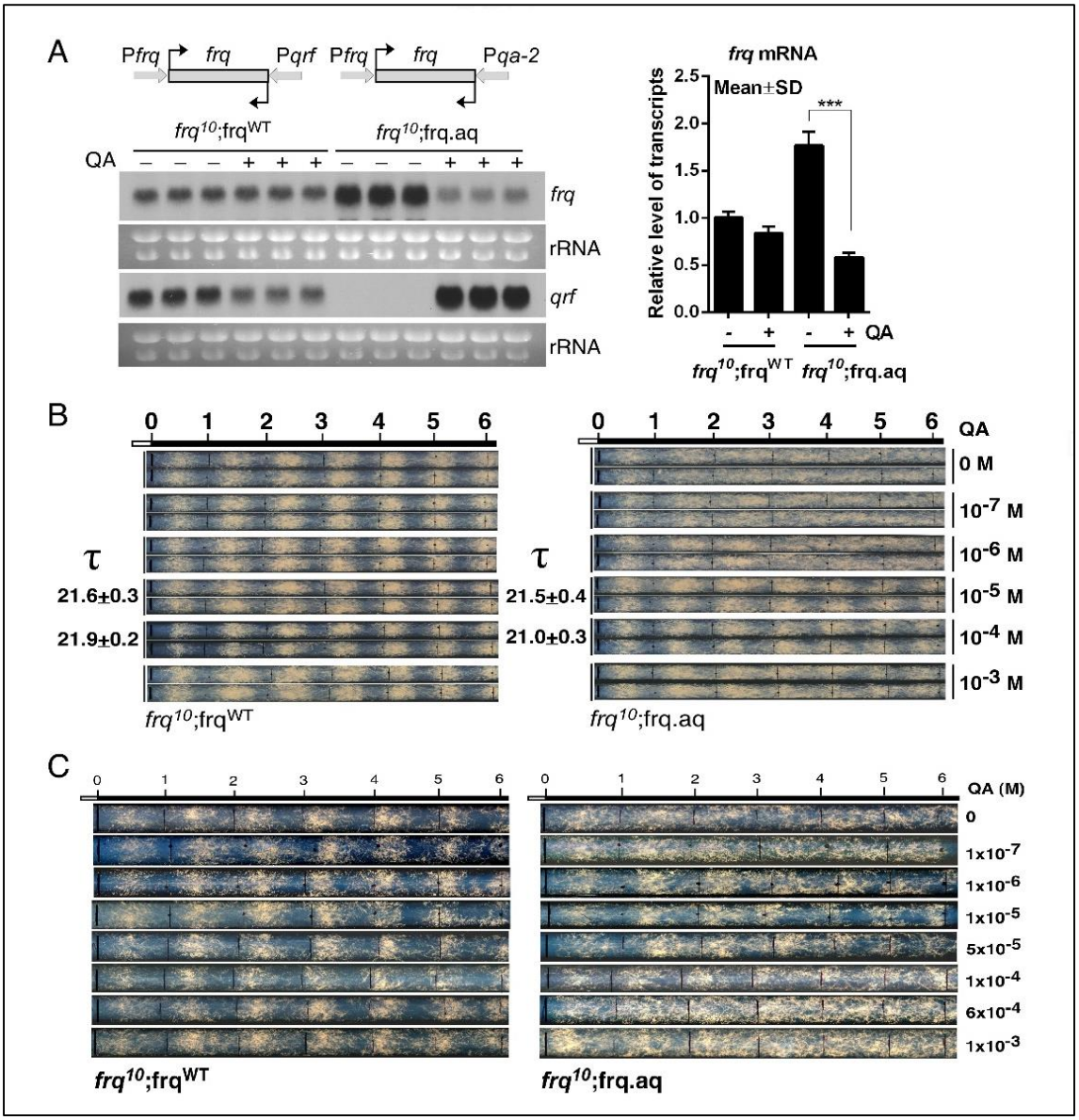

Figure 3-8 *qrf* expression is required for circadian conidiation rhythms in DD.
(A) Northern blot analysis showing the expression levels of *frq* and *qrf* in the presence or absence of $1x10^{-3}$ M QA (0.1% glucose) in the indicated strains. The densitometric analyses of the northern blot results are shown in the right panel. The asterisks indicate P value < 0.001. (B, C) Race tube analyses of the *frq*^{10};frq^{WT} and *frq*^{10};frq.aq strains in medium with 0.1% glucose (B) or 0% glucose + 0.17% arginine (C) with the indicated concentrations of QA in DD. Glucose is known to suppress leaky expression from the *qa-2* promoter in the absence of QA. The lack of glucose in medium is known to allow more efficient expression from the *qa-2* promoter. The black lines on race tubes indicate the daily growth fronts.

The restoration of circadian rhythm by QA in the *frq*^{10};frq.aq strain was also seen at FRQ expression level. In the absence of QA, after the initial light to dark transfer, the level and phosphorylation profile of FRQ were constant in DD. In the presence of QA, however, the rhythm of circadian oscillation of FRQ was restored, as indicated by the cyclic changes of FRQ phosphorylation profiles (Figure 3-9B). Furthermore, the presence of QA also resulted in a higher amplitude of frq mRNA oscillation (Figure 3-9C). These results indicate that the expression of *qrf* in the dark is required for circadian gene expression and clock function. Our data also establish that the level of *qrf* transcription must be within a certain range to permit a functional clock: When levels of *qrf* are too low or too high, the circadian expression of *frq* is abolished. In addition, we found that the promoter activity of *qrf* may not need to be regulated in a circadian manner because the *qa-2* promoter is not clock controlled (Aronson et al., 1994a).

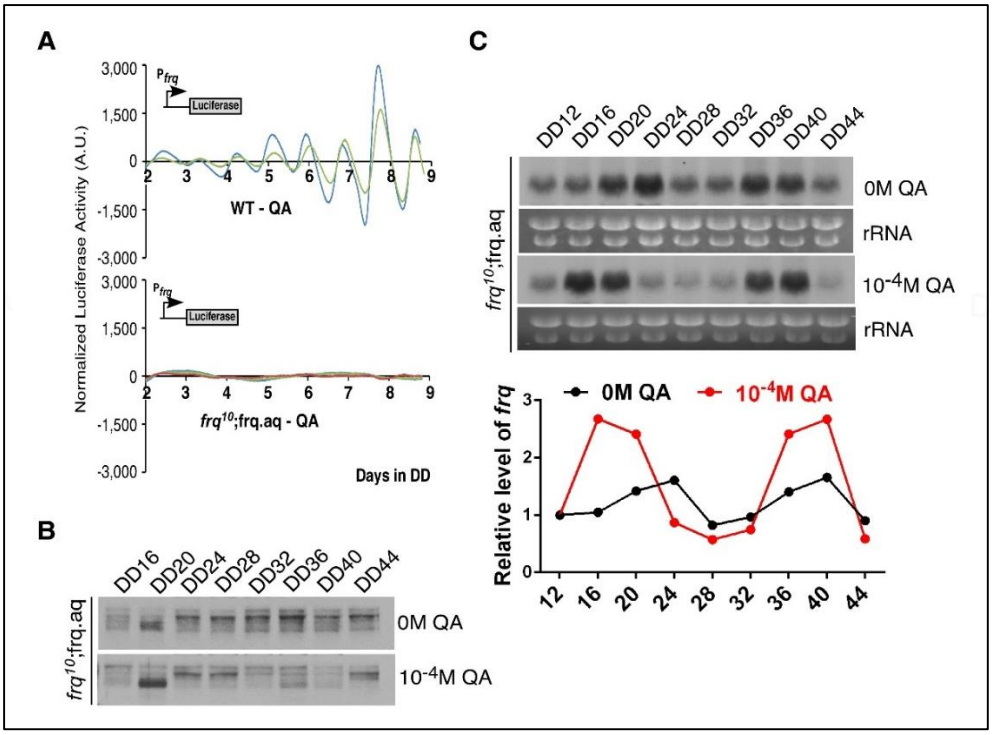

Figure 3-9 *qrf* expression is required for circadian molecular rhythms in DD.
(A) Luciferase reporter assay showing the normalized *frq* promoter activity in the *frq*^{10};frq^{WT} and *frq*^{10};frq.aq strains after one day in DD. The measurement of luciferase activity from each culture was normalized using the LumiCycle analysis software to subtract the increasing baseline luciferase signal caused by the cell growth during the experiment. (B) Western blot analysis showing the FRQ expression profiles in the *frq*^{10};frq.aq strain in the presence or absence of QA. (C) Northern blot analysis showing the *frq* expression profiles in the *frq*^{10};frq.aq strain in the presence or absence of QA. The densitometric analysis of the results is shown below.

3.3.4 frq transcription represses qrf expression

Strand-specific qRT-PCR analyses showed that the level of *qrf* transcripts exhibits a circadian oscillation in DD in the wild-type that is antiphase to that of the rhythm of the sense *frq* transcripts (Figure 3-10A), consistent with the previously reported result (Kramer et al., 2003). The rhythmic *frq* transcription requires rhythmic binding of the WC complex at the *frq* promoter (Belden et al., 2007; He et al., 2006). Thus, we examined whether the WC complex regulates *qrf* transcription in a similar manner. As shown by the WC-2 ChIP assays in Figure 3-10B, in contrast to the robust rhythm of WC complex binding at the *frq* promoter in DD, no WC binding was detected in the *qrf* promoter at different time points. Furthermore, the mutation of qLRE in the qrf promoter did not affect either *frq* or *qrf* transcripts levels in DD (Figure 3-7B). These results indicate that WC is not involved in regulating qrf transcription in the dark.

To determine whether qrf transcription is activated rhythmically, we used the promoter of *qrf* to drive the expression of luciferase reporter gene in a wild-type strain. Whereas activity from a luciferase gene driven by the *frq* promoter exhibited a robust circadian rhythm of luminescence, no rhythm of luciferase activity was seen in the P*qrf*-

luc reporter strain (Figure 3-10C). This result strongly suggests that the promoter activity of *qrf* is not rhythmically controlled.

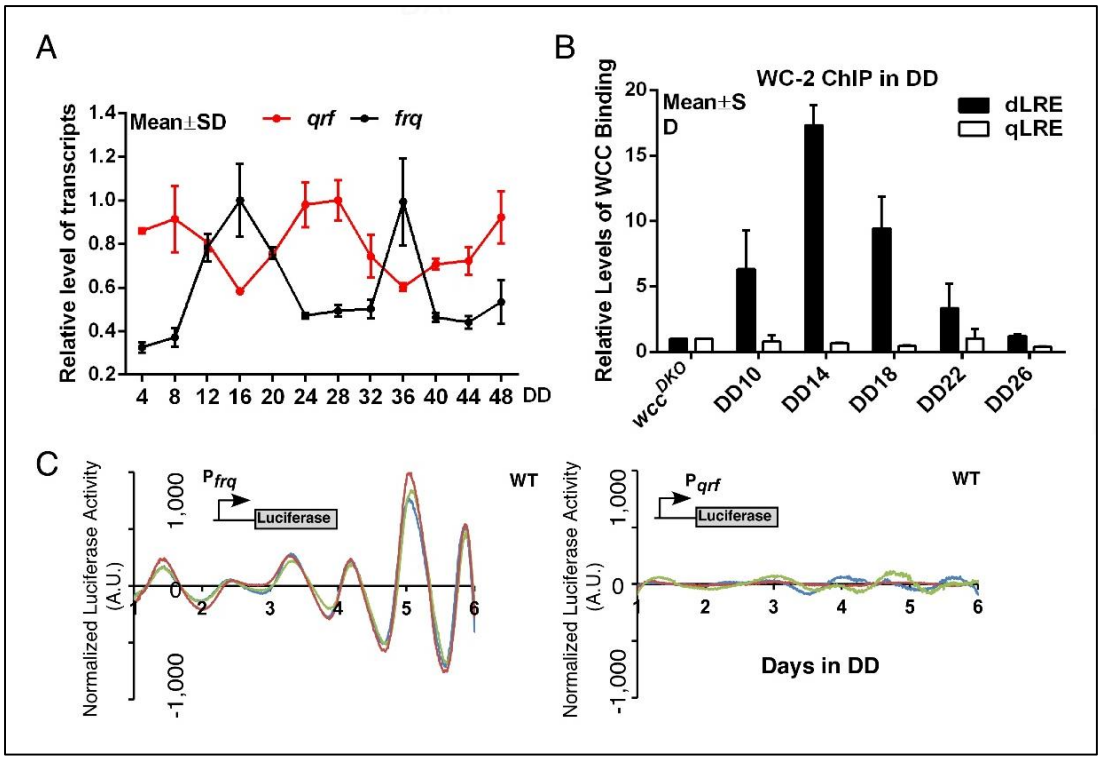

Figure 3-10 The promoter activity of *qrf* is not rhythmically controlled.
(A) Strand-specific RT-qPCR results showing the antiphase oscillation of *frq* and *qrf* in DD. Error bars are standard deviations (n=3). (B) WC complex does not bind to the *qrf* promoter in DD. WC-2 ChIP assays showing the relative levels of WC binding at the *frq* (dLRE) and *qrf* (qLRE) promoters at the indicated time points in DD. (C) Luciferase reporter assay showing the normalized *frq* (left) or *qrf* (right) promoter activity after one day in DD in wild-type strains that carry P*frq:luc* or P*qrf:luc* construct, respectively.

In the frq^9 mutant, only truncated FRQ protein is made due to a frame-shift mutation; this results in the loss of the circadian negative feedback loop and high *frq* mRNA levels (Aronson et al., 1994a). The higher level of *frq* in the frq^9 mutant was accompanied by a lower level of *qrf* RNA (Figure 3-11A), suggesting that *frq* transcription also inhibits *qrf* expression. To further test this conclusion, we examined

whether an induction in *frq* transcription leads to the inhibition of qrf expression. The *frq*^{10},frq^{qLREmut} strain grown in DD was transferred to light. Because of the mutation of qLRE in the qrf promoter, only *frq* transcription and not *qrf* expression was induced. The induction of frq transcription was, as expected, associated with a significant decrease of qrf transcription levels (Figure 3-11B). In addition, we also compared the levels of *frq* and *qrf* transcripts in DD in the wild-type and *wcc*^{DKO} strains (Figure 3-11C). At both DD time points evaluated, the decrease of *frq* mRNA levels was accompanied by a significant increase of *qrf* mRNA levels. Because WC complex does not regulate *qrf* transcription in DD, such an effect should be due to the increase in frq transcription. Together, these results indicate that *frq* transcription inhibits the expression of *qrf*.

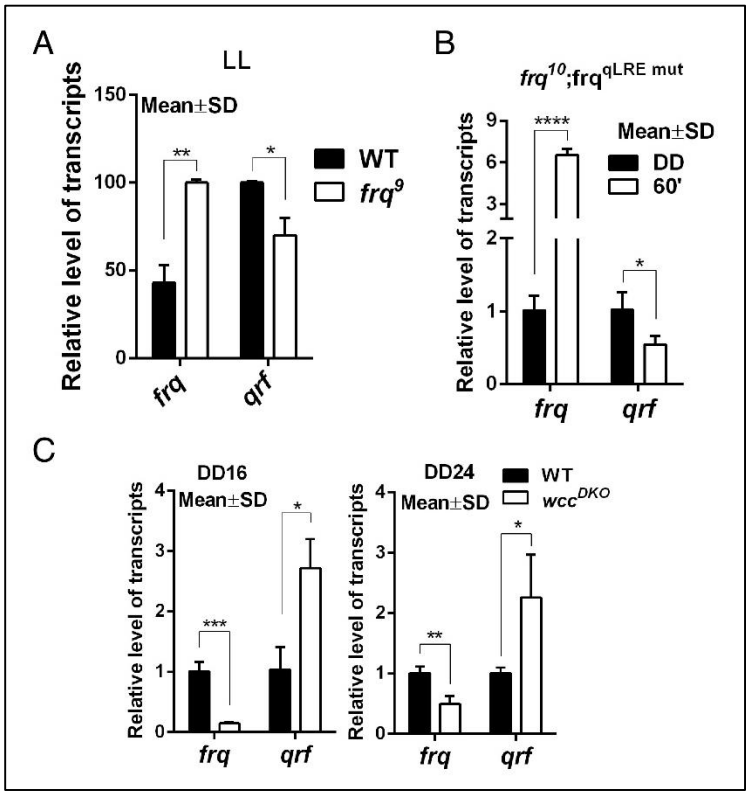

Figure 3-11 *frq* transcription represses *qrf* expression.
(A) Densitometric analyses of three independent northern blot results indicate that levels of qrf transcripts are reduced in the *frq*^{9} strains as a result of increased *frq* expression. (B) Strand-specific RT-qPCR results showing the levels of *frq* and *qrf* transcripts in the *frq*^{10};frq^{qLRE} mut strain at DD24 or 60 mins after the dark to light transfer. (C) Levels of *frq* and *qrf* transcripts in the wild-type and *wcc*^{DKO} strains measured by strand-specific RT-qPCR at the indicated DD.

3.3.5 Rhythmic frq transcription drives an antiphasic rhythm of qrf transcripts

What results in the rhythmic *qrf* transcript level without rhythmic activation of *qrf* transcription? The antiphasic relationship between *frq* and *qrf* mRNA rhythms and the repression of *qrf* by *frq* transcription raised the possibility that the antiphasic rhythm of qrf transcript levels is driven by rhythmic *frq* transcription. To test this hypothesis, we created a luciferase reporter construct (P*min-luc*-P*frq*) with convergent transcription and introduced it into a wild-type *Neurospora* strain. In this construct, the sense luciferase mRNA expression is driven by a previously described constitutive minimal promoter (Bell-Pedersen et al., 1996), and the antisense luciferase mRNA is driven by the *frq* promoter (Figure 3-12A). Wild-type strains containing the P*frq-luc* or P*min-luc* (without the frq promoter to drive the antisense luciferase RNA) construct were used as controls. As predicted, the P*min-luc*-P*frq* strain exhibited a robust circadian luminescence rhythm (Figure 3-12A). In contrast, the P*min-luc* strains failed to generate a circadian rhythm of luciferase activity (Figure 3-12B). Importantly, the phase of the P*min-luc*-P*frq* rhythm was antiphase to that of the P*frq-luc* rhythm. These results indicate that the antiphasic rhythm of *qrf* expression is driven by the rhythmic *frq* transcription. Therefore, the mutual inhibition of *frq* and *qrf* transcription forms a double negative feedback loop that results in antiphasic rhythms of *frq* and *qrf* transcripts (Figure 3-14A).

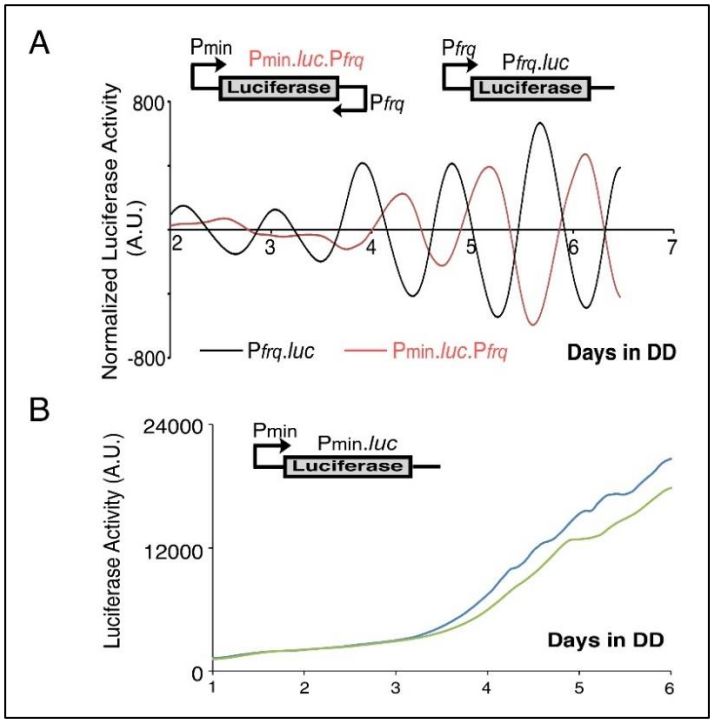

3-12 Convergent transcription drives an antiphasic oscillation of luciferase reporter. (A) Luciferase reporter assay showing the normalized luminescence levels in a wild-type strain that carries the P*frq.luc* (black) or P*mini.luc*.P*frq* (red) construct. (B) The unnormalized luciferase activity of the wild-type strain carrying the P*min-luc* construct. Results of two independent transformants were shown.

3.3.6 Mathematical modeling of the Neurospora oscillator with the double negative feedback loop

We then used mathematical modeling (Figure 3-13) to determine the importance of the double negative feedback loop and provide an explanation for our observed results. By changing two non-experimentally determined rate constants in a previous developed mathematical model for the *Neurospora* circadian oscillator (Hong et al., 2008), we found that in the absence of *qrf*, the previously known circadian feedback loops generate only a low amplitude *frq* oscillation that cannot be sustained and damps out quickly (Figure 3-14B). When the expression of *qrf* and the double negative feedback loops were introduced into the model, both *frq* and *qrf* mRNA levels oscillated robustly with antiphasic rhythms (Figure 3-14C). When *qrf* expression was increased above a certain

threshold level, the *frq* oscillation was not sustained (Figure 3-14D). Thus, our mathematical model is in good agreement with the experimental observations presented here. Our results suggest that the previously known circadian negative feedback loop, although not sufficient to sustain a persisting rhythm, are the source of the rhythmicity that is amplified and sustained by the double negative feedback loop formed by the mutual inhibition of *frq* and *qrf* transcription. Together, our results demonstrate that the double negative feedback loop and the expression of *qrf* are required for sustained and robust rhythmic *frq* expression in *Neurospora*.

$$\frac{d[frq\text{mRNA}]}{dt} = \frac{k_1[\text{WC1}_n]^2}{K + [\text{WC1}_n]^2} - k_4[frq\text{mRNA}] - k_{19}[qrf\text{mRNA}] + k_{01} \quad (1)$$

$$\frac{d[FRQ_c]}{dt} = k_2[frq\text{mRNA}] - (k_3 + k_5)[FRQ_c] \quad (2)$$

$$\frac{d[FRQ_n]}{dt} = k_3[FRQ_c] + k_{14}[FRQ_n{:}\,\text{WC1}_n] - [FRQ_n](k_6 + k_{13}[\text{WC1}_n]) \quad (3)$$

$$\frac{d[wc1\text{mRNA}]}{dt} = k_7 - k_{10}[wc1\text{mRNA}] \quad (4)$$

$$\frac{d[\text{WC1}_c]}{dt} = \frac{k_8[FRQ_c][wc1\text{mRNA}]}{K_2 + [FRQ_c]^2} - (k_9 + k_{11})[\text{WC1}_c] + k_{02}[wc1\text{mRNA}] \quad (5)$$

$$\frac{d[\text{WC1}_n]}{dt} = k_9[\text{WC1}_c] - [\text{WC1}_n](k_{12} + k_{13}[FRQ_n]) + k_{14}[FRQ_n{:}\,\text{WC1}_n] \quad (6)$$

$$\frac{d[FRQ_n{:}\,\text{WC1}_n]}{dt} = k_{13}[FRQ_n][\text{WC1}_n] - (k_{14} + k_{15})[FRQ_n{:}\,\text{WC1}_n] \quad (7)$$

$$\frac{d[qrf\text{mRNA}]}{dt} = k_{16} - k_{17}[frq\text{mRNA}] - k_{18}[qrf\text{mRNA}] \quad (8)$$

Dimensionless value (h^{-1})

k_1	k_2	k_3	k_4	k_5	k_6	k_7	k_8	k_9	k_{10}	k_{11}	k_{12}
1.2	1.8	0.15	0.23	0.27	0.07	0.16	0.8	40	0.1	0.05	0.02
k_{13}	k_{14}	k_{15}	k_{16}	k_{17}	k_{18}	k_{19}	K	K_2	k_{01}	k_{02}	
50	1.0	5	0.5	0.35	0.23	0.1	1.25	1.0	0.64	0.1	

Figure 3-13 Mathematical equations and parameters for *Neurospora* circadian oscillator simulations.

Mathematical modeling of the *Neurospora* circadian oscillator with the double negative feedback loop. The differential equations used in the model are shown. The model is identical to a previously developed model(Hong et al., 2008) with the exception of

equation 1, which in this case includes the inhibition of *frq* transcription by *qrf*, and the equation 8, which includes the inhibition of qrf transcription by *frq*. The rate constants used in the simulations were listed below.

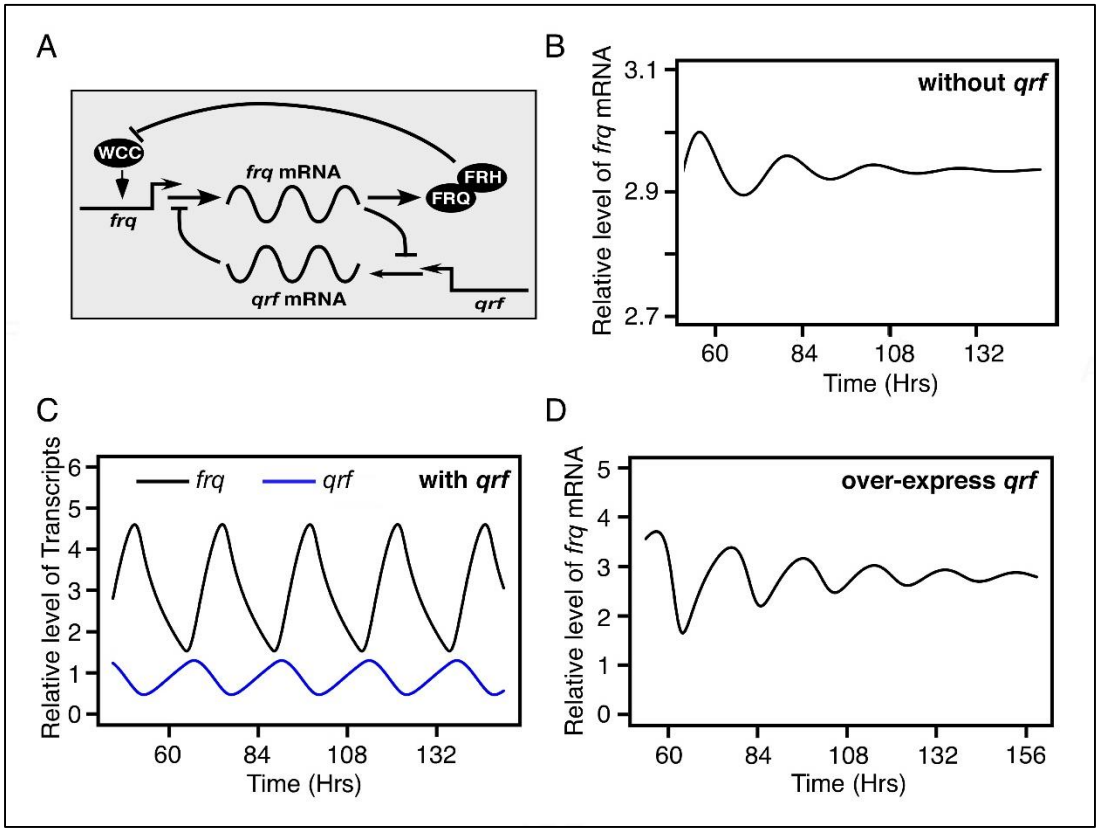

Figure 3-14 Mathematical simulations of the *Neurospora* circadian oscillator.
(A) A simple model of the *Neurospora* circadian clock that depicts the double negative feedback loop formed by the mutual inhibition of *frq* and *qrf* transcription. (B) Mathematical simulation of relative *frq* mRNA levels in DD when the double negative feedback loop is deleted by removing the expression of *qrf* (k_{19} =0). (C) Mathematical simulation of relative *frq* and *qrf* RNA levels in DD when *qrf* expression is introduced (k_{16}=0.5, k_{17}=0.35, k_{19}=0.1). (D) Mathematical simulation of relative *frq* RNA levels when *qrf* is overexpressed (k_{16} =0.91).

3.3.7 Convergent frq and qrf transcription causes stalling of RNA polymerase II

Sense and antisense transcripts of frq may form double-stranded RNA, which then can be processed into small interfering RNAs (siRNAs) to regulate transcription through

the RNAi pathway. Light-induced *frq* transcription, however, was found to be normal in both a *dicer* double mutant and in a *qde-2* (encodes the *Neurospora* Argonaute protein) mutant (Figure 3-15A, B) (Chang et al., 2012). In addition, the levels of *frq* and *qrf* were normal in both mutants (Figure 3-15C). Furthermore, the circadian conidiation rhythms of the RNAi mutants were similar to that of the wild-type strain (Figure 3-15D). Convergent transcription is also known to induce dynamic DNA methylation in the promoter region of *frq* (Belden et al., 2011; Dang et al., 2013). Deletion of two genes (*dim-2* and *dim-5*) that are required for DNA methylation in *Neurospora* had no effect on the light induced *frq* transcription (Figure 3-16A, B), however. These results indicate that double-stranded RNA formation, the RNAi pathway, and DNA methylation do not play significant roles in the mechanism that links regulation of *frq* and *qrf* transcription.

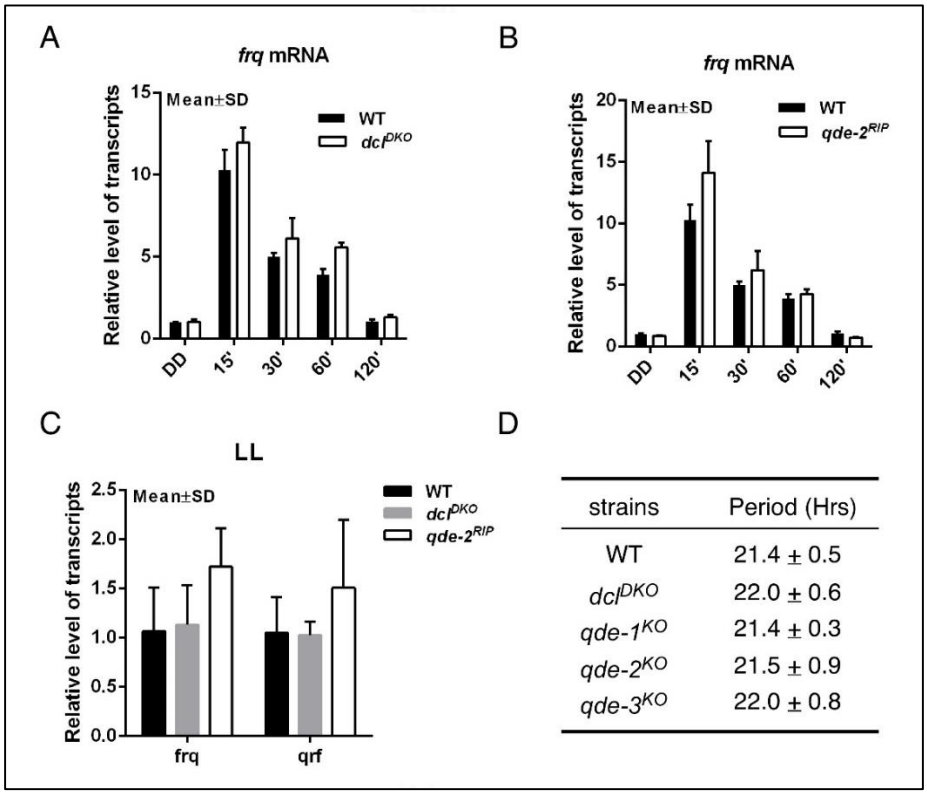

strains	Period (Hrs)
WT	21.4 ± 0.5
dcl^{DKO}	22.0 ± 0.6
qde-1^{KO}	21.4 ± 0.3
qde-2^{KO}	21.5 ± 0.9
qde-3^{KO}	22.0 ± 0.8

Figure 3-15 RNAi pathways do not significantly affect circadian clock.
(A, B) Strand-specific RT-qPCR results showing the induction of *frq* after a light pulse are similar in the indicated strains at DD24. (C) Strand-specific RT-qPCR results showing similar expression levels of *frq* and *qrf* in the indicated strains in LL. (D) A table showing the period lengths of the conidiation rhythms in the wild-type and different RNAi mutants.

We next examined whether qrf can regulate *frq in trans*. We created a *frq* construct in which the *frq* promoter was deleted and targeted it to the *csr-1* locus in the frq^{10} and frq^{10};$frq^{qLRE\ mut}$ strains (Figure 3-2D). In the frq^{10};qrf strain, the *qrf* RNA levels were restored to those of the wild-type strain without detectable expression of *frq* (Figure 3-17A), indicating the specificity of the *qrf*-expressing construct. Therefore, in the frq^{10};$frq^{qLRE\ mut}$;qrf strain, the light-induced *qrf* can only be expressed from the *csr-1* locus. Even though the levels of *qrf* transcripts were restored to normal levels in the frq^{10};$frq^{qLRE\ mut}$;qrf strains, the levels of *frq* RNA were not rescued (Figure 3-17B, C). This result indicates *qrf* can only regulate *frq* transcription *in cis*.

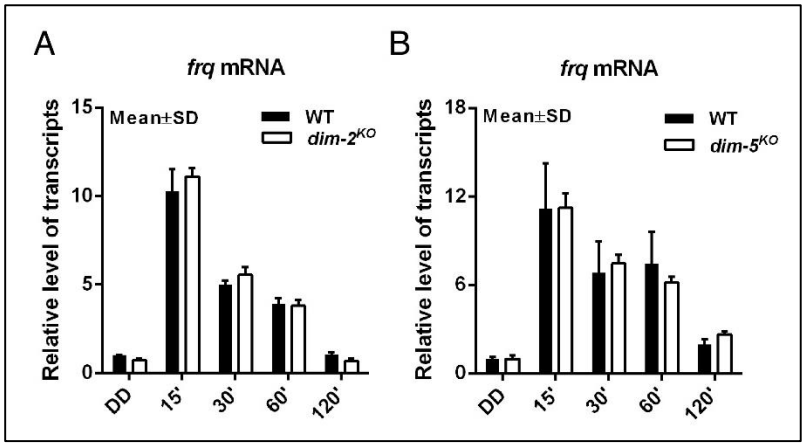

Figure 3-16 DNA methylation pathways do not play a significant role in the clock.
Strand-specific RT-qPCR results showing the induction of frq after a light pulse are similar in the indicated trains at DD24. Error bars are standard deviations (n=3).

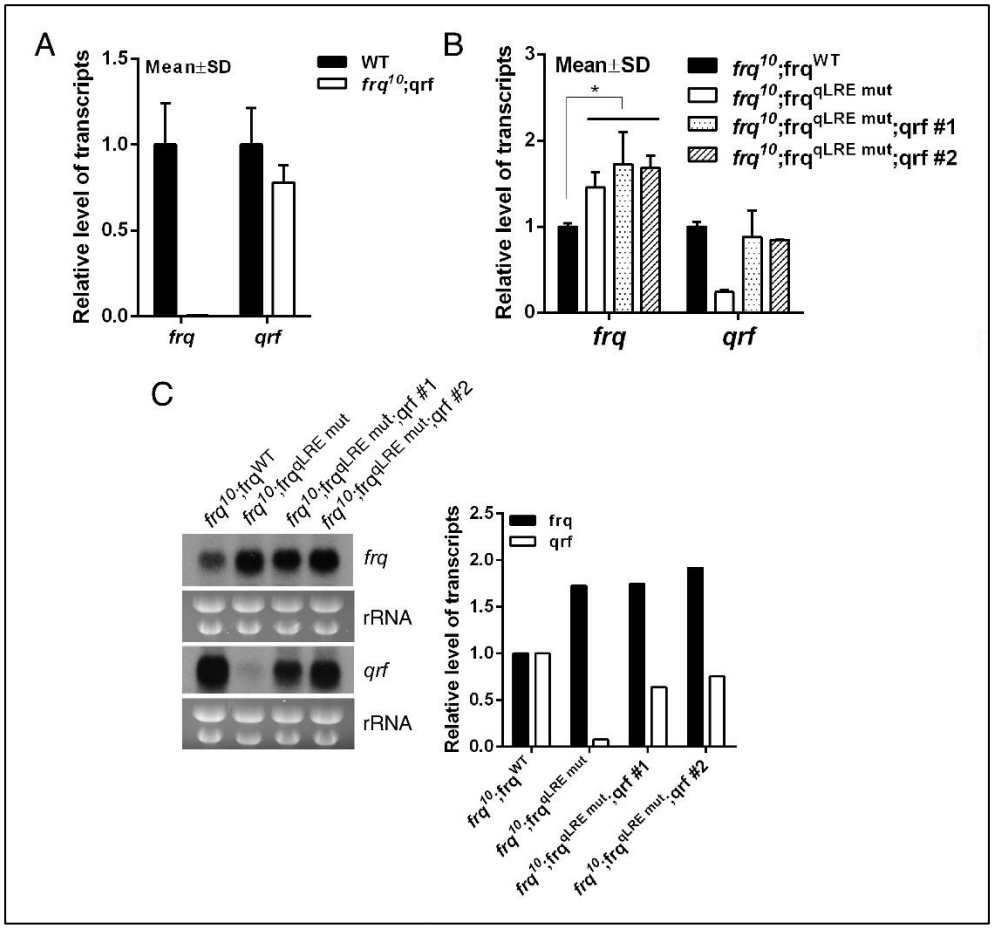

Figure 3-17 *qrf* represses *frq* expression *in cis*.
(A) Strand-specific RT-qPCR results showing that only *qrf* is expressed from the *qrf* construct in the *frq*^{10}; qrf strain. (B) Strand-specific RT-qPCR results showing the levels of *frq* and *qrf* transcripts in the indicated strains in LL. Error bars are standard deviations. Asterisk indicates P value < 0.05 (n=3). (C) Northern blot results showing that expression of *qrf in trans* in the *frq*^{10};frq$^{\text{qLRE mut}}$;qrf strains does not repress *frq* expression. Densitometric analysis of the northern blot results is shown at right.

We then examined how *qrf* affects *frq* at the transcriptional level. WC complex binding to the *frq* promoter initiates WC-dependent *frq* transcription. WC-2 ChIP assays showed that WC complex binding at the *frq* promoter was not affected by the mutation of the qLRE element in the *qrf* promoter (Figure 3-18A, B). In contrast, RT-qPCR of *frq* mRNA over an intron showed that *frq* pre-mRNA levels in LL and after a light induction

were significantly elevated in strains with mutated qLRE element (Figure 3-19A, B). On the other hand, the induction of *qrf* expression in the *frq*^{10};frq.aq strain did not affect *frq* mRNA stability (Figure 3-20). Together, these results suggest that *qrf* regulates *frq* at the transcriptional level at a step subsequent to transcriptional initiation.

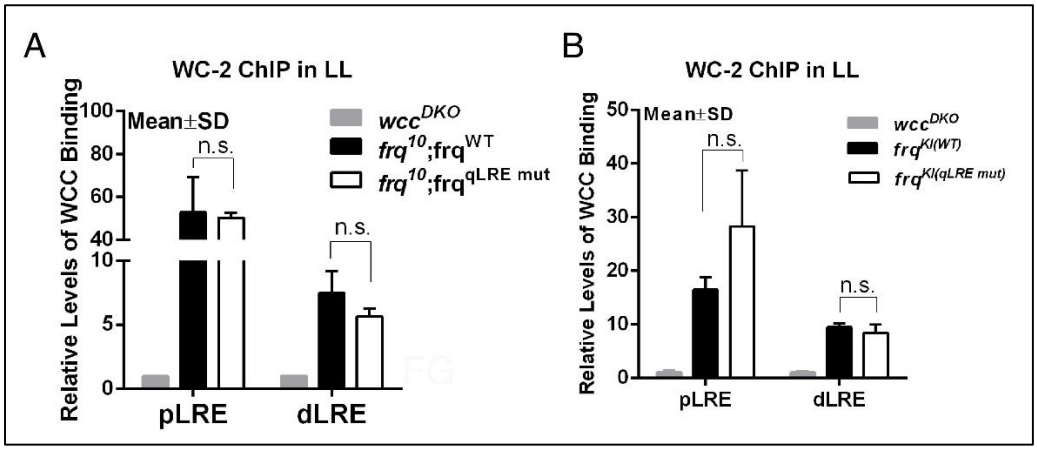

Figure 3-18 WC complex binding at the *frq* promoter was not affected by the mutation of the qLRE element.
WC-2 ChIP assays showing the relative WC binding levels at the frq promoter in LL in the indicated strains. The *wcc*^{DKO} was used as a negative control for ChIP. n.s. stands for not statistically significant (n=3).

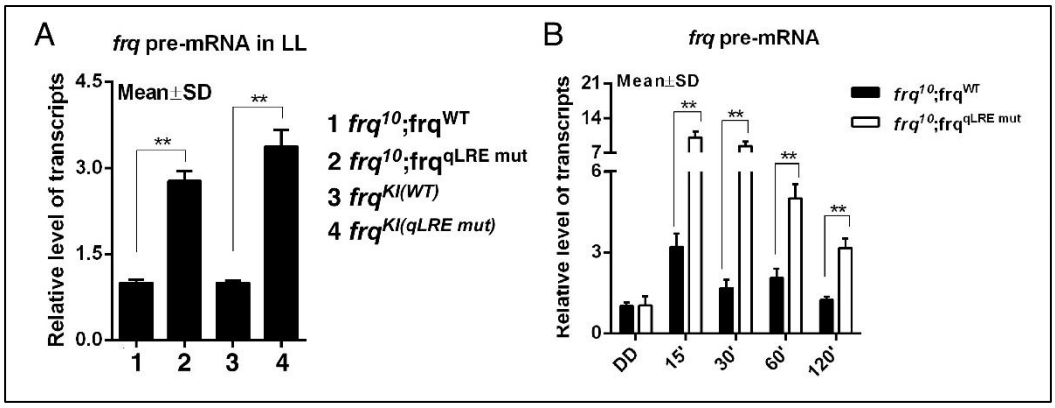

Figure 3-19 The levels of *frq* pre-mRNA are repressed by *qrf*.
(A) Strand-specific RT-qPCR results showing the levels of *frq* pre-mRNA levels in the indicated strains in LL. (B) Strand-specific RT-qPCR results showing that the mutation of the qLRE element in the *qrf* promoter results in significant increases in light-induced *frq* pre-mRNA expression.

After transcriptional initiation, the RNA polymerase II (pol II) carboxy-terminal domain (CTD) is phosphorylated at serines 2 and 5 (Hsin and Manley, 2012; Komarnitsky et al., 2000). Ser 5 phosphorylation is normally enriched in polymerases near the 5' ends of transcribed regions, whereas Ser 2 phosphorylation is enriched on polymerases bound toward the 3' ends of transcripts. In contrast to this expectation, ChIP assays of the *frq* locus using Ser 2 and Ser 5 phospho-specific pol II CTD antibodies showed that both modifications of pol II peaked at the same position in the middle of the transcribed *frq* region (Figure 3-21, two top panels). The mutation of the qLRE resulted in significant decreases of both Ser 2 and Ser 5 phosphorylation. Because stalling or collision of Pol II is known to result in accumulation of pol II in the middle of the gene (Hobson et al., 2012), these results suggest that transcribing pol II stalls in the middle of *frq* locus due to convergent transcription of *frq* and *qrf*.

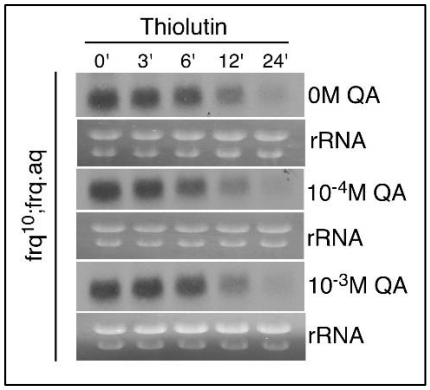

Figure 3-20 *qrf* does not affect *frq* mRNA stability. Northern blot results showing that the stability of *frq* mRNA is not affected by the transcription of *qrf*. The *frq*^{10};frq.aq strain that can induce *qrf* expression in the presence of QA was used. Thiolutin, a transcription inhibitor (Guo et al., 2009), was added in the culture to block *frq* transcription so that *frq* mRNA stability could be determined. Cultures were harvested at the indicated time points after the

Phosphorylation of pol II has been shown to recruit a histone methyltransferase to methylate histone H3 at lysine 36 (H3K36) residue (Li et al., 2003; Phatnani and Greenleaf, 2006). ChIP assays showed that H3K36me3 enrichment at the *frq* locus peaked at the same position as did the Ser 2 and 5 phosphorylation of pol II, and the

mutation of the qLRE reduced H3K36me3 (Figure 3-21, bottom panel). This result further suggests that pol II stalls in the middle of the *frq* locus.

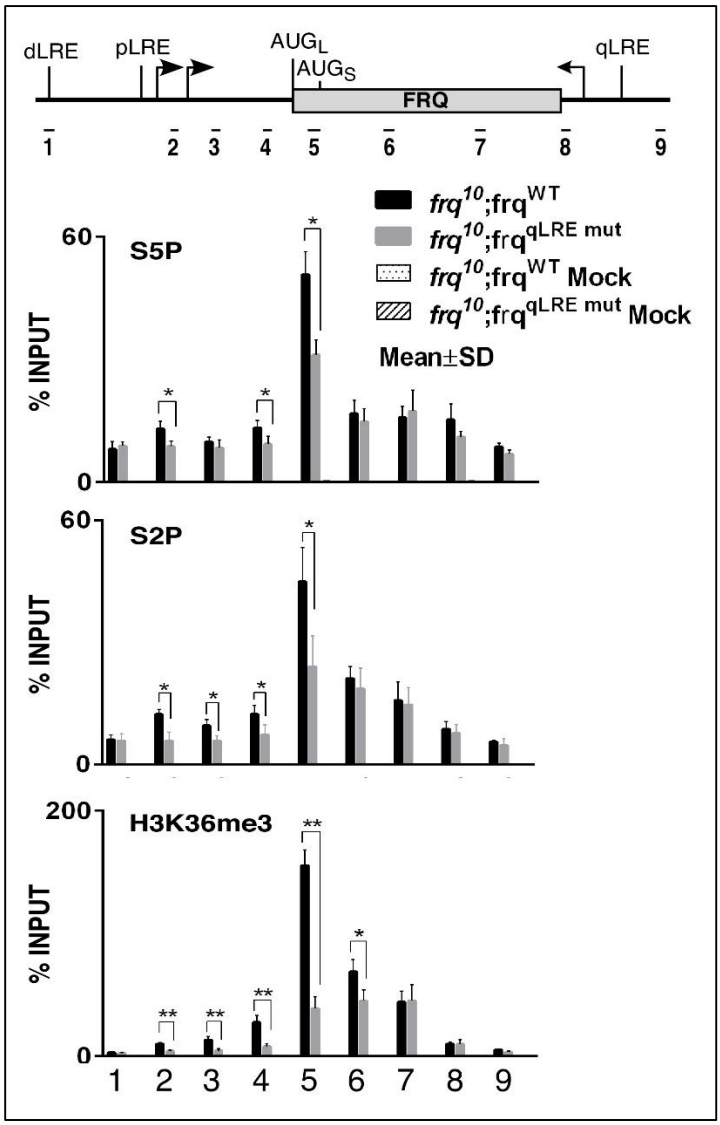

Figure 3-21 The transcribing pol II stalls in the middle of *frq* locus due to convergent transcription of *frq* and *qrf*. ChIP assays showing the relative enrichment of pol II Ser 5, pol II Ser 2, and H3K36me3 in the *frq* locus.

SET-2 has been shown to methylate H3K36 in *Neurospora* (Adhvaryu et al., 2005). To examine the role of this chromatin modification in suppressing *frq* transcription, we examined the levels of *frq* and *qrf* in *set-2^{KO}* single and *frq^{9};set-2^{KO}* double mutants. Even though the levels of *frq* and *qrf* were only modestly but significantly increased in the *set-*

2^{KO} single mutants (likely due to the negative feedback role of FRQ), their levels were markedly elevated in the frq^{9};*set-*2^{KO} double mutant (Figure 3-22), suggesting that H3K36me3 contributes to the suppression of *frq* and *qrf* transcription. Further supporting the role of H3K36me3 function, we recently showed that SET-2 is required for circadian clock function in *Neurospora* (Zhou et al., 2013).

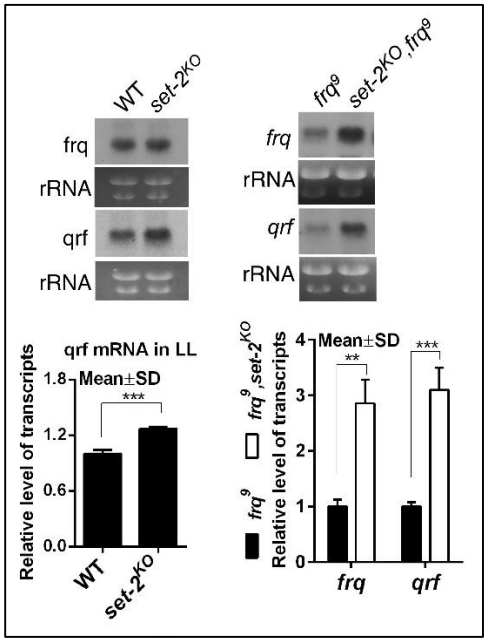

Figure 3-22 H3K36me3 contributes to the suppression of *frq* and *qrf* transcription.
Northern blot analyses showing the levels of *frq* and *qrf* in the wild-type, *set-*2^{KO}, frq^{9} and *set-*2^{KO};frq^{9} strains (top panels). The densitometric analyses of three independent experiments are shown. The asterisks indicate P values <0.01.

3.3.8 Convergent transcripiton of frq and qrf results in pre-mature transcriptional termination

When pol II proteins collide during transcription of genes in opposite orientations, the two proteins may not be able to bypass each other (Hobson et al., 2012). Rather, transcription could terminate prematurely. Thus, we expected to observe production of truncated *frq* and *qrf* transcripts from their respective 5' ends but not their 3'ends. Because such prematurely terminated transcripts are normally rapidly degraded, we first

searched a panel of *Neurospora* ribonuclease mutants for the nuclease that is involved in degrading the truncated transcripts. The *Neurospora* RNA exosome was previously shown to be involved in degrading the full-length *frq* transcripts (Guo et al., 2009). Northern blot analysis using an RNA probe (*frq*-N term) that is specific to 5' end of the sense *frq* (upstream of the detected Ser 2 and Ser 5 peak, Figure 3-23A) showed that in the wild-type strain, little truncated *frq* transcript was detected even after long exposure of the northern blot (Figure 3-23B). Silencing of *rrp44*, which encodes the catalytic subunit of exosome, however, resulted in the appearance of a low molecular weight RNA smear (~0.5 -2 kb). In contrast, when a probe (*frq*-C term) specific for the 3' half of the sense *frq* was used, no truncated *frq* transcripts were be detected (Figure 3-23C), but a *qrf*-specific probe (*qrf*-N-term) corresponding the same region detected truncated *qrf* transcripts (Figure 3-23D). Importantly, the signal intensity of the low molecular weight smear detected by the *frq*-N term probe in the WT;*dsrrp44* strain was dramatically decreased in the $frq^{KI(qLRE\ mut)}$*;dsrrp44* strain in which the qLRE was mutated at the endogenous *qrf* locus (Figure 3-23E). These results indicate that simultaneous expression of sense and antisense transcripts results in pol II collision that induces premature transcription termination. Therefore, both premature transcription termination and chromatin modifications contribute to the transcriptional inhibition of *frq* by *qrf.*

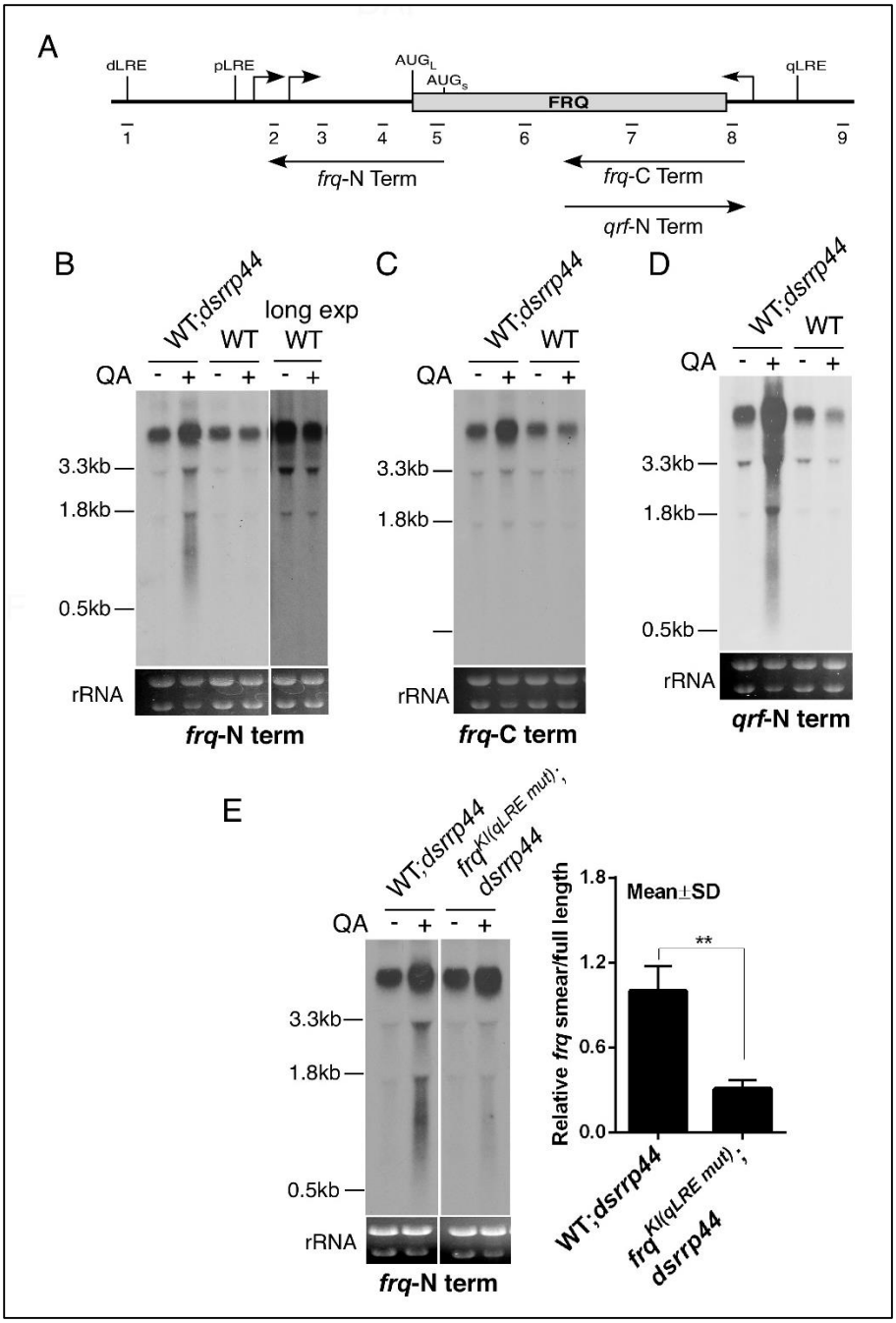

Figure 3-23 Convergent transcription of the *frq* locus results in premature transcription termination and truncated *frq* and *qrf* transcripts.
(A) A diagram depicting the strand-specific RNA probes used in northern blot analyses. (B) Northern blot analysis using a *frq* riboprobe (*frq*-N term) specific for the 5' half of the *frq* transcripts in the wild-type and WT;*dsrrp44* strains. The addition of QA results in the production of *rrp44*-specific double stranded RNA and silencing of *rrp44* expression.

(C) Northern blot analysis using a *frq* riboprobe (frq-C term) specific for the 3' half of the *frq* transcripts. (D) Northern blot analysis using a *qrf* riboprobe (qrf-N term) specific for the 5' half of the qrf transcripts. (E) Northern blot analysis using a *frq* riboprobe (*frq*-N term) specific for the 5' half of the *frq* transcripts in the WT;*dsrrp44* and $frq^{KI(qLRE^{mut})}$;*dsrrp44* strains. The ratios between truncated and full-length *frq* transcripts based on densitometric analyses in three independent experiments are shown at right. The asterisks indicate P value <0.01.

CHAPTER FOUR

CONCLUSION AND FUTURE DIRECTION

4.1 Biochemical reconstitution of an Argonaute-dependent small RNA biogenesis pathway

Argonaute-dependent sRNA biogenesis are found in many organisms. Here, by using the *Neurospora* milR-1 milRNA as an example, we established a biochemical mechanism for an Argonaute-dependent sRNA production process and uncovered the collaborative and distinct roles of the Argonaute QDE-2, exosome and QIP in the milR-1 maturation process. Our biochemical and genetic results suggest that the maturation of milR-1 is a five-step process (Figure 4-1). First, the 170-nt pri-milR-1 is directly cleaved by Dicer to generate the ~33-nt double-stranded pre-milRNA. Although we showed that the recombinant DCL-2 is sufficient to convert pri-milRNA into the functional pre-milR-1, pre-milR-1' was not produced by Dicer cleavage *in vitro*, and it is likely that additional factors are involved in this step *in vivo*. We previously showed that the down-regulation of MRPL3, a putative RNase III domain-containing protein, resulted in a decrease in the levels of pre-milR-1 (Lee et al., 2010), suggesting that MRPL-3 may also participate in this process.

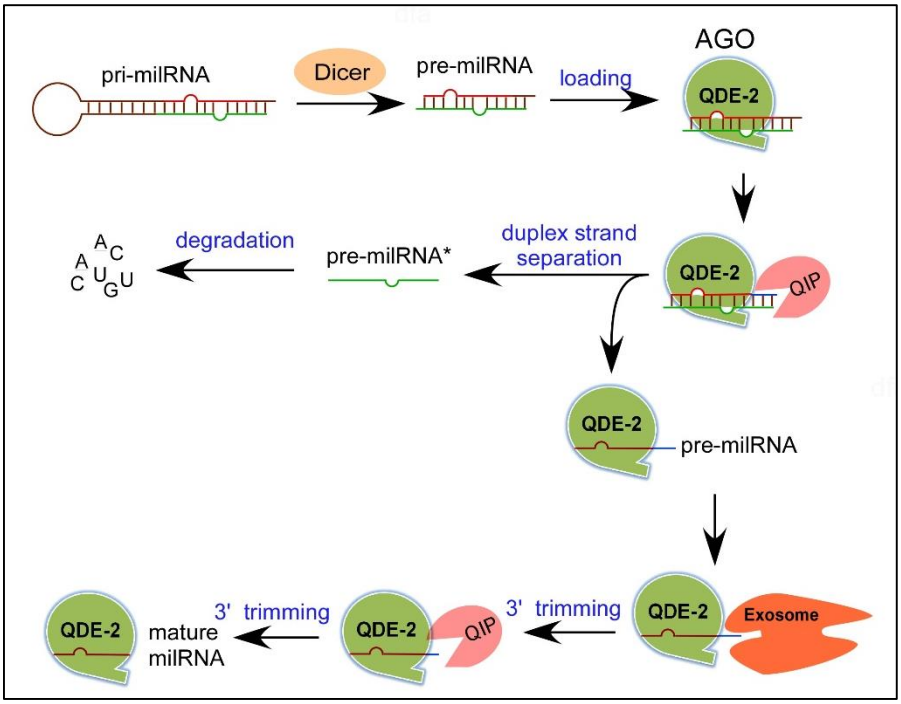

Figure 4-1 Model of milR-1 biogenesis pathway from pri-milRNA.

The second step is Argonaute QDE-2 binding of the duplex pre-milRNA. Third, QIP, which is recruited by QDE-2, separates the pre-milRNA duplex into single-stranded RNAs in collaboration with QDE-2; the pre-milRNA strand remains QDE-2-associated, and the pre-milRNA* strand is released from the complex and degraded way. We demonstrated that QIP is indeed a 3' to 5'exoribonuclease (Figure 2-3) and importantly, it also possess an activity that can trigger the stand-separation of QDE-2 associated duplex RNA *in vitro* (Figure 2-16). The role of QIP in strand-separation of the pre-milR-1 duplex *in vivo* was further supported by the increase of pre-milR-1 duplex levels in *qip* mutants (Figures 2-3 and 2-5) and by its role in converting the QDE-2-associated siRNA duplex into single strands (Maiti et al., 2007). Because both pre-milR-1 and siRNA are maintained in duplex forms in qde-2 mutants (Figure 2-3) (Maiti et al., 2007), QDE-2

should also contributes to the duplex separation process *in vivo*. This notion is consistent with the existence of low levels of single-stranded pre-milRNA in the *qip* mutants (Figure 2-5, 2-6) and with previous results that the *Drosophila* Ago1 can passively separate miRNA duplexes *in vitro* (Kawamata et al., 2009). The ability of QIP to separate QDE-2-bound duplex pre-milRNA and its role in siRNA RISC activation suggest that strand-separation of Argonaute-bound duplex siRNA and miRNA is an important step in the activation of siRISC and miRISC. Our results and the fact that the budding yeast homolog of QIP, Gfd2p, was identified as a high copy suppressor of an RNA helicase mutant (Estruch and Cole, 2003) suggest that similar exoribonucleases may also possess dsRNA strand-separation activity.

The selective dissociation of the milRNA* strand of the pre-milR-1 from QDE-2 is likely pre-determined by the asymmetric loading of the duplex pre-milRNA onto QDE-2, so that the strand separation process preferentially dissociates milRNA* strand from the complex. The asymmetric loading of siRNAs, duplex-miRNAs, and pre-piRNAs into Argonaute proteins was recently suggested to be due to the selective binding of Argonaute proteins to small RNAs with a 5' U (Kawaoka et al., 2011; Mi et al., 2008; Seitz et al., 2011). The pre-milR-1 milRNA strand also has a strong preference for 5' U, thus, the asymmetric loading of the pre-milRNA duplex may be due to the selective binding of QDE-2 to the pre-milRNA strand.

In the fourth step, the exosome trims the QDE-2 bound pre-milRNAs from 3' to 5' end into sRNAs of intermediate sizes. Our conclusion that the exosome carries out this trimming is supported by several lines of evidence. Recombinant QIP cannot efficiently

process the single-stranded full-length pre-milR-1and prefers shorter pre-milR-1 substrates (Figure 2-4). In addition, there is the accumulation of a ladder of single-stranded pre-milRNAs with sizes between the mature milR-1 and pre-milR-1 in the *qip* mutants (Figure 2-5), indicating that QIP can only efficiently process pre-processed pre-milR-1. Importantly, the silencing of the essential exosome components in *Neurospora* abolishes the QDE-2-dependent maturation of milR-1 and the production of the processed pre-milRNA ladder, indicating that the exosome is required for milR-1 maturation and is responsible for the generation of the pre-milR-1 substrates for QIP. Furthermore, even in the absence of QIP, a low level of the processed pre-miRNA with sizes similar to the mature milR-1 can be observed (Figures 2-5, 6), suggesting that exosome alone is able to convert pre-milRNA into mature milRNA, albeit very inefficiently.

In the fifth and final step, the exosome-processed pre-milRNAs are further processed into mature milRNAs in a process involving both QIP and exosome. The accumulation of the intermediate-sized partially processed pre-milRNAs in the *qip* mutants indicates that they are substrates of QIP. Supporting this notion, QIP can efficiently convert this ladder of processed pre-milRNAs into mature milRNA *in vitro* (Figure 2-16). In addition, we found that the addition of exosome strongly promoted the QIP-mediated maturation of QDE-2-bound pre-milRNA (Figure 2-18), indicating that QIP and exosome collaborate in the 3’ to 5’ progressive trimming of pre-milR-1 into the mature milRNAs.

Our results also shed important insights in the role of Argonauate protein in small RNA maturation. Based on our results, the Argonaute QDE-2 has three essential roles in the milR-1 maturation process: 1) it binds to pre-milR-1 and determines which milR-1 strand will be matured, 2) it recruits exoribonucleases to process pre-milR-1, and 3) it determines the sizes of milR-1 by protecting the mature milR-1 from further processing. We showed that the duplex pre-milR-1 was first become single-stranded before being proceed, however, pre-milR-1 and pre-milR-1* have complete different outcome after processing: while pre-milR-1 was matured into milR-1, the pre-milR-1* was degraded away. In addition, we showed that although the single-stranded pre-milR-1 is associated with QDE-2, the single-stranded pre-milR-1* is not (Figure 2-16). This result is also consistent with the much slower degradation kinetics of pre-milR-1* than that of pre-milR-1 (Figure 2-16) and the fact that QIP can degrade the synthetic unprotected pre-milR-1 into very small RNA fragments (Figure 2-3). Thus, the different processing outcomes of pre-milR-1 and pre-milR-1* is due to the binding of pre-milR-1 by QDE-2.

Crystal structure of an archaeal Argonaute suggested both the 5’ and 3’ ends of the guide RNA are anchored on the protein and the 5’ end of the guide RNA is anchored within a highly conserved basic pocket, suggesting that when in a complex, ~21nt from the 5’end of the small RNA are in complex with and protected by Argonaute (Ma et al., 2005; Parker et al., 2004; Wang et al., 2008). Although the association between QDE-2 and pre-milR-1 protect the region containing the mature milR-1, the 3’ ends of the large pre-milR-1 should be accessible by the nucleases. Thus, the sizes of mature milR-1 are

determined by the region of pre-milR-1 that is protected by QDE-2 from further processing.

Recently, a cell-free system derived from a silkworm ovary-derived cell line was established and was shown to recapitulate key steps of animal piRNA biogenesis (Kawaoka et al., 2011). The proposed 3' end trimming model for piRNA maturation is very similar to that we proposed for biogenesis of the *Neurospora* milR-1. However, the enzyme or enzymes that trim the piRNA-precursor in a PIWI-dependent manner have not been identified. Our study suggests that the highly conserved RNA exosome and DEDDh superfamily of exonucleases may function as the trimmer enzymes in piRNA and other small RNA processing. Since the submission of our paper, the putative exoribonuclease Nibbler has been shown to modify the 3' ends of mature miR-34 miRNAs in *Drosophila* (Han et al., 2011; Liu et al., 2011). Interestingly, even though QIP and Nibbler are not sequence homologs, they both belong to the DEDDh superfamily of the ribonuclease.

Exosome components were previously suggested to be involved in small RNA decay (Bail et al., 2010; Halic and Moazed, 2010; Ibrahim et al., 2010), and exosome has also been shown to process the 3' ends of some *Drosophila* mirtron-derived miRNAs (Flynt et al., 2010). In the fission yeast, the Argonaute-dependent priRNA levels and size distributions were found to be modestly effected in a *dis3* mutant (Halic and Moazed, 2010), but a clear role for exosome in priRNA production is still unclear. In *Neurospora*, exosome is clearly essential for *Neurospora* milR-1 maturation. On the other hand, we found that the silencing of the exosome components resulted in the significant accumulation of siRNA and other milRNAs examined (Figure 2-19), indicating that

exosome also functions in sRNA decay pathways in *Neurospora*. Therefore, exosome has at least two opposing roles in regulating sRNA levels.

4.2 Transcriptional interference by sense and antisense of *frequency* forms a double negative feedback loop that is required for circadian gene expression

In eukaryotic circadian oscillators, the core circadian negative feedback loops are thought to be able to generate the endogenous oscillations of expression of clock genes and clock-controlled genes (Bell-Pedersen et al., 2005; Dunlap, 1999; Young and Kay, 2001). In this study, we discovered that sense and antisense transcription of *frq* forms a novel double negative feedback loop that is interlocked with the previously characterized core circadian feedback loops in *Neurospora*. The transcription of qrf inhibits the transcription of *frq*, and the transcription of *frq* represses the transcription of *qrf*. Moreover, the rhythmic *frq* transcription drives an antiphasic oscillation of *qrf* level. The antiphasic oscillations of *frq* and *qrf* expression are expected to resonate to achieve high amplitude robust circadian gene expression. When *frq* RNA expression is high the impact of transcriptional collision from convergently transcribed *frq* and *qrf* is low. When expression of *frq* is repressed via FRQ-FRH feedback on the WCC however, *frq* expression is further reduced due to the high expression of *qrf* and the resultant transcriptional collision of pol II complexes. Supporting this conclusion, our genetic results and mathematical modeling demonstrated that the expression of *qrf* and the double negative feedback loop are required for sustained and robust circadian gene expression. In the absence of *qrf* expression, the amplitude of the circadian rhythm was low and

damped out quickly. Therefore, to achieve robust and sustained circadian gene expression, the basic oscillation generated the core circadian feedback loops must be amplified and sustained by this double negative feedback loop.

In the silkmoth and mouse liver, antisense RNAs of the core animal clock gene *per* are present (Koike et al., 2012; Sauman and Reppert, 1996; Vollmers et al., 2012). Interestingly, the sense and antisense per RNAs oscillate in antiphase to each other as do *frq* and *qrf*. Because of the similar roles of FRQ and PER in circadian clocks, our results suggest that a double negative feedback loop formed by sense and antisense *per* transcription may function in animal circadian systems. Thus regulation of core clock components by antisense RNA is a common circadian architecture in fungi and animal circadian systems.

Our results also provide insight into how antisense transcription inhibits the transcription of sense RNAs. Thousands of antisense RNAs have been discovered by genomic-wide RNA sequencing studies in eukaryotic organisms (Berretta and Morillon, 2009; Osato et al., 2007; Xu et al., 2009). Several mechanisms have been proposed to explain the suppression of sense transcription by antisense RNAs including chromatin modifications, small RNA formation and pol II collision (Camblong et al., 2007; Hobson et al., 2012; Osato et al., 2007; Prescott and Proudfoot, 2002).Our results show that frq and qrf regulate each in a non-sequence specific manner. Neither the RNAi pathway nor DNA methylation contribute significantly to the suppression of frq by qrf transcription. ChIP assays using pol II Ser 2 and Ser 5 phospho-specific antibodies suggest that pol II proteins collide and stall in the middle of the transcribed frq region due to convergent

transcription (Fig 3-21), resulting in premature transcriptional termination (Figure 3-23). The prematurely terminated frq and qrf transcripts are then rapidly degraded by the RNA exosome. In addition, the convergent transcription also results in changes in H3K36me3 profile that can regulate frq and qrf expression. Transcriptional interference refers to the inhibitory effect of one transcriptional process on another transcriptional process in cis (Mazo et al., 2007a; Shearwin et al., 2005). Together, our results suggest that the inhibition of frq transcription by qrf is due to transcriptional interference of convergent transcription that results in pol II collision triggered transcriptional termination and chromatin modification.

BIBLIOGRAPHY

Adhvaryu, K.K., Morris, S.A., Strahl, B.D., and Selker, E.U. (2005). Methylation of histone H3 lysine 36 is required for normal development in Neurospora crassa. Eukaryot Cell *4*, 1455-1464.

Ambros, V. (2004). The functions of animal microRNAs. Nature *431*, 350-355.
Aronson, B., Johnson, K., Loros, J.J., and Dunlap, J.C. (1994a). Negative feedback defining a circadian clock: autoregulation in the clock gene *frequency*. Science *263*, 1578-1584.

Aronson, B.D., Johnson, K.A., and Dunlap, J.C. (1994b). The circadian clock locus *frequency*: A single ORF defines period length and temperature compensation. Proc Natl Acad Sci USA *91*, 7683 - 7687.

Bail, S., Swerdel, M., Liu, H., Jiao, X., Goff, L.A., Hart, R.P., and Kiledjian, M. (2010). Differential regulation of microRNA stability. RNA *16*, 1032-1039.

Baker, C.L., Loros, J.J., and Dunlap, J.C. (2012). The circadian clock of Neurospora crassa. FEMS Microbiol Rev *36*, 95-110.

Bardiya, N., and Shiu, P.K. (2007). Cyclosporin A-resistance based gene placement system for Neurospora crassa. Fungal genetics and biology : FG & B *44*, 307-314.

Barlow, J.J., Mathias, A.P., Williamson, R., and Gammack, D.B. (1963). A series of six compact fungal transformation vectors containing polylinkers with multiple unique restriction sites. Biochemical and biophysical research communications *13*, 61-66.

Bartel, D.P. (2004). MicroRNAs: Genomics, Biogenesis, Mechanism, and Function. Cell *116*, 281-297.

Batista, Pedro J., and Chang, Howard Y. (2013). Long Noncoding RNAs: Cellular Address Codes in Development and Disease. Cell *152*, 1298-1307.

Belden, W.J., Lewis, Z.A., Selker, E.U., Loros, J.J., and Dunlap, J.C. (2011). CHD1 remodels chromatin and influences transient DNA methylation at the clock gene frequency. PLoS Genet *7*, e1002166.

Belden, W.J., Loros, J.J., and Dunlap, J.C. (2007). Execution of the circadian negative feedback loop in Neurospora requires the ATP-dependent chromatin-remodeling enzyme CLOCKSWITCH. Mol Cell *25*, 587-600.

Bell-Pedersen, D., Cassone, V.M., Earnest, D.J., Golden, S.S., Hardin, P.E., Thomas, T.L., and Zoran, M.J. (2005). Circadian rhythms from multiple oscillators: lessons from diverse organisms. Nat Rev Genet *6*, 544-556.

Bell-Pedersen, D., Dunlap, J.C., and Loros, J.J. (1996). Distinct cis-acting elements mediate clock, light, and developmental regulation of the *Neurospora crassa eas* (*ccg-2*) gene. Molecular and Cellular Biology *16*, 513 - 521.

Bernstein, E., Caudy, A.A., Hammond, S.M., and Hannon, G.J. (2001). Role for a bidentate ribonuclease in the initiation step of RNA interference. Nature *409*, 363-366.

Berretta, J., and Morillon, A. (2009). Pervasive transcription constitutes a new level of eukaryotic genome regulation. EMBO Rep *10*, 973-982.

Borkovich, K.A., Alex, L.A., Yarden, O., Freitag, M., Turner, G.E., Read, N.D., Seiler, S., Bell-Pedersen, D., Paietta, J., Plesofsky, N., *et al.* (2004). Lessons from the genome sequence of Neurospora crassa: tracing the path from genomic blueprint to multicellular organism. Microbiol Mol Biol Rev *68*, 1-108.

Brennecke, J., Aravin, A.A., Stark, A., Dus, M., Kellis, M., Sachidanandam, R., and Hannon, G.J. (2007). Discrete small RNA-generating loci as master regulators of transposon activity in Drosophila. Cell *128*, 1089-1103.

Buhler, M., and Moazed, D. (2007). Transcription and RNAi in heterochromatic gene silencing. Nat Struct Mol Biol *14*, 1041-1048.

Callahan, K.P., and Butler, J.S. (2010). TRAMP complex enhances RNA degradation by the nuclear exosome component Rrp6. J Biol Chem *285*, 3540-3547.

Camblong, J., Iglesias, N., Fickentscher, C., Dieppois, G., and Stutz, F. (2007). Antisense RNA stabilization induces transcriptional gene silencing via histone deacetylation in S. cerevisiae. Cell *131*, 706-717.

Carthew, R.W., and Sontheimer, E.J. (2009). Origins and Mechanisms of miRNAs and siRNAs. Cell *136*, 642-655.

Catalanotto, C., Pallotta, M., ReFalo, P., Sachs, M.S., Vayssie, L., Macino, G., and Cogoni, C. (2004). Redundancy of the two dicer genes in transgene-induced posttranscriptional gene silencing in Neurospora crassa. Mol Cell Biol *24*, 2536-2545.

Chang, S.S., Zhang, Z., and Liu, Y. (2012). RNA interference pathways in fungi: mechanisms and functions. Annu Rev Microbiol *66*, 305-323.

Cheng, P., He, Q., He, Q., Wang, L., and Liu, Y. (2005). Regulation of the Neurospora circadian clock by an RNA helicase. Genes Dev *19*, 234-241.

Cheng, P., Yang, Y., and Liu, Y. (2001). Interlocked feedback loops contribute to the robustness of the *Neurospora* circadian clock. Proc Natl Acad Sci USA *98*, 7408-7413.

Choudhary, S., Lee, H.-C., Maiti, M., He, Q., Cheng, P., Liu, Q., and Liu, Y. (2007). A Double-Stranded-RNA Response Program Important for RNA Interference Efficiency. Molecular and Cellular Biology *27*, 3995-4005.

Cogoni, C., and Macino, G. (1999). Gene silencing in Neurospora crassa requires a protein homologous to RNA-dependent RNA polymerase. Nature *399*, 166-169.

Colot, H.V., Park, G., Turner, G.E., Ringelberg, C., Crew, C.M., Litvinkova, L., Weiss, R.L., Borkovich, K.A., and Dunlap, J.C. (2006). A high-throughput gene knockout procedure for Neurospora reveals functions for multiple transcription factors. Proc Natl Acad Sci U S A *103*, 10352-10357.

Costa, F.F. (2008). Non-coding RNAs, epigenetics and complexity. Gene *410*, 9-17.

Crosthwaite, S.K., Loros, J.J., and Dunlap, J.C. (1995). Light-Induced resetting of a circadian clock is mediated by a rapid increase in *frequency* transcript. Cell *81*, 1003 - 1012.

Czech, B., and Hannon, G.J. (2011). Small RNA sorting: matchmaking for Argonautes. Nat Rev Genet *12*, 19-31.

Dang, Y., Li, L., Guo, W., Xue, Z., and Liu, Y. (2013). Convergent Transcription Induces Dynamic DNA Methylation at disiRNA Loci. PLoS Genet *9*, e1003761.

Dang, Y., Yang, Q., Xue, Z., and Liu, Y. (2011). RNA Interference in Fungi: Pathways, Functions, and Applications. Eukaryotic Cell *10*, 1148-1155.

Davis, R.L., and deSerres, D. (1970). Genetic and microbial research techniques for *Neurospora crassa*. Methods in Enzymology *27A*, 79-143.

Denault, D.L., Loros, J.J., and Dunlap, J.C. (2001). WC-2 mediates WC-1–FRQ interaction within the PAS protein-linked circadian feedback loop of *Neurospora*. EMBO J *20*, 109-117.

Deuve, J.L., and Avner, P. (2011). The coupling of X-chromosome inactivation to pluripotency. Annu Rev Cell Dev Biol *27*, 611-629.

Dunlap, J.C. (1999). Molecular bases for circadian clocks. Cell *96*, 271-290.

Dziembowski, A., Lorentzen, E., Conti, E., and Seraphin, B. (2007). A single subunit, Dis3, is essentially responsible for yeast exosome core activity. Nat Struct Mol Biol *14*, 15-22.

Elbashir, S.M., Lendeckel, W., and Tuschl, T. (2001). RNA interference is mediated by 21- and 22-nucleotide RNAs. Genes & Development *15*, 188-200.

Ermentrout, B. (2007). XPPAUT. Scholarpedia *2*, 1399.

Estruch, F., and Cole, C.N. (2003). An Early Function during Transcription for the Yeast mRNA Export Factor Dbp5p/Rat8p Suggested by Its Genetic and Physical Interactions with Transcription Factor IIH Components. Molecular Biology of the Cell *14*, 1664-1676.

Fabian, M.R., Sonenberg, N., and Filipowicz, W. (2010). Regulation of mRNA Translation and Stability by microRNAs. Annual Review of Biochemistry *79*, 351-379.

Flynt, A.S., Greimann, J.C., Chung, W.J., Lima, C.D., and Lai, E.C. (2010). MicroRNA biogenesis via splicing and exosome-mediated trimming in Drosophila. Mol Cell *38*, 900-907.

Froehlich, A.C., Liu, Y., Loros, J.J., and Dunlap, J.C. (2002). White Collar-1, a circadian blue light photoreceptor, binding to the frequency promoter. Science *297*, 815-819.

Fulci, V., and Macino, G. (2007). Quelling: post-transcriptional gene silencing guided by small RNAs in Neurospora crassa. Curr Opin Microbiol *10*, 199-203.

Gear, C. (1971). Simultaneous Numerical Solution of Differential-Algebraic Equations. Circuit Theory, IEEE Transactions on *18*, 89-95.

Ghildiyal, M., and Zamore, P.D. (2009). Small silencing RNAs: an expanding universe. Nat Rev Genet *10*, 94-108.

Giles, N.H., Case, M.E., Baum, J., Geever, R., Huiet, L., Patel, V., and Tyler, B. (1985). Gene organization and regulation in the qa (quinic acid) gene cluster of Neurospora crassa. Microbiological Reviews *49*, 338-358.

Gooch, V.D., Mehra, A., Larrondo, L.F., Fox, J., Touroutoutoudis, M., Loros, J.J., and Dunlap, J.C. (2008). Fully codon-optimized luciferase uncovers novel temperature characteristics of the Neurospora clock. Eukaryot Cell *7*, 28-37.

Gu, S., and Kay, M. (2010). How do miRNAs mediate translational repression? Silence *1*, 11.

Gunawardane, L.S., Saito, K., Nishida, K.M., Miyoshi, K., Kawamura, Y., Nagami, T., Siomi, H., and Siomi, M.C. (2007). A slicer-mediated mechanism for repeat-associated siRNA 5' end formation in Drosophila. Science *315*, 1587-1590.

Guo, J., Cheng, P., Yuan, H., and Liu, Y. (2009). The exosome regulates circadian gene expression in a posttranscriptional negative feedback loop. Cell *138*, 1236-1246.

Haley, B., and Zamore, P.D. (2004). Kinetic analysis of the RNAi enzyme complex. Nat Struct Mol Biol *11*, 599-606.

Halic, M., and Moazed, D. (2010). Dicer-independent primal RNAs trigger RNAi and heterochromatin formation. Cell *140*, 504-516.

Han, Bo W., Hung, J.-H., Weng, Z., Zamore, Phillip D., and Ameres, Stefan L. (2011). The 3'-to-5' Exoribonuclease Nibbler Shapes the 3' Ends of MicroRNAs Bound to Drosophila Argonaute1. Current biology : CB *21*, 1878-1887.

Hannon, G.J. (2002). RNA interference. Nature *418*, 244-251.

He, Q., Cha, J., He, Q., Lee, H., Yang, Y., and Liu, Y. (2006). CKI and CKII mediate the FREQUENCY-dependent phosphorylation of the WHITE COLLAR complex to close the Neurospora circadian negative feedback loop. Genes & Dev *20*, 2552-2565.

He, Q., Cheng, P., Yang, Y., Wang, L., Gardner, K.H., and Liu, Y. (2002). White collar-1, a DNA binding transcription factor and a light sensor. Science *297*, 840-843.

He, Q., and Liu, Y. (2005). Molecular mechanism of light responses in Neurospora: from light-induced transcription to photoadaptation. Genes & Development *19*, 2888-2899.

Heintzen, C., and Liu, Y. (2007). The Neurospora crassa circadian clock. Adv Genet *58*, 25-66.

Hobson, D.J., Wei, W., Steinmetz, L.M., and Svejstrup, J.Q. (2012). RNA polymerase II collision interrupts convergent transcription. Mol Cell *48*, 365-374.

Holley, R.W., Apgar, J., Everett, G.A., Madison, J.T., Marquisee, M., Merrill, S.H., Penswick, J.R., and Zamir, A. (1965). STRUCTURE OF A RIBONUCLEIC ACID. Science *147*, 1462-1465.

Hong, C.I., Jolma, I.W., Loros, J.J., Dunlap, J.C., and Ruoff, P. (2008). Simulating dark expressions and interactions of frq and wc-1 in the Neurospora circadian clock. Biophys J *94*, 1221-1232.

Houseley, J., LaCava, J., and Tollervey, D. (2006). RNA-quality control by the exosome. Nat Rev Mol Cell Biol *7*, 529-539.

Houseley, J., and Tollervey, D. (2006). Yeast Trf5p is a nuclear poly(A) polymerase. EMBO Rep *7*, 205-211.

Hsin, J.P., and Manley, J.L. (2012). The RNA polymerase II CTD coordinates transcription and RNA processing. Genes Dev *26*, 2119-2137.

Huntzinger, E., and Izaurralde, E. (2011). Gene silencing by microRNAs: contributions of translational repression and mRNA decay. Nat Rev Genet *12*, 99-110.

Ibrahim, F., Rymarquis, L.A., Kim, E.J., Becker, J., Balassa, E., Green, P.J., and Cerutti, H. (2010). Uridylation of mature miRNAs and siRNAs by the MUT68 nucleotidyltransferase promotes their degradation in Chlamydomonas. Proc Natl Acad Sci U S A *107*, 3906-3911.

Jacob, F., and Monod, J. (1961). Genetic regulatory mechanisms in the synthesis of proteins. Journal of Molecular Biology *3*, 318-356.

Kawamata, T., Seitz, H., and Tomari, Y. (2009). Structural determinants of miRNAs for RISC loading and slicer-independent unwinding. Nat Struct Mol Biol *16*, 953-960.

Kawaoka, S., Izumi, N., Katsuma, S., and Tomari, Y. (2011). 3' end formation of PIWI-interacting RNAs in vitro. Mol Cell *43*, 1015-1022.

Kim, V.N., Han, J., and Siomi, M.C. (2009). Biogenesis of small RNAs in animals. Nat Rev Mol Cell Biol *10*, 126-139.

Klattenhoff, C., and Theurkauf, W. (2008). Biogenesis and germline functions of piRNAs. Development *135*, 3-9.

Koike, N., Yoo, S.H., Huang, H.C., Kumar, V., Lee, C., Kim, T.K., and Takahashi, J.S. (2012). Transcriptional architecture and chromatin landscape of the core circadian clock in mammals. Science *338*, 349-354.

Komarnitsky, P., Cho, E.J., and Buratowski, S. (2000). Different phosphorylated forms of RNA polymerase II and associated mRNA processing factors during transcription. Genes Dev *14*, 2452-2460.

Kramer, C., Loros, J.J., Dunlap, J.C., and Crosthwaite, S.K. (2003). Role for antisense RNA in regulating circadian clock function in Neurospora crassa. Nature *421*, 948-952.

LaCava, J., Houseley, J., Saveanu, C., Petfalski, E., Thompson, E., Jacquier, A., and Tollervey, D. (2005). RNA degradation by the exosome is promoted by a nuclear polyadenylation complex. Cell *121*, 713-724.

Lapidot, M., and Pilpel, Y. (2006). Genome-wide natural antisense transcription: coupling its regulation to its different regulatory mechanisms. EMBO Rep *7*, 1216-1222.

Lee, H.-C., Chang, S.-S., Choudhary, S., Aalto, A.P., Maiti, M., Bamford, D.H., and Liu, Y. (2009). qiRNA is a new type of small interfering RNA induced by DNA damage. Nature *459*, 274-277.

Lee, H.-C., Li, L., Gu, W., Xue, Z., Crosthwaite, S.K., Pertsemlidis, A., Lewis, Z.A., Freitag, M., Selker, E.U., Mello, C.C., *et al.* (2010). Diverse Pathways Generate MicroRNA-like RNAs and Dicer-Independent Small Interfering RNAs in Fungi. Molecular Cell.

Lee, R.C., Feinbaum, R.L., and Ambros, V. (1993). The C. elegans heterochronic gene lin-4 encodes small RNAs with antisense complementarity to lin-14. Cell *75*, 843-854.

Li, B., Howe, L., Anderson, S., Yates, J.R., 3rd, and Workman, J.L. (2003). The Set2 histone methyltransferase functions through the phosphorylated carboxyl-terminal domain of RNA polymerase II. J Biol Chem *278*, 8897-8903.

Li, C., Vagin, V.V., Lee, S., Xu, J., Ma, S., Xi, H., Seitz, H., Horwich, M.D., Syrzycka, M., Honda, B.M., *et al.* (2009). Collapse of germline piRNAs in the absence of Argonaute3 reveals somatic piRNAs in flies. Cell *137*, 509-521.

Li, L., Chang, S.-s., and Liu, Y. (2010). RNA interference pathways in filamentous fungi. Cellular and Molecular Life Sciences *67*, 3849-3863.

Liu, N., Abe, M., Sabin, L.R., Hendriks, G.J., Naqvi, A.S., Yu, Z., Cherry, S., and Bonini, N.M. (2011). The exoribonuclease Nibbler controls 3' end processing of microRNAs in Drosophila. Curr Biol *21*, 1888-1893.

Liu, Q., Greimann, J.C., and Lima, C.D. (2006). Reconstitution, activities, and structure of the eukaryotic RNA exosome. Cell *127*, 1223-1237.

Liu, Q., and Paroo, Z. (2010). Biochemical Principles of Small RNA Pathways. Annual Review of Biochemistry *79*, 295-319.

Liu, Q., Rand, T.A., Kalidas, S., Du, F., Kim, H.E., Smith, D.P., and Wang, X. (2003). R2D2, a bridge between the initiation and effector steps of the Drosophila RNAi pathway. Science *301*, 1921-1925.

Liu, Y., and Bell-Pedersen, D. (2006). Circadian rhythms in Neurospora crassa and other filamentous fungi. Eukaryot Cell *5*, 1184-1193.

Liu, Y., Garceau, N.Y., Loros, J.J., and Dunlap, J.C. (1997). Thermally Regulated Translational Control of FRQ Mediates Aspects of Temperature Responses in the Neurospora Circadian Clock. Cell *89*, 477-486.

Ma, J.B., Yuan, Y.R., Meister, G., Pei, Y., Tuschl, T., and Patel, D.J. (2005). Structural basis for 5'-end-specific recognition of guide RNA by the A. fulgidus Piwi protein. Nature *434*, 666-670.

Maiti, M., Lee, H.-C., and Liu, Y. (2007). QIP, a putative exonuclease, interacts with the Neurospora Argonaute protein and facilitates conversion of duplex siRNA into single strands. Genes & Development *21*, 590-600.

Malone, C.D., Brennecke, J., Dus, M., Stark, A., McCombie, W.R., Sachidanandam, R., and Hannon, G.J. (2009). Specialized piRNA pathways act in germline and somatic tissues of the Drosophila ovary. Cell *137*, 522-535.

Matranga, C., Tomari, Y., Shin, C., Bartel, D.P., and Zamore, P.D. (2005). Passenger-strand cleavage facilitates assembly of siRNA into Ago2-containing RNAi enzyme complexes. Cell *123*, 607-620.

Mattick, J.S., and Makunin, I.V. (2006). Non-coding RNA. Human Molecular Genetics *15*, R17-R29.

Mazo, A., Hodgson, J.W., Petruk, S., Sedkov, Y., and Brock, H.W. (2007). Transcriptional interference: an unexpected layer of complexity in gene regulation. Journal of cell science *120*, 2755-2761.

Meister, G. (2013). Argonaute proteins: functional insights and emerging roles. Nat Rev Genet *14*, 447-459.

Mercer, T.R., Dinger, M.E., and Mattick, J.S. (2009). Long non-coding RNAs: insights into functions. Nat Rev Genet *10*, 155-159.

Mi, S., Cai, T., Hu, Y., Chen, Y., Hodges, E., Ni, F., Wu, L., Li, S., Zhou, H., Long, C., *et al.* (2008). Sorting of small RNAs into Arabidopsis argonaute complexes is directed by the 5' terminal nucleotide. Cell *133*, 116-127.

Moazed, D. (2009). Small RNAs in transcriptional gene silencing and genome defence. Nature *457*, 413-420.

Nagano, T., Mitchell, J.A., Sanz, L.A., Pauler, F.M., Ferguson-Smith, A.C., Feil, R., and Fraser, P. (2008). The Air noncoding RNA epigenetically silences transcription by targeting G9a to chromatin. Science *322*, 1717-1720.

Nolan, T., and Cogoni, C. (2004). The long hand of the small RNAs reaches into several levels of gene regulation. Biochem Cell Biol *82*, 472-481.

Ogawa, Y., Sun, B.K., and Lee, J.T. (2008). Intersection of the RNA interference and X-inactivation pathways. Science *320*, 1336-1341.

Osato, N., Suzuki, Y., Ikeo, K., and Gojobori, T. (2007). Transcriptional interferences in cis natural antisense transcripts of humans and mice. Genetics *176*, 1299-1306.

Pall, G.S., Codony-Servat, C., Byrne, J., Ritchie, L., and Hamilton, A. (2007). Carbodiimide-mediated cross-linking of RNA to nylon membranes improves the detection of siRNA, miRNA and piRNA by northern blot. Nucleic Acids Research *35*, e60.

Pall, M.L. (1993). The use of Ignite (Basta; glufosinate;phosphinothricin) to select transformants of bar-containing plasmids in Neurospora crassa. Fungal Genetics Newsletter *40*.

Parker, J.S., Roe, S.M., and Barford, D. (2004). Crystal structure of a PIWI protein suggests mechanisms for siRNA recognition and slicer activity. The EMBO journal *23*, 4727-4737.

Phatnani, H.P., and Greenleaf, A.L. (2006). Phosphorylation and functions of the RNA polymerase II CTD. Genes Dev *20*, 2922-2936.

Pickford, A.S., and Cogoni, C. (2003). RNA-mediated gene silencing. Cell Mol Life Sci *60*, 871-882.

Ponting, C.P., Oliver, P.L., and Reik, W. (2009). Evolution and Functions of Long Noncoding RNAs. Cell *136*, 629-641.

Prescott, E.M., and Proudfoot, N.J. (2002). Transcriptional collision between convergent genes in budding yeast. Proc Natl Acad Sci U S A *99*, 8796-8801.

Rinn, J.L., and Chang, H.Y. (2012). Genome Regulation by Long Noncoding RNAs. Annual Review of Biochemistry *81*, 145-166.

Romano, N., and Macino, G. (1992). Quelling: transient inactivation of gene expression in Neurospora crassa by transformation with homologous sequences. Molecular microbiology *6*, 3343-3353.

Ruoff, P., Loros, J.J., and Dunlap, J.C. (2005). The relationship between FRQ-protein stability and temperature compensation in the Neurospora circadian clock. Proc Natl Acad Sci U S A *102*, 17681-17686.

Ruoff, P., Vinsjevik, M., Monnerjahn, C., and Rensing, L. (1999). The Goodwin oscillator: on the importance of degradation reactions in the circadian clock. Journal of biological rhythms *14*, 469-479.

Sauman, I., and Reppert, S.M. (1996). Circadian clock neurons in the silkmoth Antheraea pernyi: novel mechanisms of Period protein regulation. Neuron *17*, 889-900.

Schafmeier, T., Haase, A., Kaldi, K., Scholz, J., Fuchs, M., and Brunner, M. (2005). Transcriptional feedback of neurospora circadian clock gene by phosphorylation-dependent inactivation of its transcription factor. Cell *122*, 235-246.

Schneider, C., Anderson, J.T., and Tollervey, D. (2007). The exosome subunit Rrp44 plays a direct role in RNA substrate recognition. Mol Cell *27*, 324-331.

Seitz, H., Tushir, J., and Zamore, P. (2011). A 5'-uridine amplifies miRNA/miRNA* asymmetry in Drosophila by promoting RNA-induced silencing complex formation. Silence *2*, 4.

Sharma, V., and Misteli, T. (2013). Non-coding RNAs in DNA damage and repair. FEBS letters *587*, 1832-1839.

Shearwin, K.E., Callen, B.P., and Egan, J.B. (2005). Transcriptional interference – a crash course. Trends in Genetics *21*, 339-345.

Siomi, H., and Siomi, M.C. (2009). On the road to reading the RNA-interference code. Nature *457*, 396-404.

Smith, K.M., Sancar, G., Dekhang, R., Sullivan, C.M., Li, S., Tag, A.G., Sancar, C., Bredeweg, E.L., Priest, H.D., McCormick, R.F., *et al.* (2010). Transcription factors in light and circadian clock signaling networks revealed by genomewide mapping of direct targets for neurospora white collar complex. Eukaryot Cell *9*, 1549-1556.

Thomson, T., and Lin, H. (2009). The Biogenesis and Function of PIWI Proteins and piRNAs: Progress and Prospect. Annual Review of Cell and Developmental Biology *25*, 355-376.

Vanacova, S., Wolf, J., Martin, G., Blank, D., Dettwiler, S., Friedlein, A., Langen, H., Keith, G., and Keller, W. (2005). A new yeast poly(A) polymerase complex involved in RNA quality control. PLoS Biol *3*, e189.

Voinnet, O. (2009). Origin, Biogenesis, and Activity of Plant MicroRNAs. *136*, 669-687.
Vollmers, C., Schmitz, R.J., Nathanson, J., Yeo, G., Ecker, J.R., and Panda, S. (2012). Circadian oscillations of protein-coding and regulatory RNAs in a highly dynamic mammalian liver epigenome. Cell Metab *16*, 833-845.

Wang, Kevin C., and Chang, Howard Y. (2011). Molecular Mechanisms of Long Noncoding RNAs. Molecular cell *43*, 904-914.

Wang, Y., Sheng, G., Juranek, S., Tuschl, T., and Patel, D.J. (2008). Structure of the guide-strand-containing argonaute silencing complex. Nature *456*, 209-213.

Xu, Z., Wei, W., Gagneur, J., Perocchi, F., Clauder-Munster, S., Camblong, J., Guffanti, E., Stutz, F., Huber, W., and Steinmetz, L.M. (2009). Bidirectional promoters generate pervasive transcription in yeast. Nature *457*, 1033-1037.

Yang, J.-S., and Lai, Eric C. (2011). Alternative miRNA Biogenesis Pathways and the Interpretation of Core miRNA Pathway Mutants. Molecular Cell *43*, 892-903.

Young, M.W., and Kay, S.A. (2001). Time zones: a comparative genetics of circadian clocks. Nat Rev Genet *2*, 702-715.

Yu, Y., Dong, W., Altimus, C., Tang, X., Griffith, J., Morello, M., Dudek, L., Arnold, J., and Schuttler, H.B. (2007). A genetic network for the clock of Neurospora crassa. Proc Natl Acad Sci U S A *104*, 2809-2814.

Zaratiegui, M., Irvine, D.V., and Martienssen, R.A. (2007). Noncoding RNAs and Gene Silencing. Cell *128*, 763-776.

Zhao, Y., Shen, Y., Yang, S., Wang, J., Hu, Q., Wang, Y., and He, Q. (2010). Ubiquitin Ligase Components Cullin4 and DDB1 Are Essential for DNA Methylation in Neurospora crassa. Journal of Biological Chemistry *285*, 4355-4365.

Zhou, Z., Liu, X., Hu, Q., Zhang, N., Sun, G., Cha, J., Wang, Y., Liu, Y., and He, Q. (2013). Suppression of WC-independent frequency transcription by RCO-1 is essential for Neurospora circadian clock. submitted.